Immunoepidemiological Modeling of Dengue Viral Infection

Ryan Nikin-Beers

Dissertation submitted to the Faculty of the
Virginia Polytechnic Institute and State University
in partial fulfillment of the requirements for the degree of

Doctor of Philosophy
in
Mathematics

Stanca M. Ciupe, Chair
Lauren M. Childs
Julie C. Blackwood
Leah R. Johnson

March 16, 2018
Blacksburg, Virginia

Keywords: Mathematical Modeling, Dengue Viral Infection, Differential Equations

Immunoepidemiological Modeling of Dengue Viral Infection

Ryan Nikin-Beers

ABSTRACT

Dengue viral infection is a mosquito-borne disease prevalent in tropical areas, resulting in over 300 million cases each year, a quarter of which are symptomatic. Dengue virus has four distinct serotypes, where the interactions between these strains have implications on the severity of the disease outcomes. During primary infections with one strain, dengue infection is largely asymptomatic, sometimes resulting in mild dengue fever. However, patients that develop a secondary infection with a different strain are at an increased risk of more severe disease, such as dengue hemorrhagic fever or dengue shock syndrome.

The two competing hypotheses for the increased severity during secondary infections are antibody dependent enhancement and original antigenic sin. Antibody dependent enhancement suggests that long-lived antibodies from primary infection dominate antibody responses to secondary virus strains. The pre-existing antibody does not remove virus; instead, it signals phagocytes to migrate to the site of infection and ingest antibody-virus particles. Once inside the cell, virus unbinds and infects the phagocyte, which leads to enhanced infection and more severe disease. Original antigenic sin proposes that T lymphocytes specific to primary infection dominate cellular immune responses during secondary infections, but are inefficient at clearing cells infected with non-specific strains. Thus, the infected cells are not cleared quickly enough, leading to the immune cells remaining for longer periods, producing more cytokines, and leading to more severe disease.

To analyze these hypotheses, we developed and analyzed within-host mathematical models. In previous work, we developed models of neutralizing and non-neutralizing antibody response. We found that in order to fit the secondary infection model to data, we must predict a decreased non-neutralizing antibody effect during secondary infection. Since this effect accounts for decreased viral clearance and the virus is in quasi-equilibrium with infected cells, we could be accounting for reduced cell killing and the original antigenic sin hypothesis.

To further understand these interactions, we then develop a model of T cell responses to primary and secondary dengue virus infections that considers the effect of T cell cross-reactivity in disease enhancement. We fit the models to published patient data and show that the overall infected cell killing is similar in dengue heterologous infections, resulting in dengue fever and dengue hemorrhagic fever. The contribution to overall killing, however, is dominated by non-specific T cell responses during the majority of secondary dengue hemorrhagic fever cases. By contrast, more than half of secondary dengue fever cases have predominant strain-specific T cell responses with high avidity. These results support the hypothesis that cross-reactive T cell responses occur mainly during severe disease cases of heterologous dengue virus infections.

Finally, using the results from our within-host models and making certain simplifying assumptions, we develop an immunoepidemiological model of dengue viral infection which couples the within-host virus dynamics to the population level through a system of partial differential equations. The resulting multiscale model examines the dynamics of between-host infections in the presence of two circulating virus strains that involves feedback from the within-host and between-host interactions. We analytically determine the relationship between the model parameters and the characteristics of the solutions to the model, and find analytical thresholds under which infections persist in the population. Furthermore, we develop and implement a full numerical scheme for our immunoepidemiological model, allowing the simulation of population dynamics under variable parameter conditions.

Immunoepidemiological Modeling of Dengue Viral Infection

Ryan Nikin-Beers

GENERAL AUDIENCE ABSTRACT

Dengue viral infection is a mosquito-borne disease with four distinct strains, where the interactions between these strains have implications on the severity of the disease outcomes. The two competing hypotheses for the increased severity during secondary infections are antibody dependent enhancement and original antigenic sin. Antibody dependent enhancement suggests that long-lived antibodies from primary infection remain during secondary infection but do not neutralize the virus. Original antigenic sin proposes that T cells specific to primary infection dominate cellular immune responses during secondary infections, but are inefficient at clearing cells infected with non-specific strains.

To analyze these hypotheses, we developed within-host mathematical models. In previous work, we predicted a decreased non-neutralizing antibody effect during secondary infection. Since this effect accounts for decreased viral clearance and the virus is in quasi-equilibrium with infected cells, we could be accounting for reduced cell killing and the original antigenic sin hypothesis.

To further understand these interactions, we develop a model of T cell responses to primary and secondary dengue virus infections that considers the effect of T cell cross-reactivity in disease enhancement. We fit the models to published patient data and show that the overall infected cell killing is similar in dengue heterologous infections, resulting in dengue fever and dengue hemorrhagic fever. The contribution to overall killing, however, is dominated by non-specific T cell responses during the majority of secondary dengue hemorrhagic fever cases. By contrast, more than half of secondary dengue fever cases have predominant strain-specific T cell responses. These results support the hypothesis that cross-reactive T cell responses occur mainly during severe disease cases of heterologous dengue virus infections.

Finally, using the results from our within-host models, we develop a multiscale model of dengue viral infection which couples the within-host virus dynamics to the population level dynamics through a system of partial differential equations. We analytically determine the relationship between the model parameters and the characteristics of the solutions, and find thresholds under which infections persist in the population. Furthermore, we develop and implement a full numerical scheme for our model.

Acknowledgments

Firstly, I would like to thank my advisor Dr. Stanca Ciupe for her help, guidance, and advice during my time at Virginia Tech. The knowledge and insight I have gained have been invaluable.

I greatly appreciate the assistance I have received from my collaborators, especially the support from Dr. Lauren Childs, Dr. Julie Blackwood, and Dr. Kaja Abbas.

A special thanks is also required to Dr. Leah Johnson for her cooperation in the past months.

Finally, I wish to express my gratitude to my mother and father for always encouraging me to pursue my education.

Contents

List of Figures

List of Tables

Chapter 1

Introduction

The outline of this dissertation is as follows. In the second chapter, we review the biological background necessary for understanding the studies, including the epidemiology and immunology of dengue viral infection. The hypotheses of original antigenic sin and antibody dependent enhancement are discussed. In the third chapter, we review the mathematical background of modeling disease dynamics, including an overview of epidemiological, immunological, and immunoepidemiological models. We summarize the results from our review of HIV immunonepidemiological models, which was joint work with Dr. Narges Dorratoltaj, Dr. Stanca Ciupe, Dr. Stephen Eubank, and Dr. Kaja Abbas. In the fourth chapter, we describe a within-host model of original antigenic sin in dengue viral infection. This study, completed under the guidance of Dr. Stanca Ciupe, was motivated by the results from a previous within-host model of antibody dependent enhancement, which we describe briefly in chapter three. In the fifth chapter, we describe an immunoepidemiological model of dengue viral infection, which was joint work with Dr. Julie Blackwood, Dr. Lauren Childs, and Dr. Stanca Ciupe. This model used the results from our within-host models in order to understand how the within-host dynamics of dengue viral infection affect the extinction, persistence of a single strain, or coexistence of multiple strains at the population level. In the sixth chapter, we summarize our main results and describe future work.

1.1 Manuscripts used in this dissertation

This dissertation includes published material and material being prepared for publication.

- **R. Nikin-Beers** and S. M. Ciupe. Modelling original antigenic sin in dengue viral infection. *Math. Med. Biol.*, page dqx002, 2017.
- N. Dorratoltaj*, **R. Nikin-Beers***, S. M. Ciupe, S. G. Eubank, and K. M. Abbas. Multi-scale immunoepidemiological modeling of within-host and between-host HIV dynamics: systematic review of mathematical models. *PeerJ*, 5:e3877, 2017.
- **R. Nikin-Beers**, J. Blackwood, L. Childs, and S. M. Ciupe. Unraveling within-host signatures of dengue infection at the population level. *J. Theor. Biol.*, 446:79-86, 2018.

*Denotes equal contribution

Chapter 2

Biological Background

2.1 Epidemiology

Epidemiology is the study of how and why diseases spread in populations. To properly study these effects, and to institute proper control measures against diseases, reliable and accurate data must be obtained [92]. The intensity of a disease often focuses on three measures: the incidence, which is the number of new cases in a specific time period; the prevalence, which is the number of current cases at a particular time point; and the severity, which describes a specific stage of development of the disease (for example, the size of a lesion or the volume of a tumor) [92].

2.1.1 Epidemiology of dengue

Dengue viral infection is a mosquito-borne disease prevalent in tropical areas, resulting in over 300 million cases each year, a quarter of which are symptomatic [13]. Dengue virus has four distinct serotypes, namely DENV 1-4. The interactions between these strains have implications on the severity of the disease outcomes. During primary infections with one strain, dengue infection is largely asymptomatic, sometimes resulting in mild dengue fever

(DF). DF is characterized by rash, headache, and nausea [82]. After infection, lifelong immunity from reinfection with homologous serotype is developed, and a period of cross-protection against other strains occurs for one to three months [59]. However, after this period of cross-protection, patients that develop a secondary infection with a different strain are at an increased risk of more severe disease, such as dengue hemorrhagic fever (DHF) or dengue shock syndrome (DSS) [13]. DHF is characterized by symptoms such as high blood platelet count, bleeding, and liver damage, whereas DSS involves high blood pressure, weak pulse, internal bleeding, and shock if not treated properly [82].

Illnesses with symptoms similar to DF have been documented since 400 AD in the Chin dynasty [38]. Although long known to be associated with insects, dengue virus has only been recently discovered to be transmitted by mosquitos within the past hundred years [83]. Epidemics are caused mostly by transmission through the vector *Aedes aegypti*, although slow-moving outbreaks caused by the less efficient *Aedes albopictus* vector have also been observed [32, 44]. While DF has had a long history, the more severe diseases of DHF and DSS have only been recently documented, with the first observed case of DHF occurring in 1953 [38]. Although dengue occurs mostly in tropical and subtropical areas, up to 3.6 billion people are thought to be living in areas susceptible to dengue, with seventy-five percent of the susceptible population living in the Asia-Pacific region [124]. The range and spread of dengue viral infection has been increasing in recent years, along with the number of severe cases [83]. Before 1970, only nine countries reported having severe cases of dengue, while the number of countries currently with severe cases of dengue is over thirty [82, 83]. Since the spread of the mosquito vector is correlated with temperature, one hypothesis for this increased spread has been the increase in global temperature over recent decades, although other factors such as globalization and wider movement of people may be contributing factors [83]. One of the most striking cases of the emergence of more severe disease was seen in Cuba in the early 1980s. After a vector control campaign had eliminated most cases of dengue fever prior to 1970, the campaign was discontinued [83]. In 1977, an epidemic involving strain DENV-1 occurred, although most cases were asymptomatic, and the most severe cases were

mild dengue fever [73]. However, in 1981, after a strain of DENV-2 had been introduced into the region, a severe outbreak occurred, with thousands of cases of DHF and DSS, along with many more thousands of cases of overt DF [44]. The more severe cases often occurred in patients who had been infected with DENV-1 in 1977 [43].

Due to the increased prominence of dengue viral infection in the past few decades, much effort has been made recently to develop a dengue vaccine. Populations presumed to most benefit from a dengue vaccine are residents of and travelers to endemic areas, and thus any vaccine should be effective across all age groups [82]. Currently, there is one licensed dengue vaccine, Dengvaxia, that has undergone clinical trials. Two other vaccines, TDV and LATV, are currently in phase III clinical trials [45]. One of the reasons that dengue vaccines have not been developed earlier is due to the significant complications that may arise when introducing a dengue vaccine into a population. Due to the higher risk of more severe disease during secondary infections, any vaccine that is not protective across all strains may induce prevalence of more severe diseases [45]. While Dengvaxia has been licensed, Halstead raises concerns that results from the trials show evidence of vaccine-enhanced infection [45], which raises significant ethical quandaries.

2.2 Immunology

Immunology studies the different reactions of an immune system within a host to the invasion of the host by a foreign particle, often a virus, parasite, or fungus. The immune system response can be split into two main parts, namely innate immunity and adaptive immunity. Innate immunity contains no memory, and involves a non-specific response to any invading pathogen. Adaptive immunity relies on memory of previous infections, and develops a specific response depending on the pathogen [6].

The adaptive immune responses consists of two main types: an antibody response often carried out by B cells and a cell-mediated immune response often carried out by T cells.

The antibody response activates B cells, which mature into plasma cells and produce antibodies, which then bind to the infiltrating pathogen. Antibodies can be classified as either neutralizing, meaning the antibody-pathogen particle is refrained from the ability to bind to a target cell; or non-neutralizing, meaning that while the antibody-pathogen particle can still infect a target cell, the antibody marks the cell to be ingested by phagocytes, which are cells that exist specifically to eliminate infected cells [17].

In cell-mediated immune responses, activated T cells eliminate infected cells that have virus proteins on their surface, destroying infected cells before the virus has a chance to replicate inside them [6]. Certain kinds of T cells release cytokines, which can inhibit viral production, increase the chance infected cells are recognized, and actively recruit more effector cells to the infection site [17].

2.2.1 Immunology of dengue

In patients with dengue viral infection, the immune response is thought to contribute to the incidence of more severe disease during secondary heterologous infection. While cases of DHF and DSS can occur during primary infection, they much more often occur during secondary infection [113]. These cases are associated with viraemia levels much higher than those associated with cases of DF [113]. During primary infection, the immune response to dengue viral infection is relatively typical, with an early Immunoglobulin M (IgM) response followed by a later Immunoglobulin G (IgG) response [59], where the term *immunoglobulins* is used to characterize different types of antibody molecules [17]. During secondary infection with a different strain, a faster IgG response occurs, often with a lesser IgM response [59]. Protective antibodies are produced against all four strains, even if the patient has only been infected with two strains, which is why cases of tertiary or quaternary infection rarely occur [82].

The two competing hypotheses for the increased severity during secondary heterologous infections are antibody dependent enhancement and original antigenic sin. Antibody de-

pendent enhancement suggests that long-lived antibodies from primary infection dominate antibody responses to secondary virus strains. The pre-existing antibody does not remove virus; instead, the antibody-virus particles bind to receptors on circulating monocytes for the fragment crystallizable region of IgG antibody molecules (Fcγ receptors) [17]. Monocytes of this type are not normally infected during primary infection. However, once inside these monocytes, virus unbinds and infects these cells, which leads to enhanced infection and more severe disease [46, 25].

Original antigenic sin proposes that T lymphocytes specific to primary infection dominate cellular immune responses during secondary infections, but are inefficient at clearing cells infected with non-specific strains. Thus, the infected cells are not cleared quickly enough, leading to the immune cells remaining for longer periods, producing more cytokines, and leading to more severe disease [112, 120]. More severe disease has been shown to be associated with higher dengue-specific CD8+ T cell responses [80].

Chapter 3

Mathematical Background

Mathematical modeling can be used in a variety of ways, but in the context of this thesis, we will discuss the ways it can be used to describe the dynamics of infectious diseases. Models can make quantitative predictions or discover qualitative aspects about the underlying system. In lieu of large-scale experimental studies, models can analyze the costs and benefits of vaccination campaigns, drug therapies, and control measures. They allow biologists to gain insight into the interactions occurring within hosts, between hosts, or the interplay between these two levels. Due to the complexities of most biological systems, we often make simplifying assumptions so that we can work practically with the models. An understanding of the most important biological aspects of a system is required to make the model outcomes biologically relevant. Due to recent technological advances, vast amounts of new data can help to refine our mathematical models, which can then help to refine the biological experiments performed. Models can use a variety of different methods to describe the behavior of biological systems, including ordinary or partial differential equations, difference equations, stochastic equations, and individual-based models. For the purposes of this thesis, we will focus mostly on describing models of differential equations.

3.1 Epidemiological modeling background

One of the simplest models used to describe how a disease spreads throughout a population is the compartmental SIR model, which describes the interaction between susceptible individuals (S), infected individuals (I), and recovered individuals (R) [28, 54]. It is assumed that infected individuals infect susceptible individuals at rate β, individuals recover at rate γ, each class dies at rate μ, and susceptible individuals are birthed at rate μ. Due to the equal birth and death rates, the population remains constant. Note that the mean duration of infection is $\frac{1}{\gamma}$ and the mean lifetime of an individual is $\frac{1}{\mu}$. A diagram of this model is shown below in Figure 3.1. We can then write this model as the following system of differential equations,

$$\begin{aligned} \frac{dS}{dt} &= \mu - \beta SI - \mu S, \\ \frac{dI}{dt} &= \beta SI - (\gamma + \mu)I, \\ \frac{dR}{dt} &= \gamma I - \mu R. \end{aligned} \tag{3.1}$$

While the model in this form assumes each class describes proportions of the population, and thus $S + I + R = 1$, the model can be modified so that each class describes a number of individuals. By setting each of the rates equal to zero, we can solve for the two equilibria $(\overline{S}, \overline{I}, \overline{R})$ of this system, namely,

$$\begin{aligned} E_1 &= (1, 0, 0), \\ E_2 &= \left(\frac{\gamma + \mu}{\beta}, \frac{\mu(\beta - (\gamma + \mu))}{\beta(\gamma + \mu)}, \frac{\gamma(\beta - (\gamma + \mu))}{\beta(\gamma + \mu)} \right). \end{aligned} \tag{3.2}$$

The steady state E_1 is known as the epidemic equilibrium, while E_2 is known as the endemic equilibrium. If the system reaches the epidemic steady state, this means the disease will eventually clear from the population, possibly after one epidemic. However, to reach the endemic steady state, multiple epidemics usually occur, and eventually there will always be

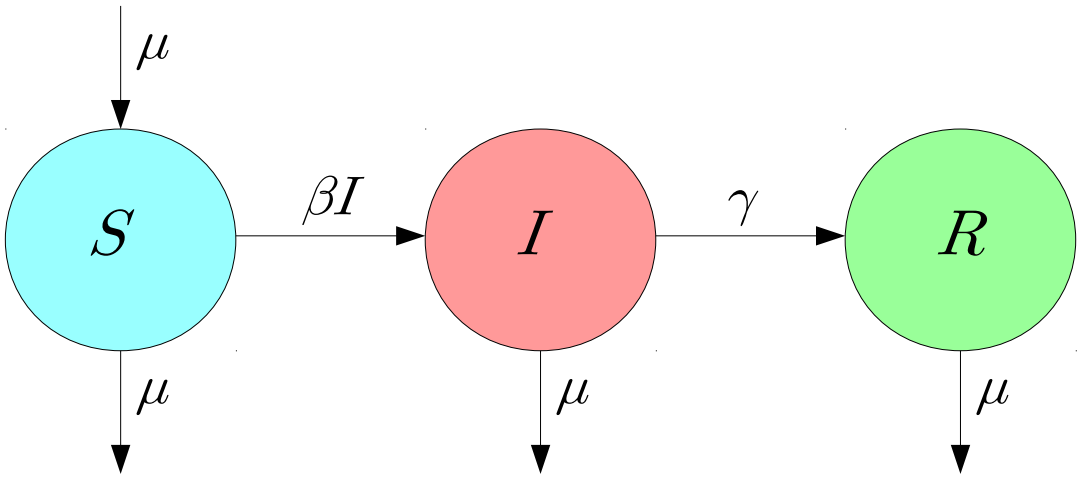

Figure 3.1: **SIR model.** A diagram of model (3.1), showing the interactions between susceptible (S), infected (I), and recovered (R) individuals.

a number of people in the population who are infected. We can define the reproduction number

$$R_0 = \frac{\beta}{\gamma + \mu},$$

which describes the number of new infections produced by each infected individual [28]. It can be shown that the epidemic steady state is locally asymptotically stable if $R_0 < 1$ (and unstable if $R_0 > 1$), and the endemic steady state is locally asymptotically stable if $R_0 > 1$ (and unstable if $R_0 < 1$). Thus, one goal of any intervention in an endemic area is to attempt to diminish R_0 below 1 to force extinction of the disease.

While this model has mostly been used in theoretical contexts, it can be used to derive estimates for R_0 in populations. Using the incidence rate at endemic equilibrium of $\beta \overline{I}_{E_2}$ and an assumption of an exponential waiting time in S, then the average age of infection can be calculated as

$$A = \frac{1}{\beta \overline{I}_{E_2}}.$$

Thus, using the average lifetime of the population

$$L = \frac{1}{\mu},$$

it can be shown that $R_0 = 1 + \frac{L}{A}$. This estimate has been used to calculate R_0 for multiple diseases in developed countries, such as measles, chicken pox, mumps, and rubella [53]. These estimates for R_0 can then be used to determine estimates for minimum values of herd immunity

$$h = 1 - \frac{1}{R_0},$$

which tells the proportion of the population that must have immunity, whether disease- or vaccination-induced, such that an epidemic does not occur [54].

3.1.1 Epidemiological modeling in dengue

Many models have been developed to describe the dynamics of dengue viral infection in a population. They can incorporate one or multiple strains, explicitly model both the vector population and the host population, or implicitly model the vector population through direct contact [7]. One of the earliest models developed to describe dengue dynamics assumed just a single strain in the population [10]. The model explicitly accounted for both the vector and human populations, where the human population is modeled by an SIR model, with susceptible, infected, and recovered classes S_h, I_h, and R_h, respectively; while the vector population is modeled by an SI model, with susceptible and infected classes S_v and I_v, respectively. It is assumed that mosquitos stay infected until death and that the total host population $N_h = S_h + I_h + R_h$. The model assumes transmission probabilities from infected vector to susceptible host β_h and from infected host to susceptible vector β_v. The biting rate b, which is the mean number of bites per vector per unit of time, is also accounted for, and affects the transmission between vectors and hosts. The mosquito population is regenerated by the recruitment rate r, which is assumed to be some constant proportion of eggs out

of the mosquito population that mature into adult females, which are the only mosquitos that can infect humans with dengue. The host recovery rate is γ_h, and the host and vector death rates are μ_h and μ_v, respectively. The situation is summarized in Figure 3.2, and the equations are given as

$$\begin{aligned}
\frac{dS_h}{dt} &= \mu_h N_h - \frac{\beta_h b}{N_h} S_h I_v - \mu_h S_h, \\
\frac{dI_h}{dt} &= \frac{\beta_h b}{N_h} S_h I_v - (\gamma_h + \mu_h) I_h, \\
\frac{dR_h}{dt} &= \gamma_h I_h - \mu_h R_h, \\
\frac{dS_v}{dt} &= r - \frac{\beta_v b}{N_h} S_v I_h - \mu_v S_v, \\
\frac{dI_v}{dt} &= \frac{\beta_v b}{N_h} S_v I_h - \mu_v I_v.
\end{aligned} \tag{3.3}$$

Many epidemiological dengue models are based on an extension of this model, looking at impact of travellers, temperature, stages of mosquito, predicting control measures on outbreaks [33, 68, 97]. For example, Luz et al extended the model to include both larvae and adult populations of mosquitos to analyze different control measures [68]. They found that while applying insecticide to larvae may reduce outbreaks drastically in the short term, could result in large outbreaks in the future due to resistance developing. They found the optimal and most cost-effective strategy, applying insecticide to adult population six times per year [68].

Due to the enhanced disease effects from the interactions between different strains, more recent models have taken into account multiple serotypes in a region. Two different hypotheses for enhanced disease are suspected: either susceptibllity enhancement, which assumes that individuals are more susceptible to secondary infection if they are infected with primary infection; or transmission enhacement, which assumes that the transmission rate is higher for individuals with secondary infection [7]. Although there is still controversy about which effect has more of an impact, most dengue models involving multiple serotypes assume transmission enhancement [7].

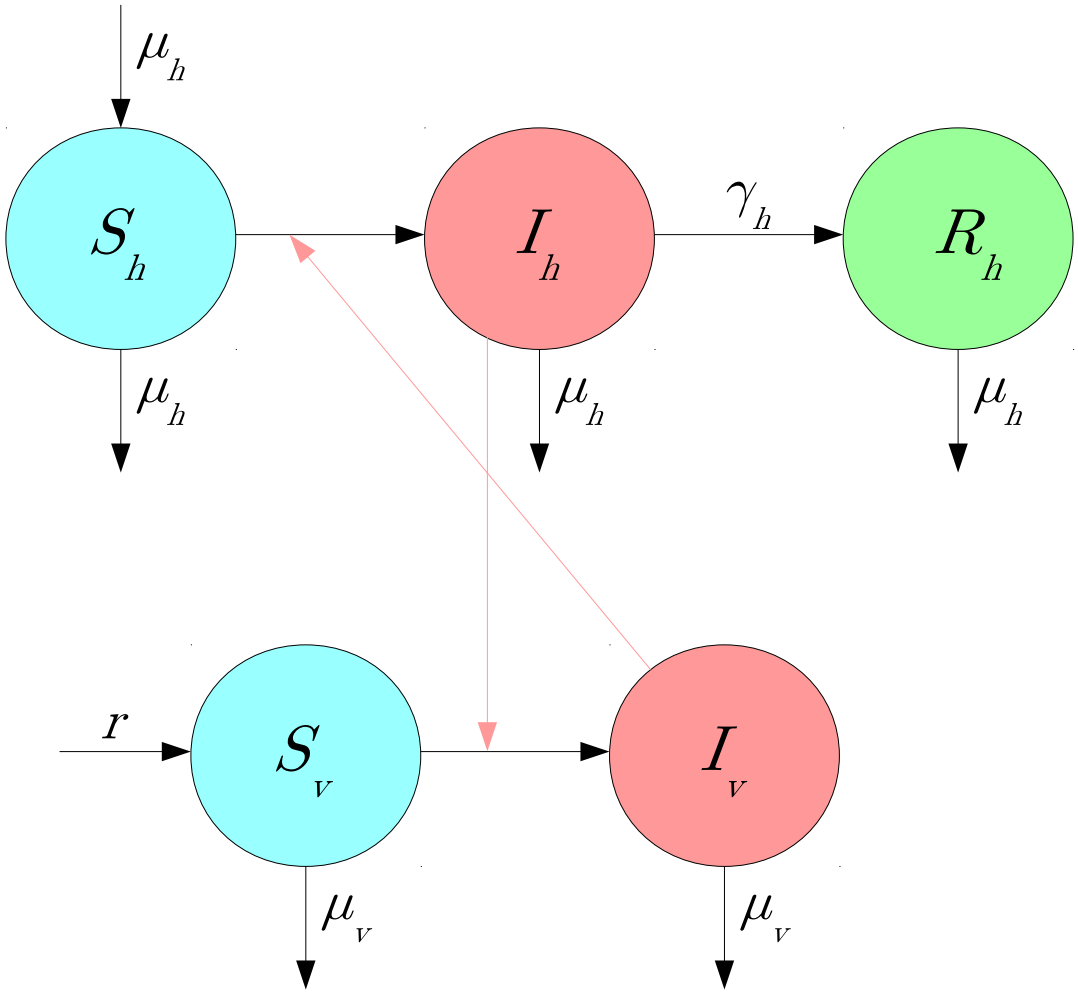

Figure 3.2: **Host-vector model.** A diagram of model (3.3), showing the interactions between susceptible (S_h), infected (I_h), and recovered (R_h) hosts, and susceptible (S_v) and infected (I_v) vectors.

Hartley et al developed a model of multiple serotypes in order to determine which parameters varied by seasonality were most impactful on outbreaks. Comparing their model with data from an outbreak in Thailand, they found that parameters such as biting rate, vector mortality, and the infectious period of hosts were the most important [50].

Dengue epidemiological models may also model the mosquito population implicitly by using models of direct contact. These models account for the mosquito population through transmission by direct contact between hosts, since individuals infect mosquitos, which then infect other individuals [34]. Billings et al used a model of this type to study the effect of transmission enhancement and cross-immunity, including vaccines protecting against a single strain and vaccines protecting against multiple strains [16]. They found that using separate vaccines to protect against each serotype would not lead to the eradication of the disease, consistent with the knowledge that a vaccine must be protective against all strains at once in order to be effective [16].

3.2 Immunological modeling background

Mathematical models can also be used to study the underlying dynamics occcurring within a single host, often involving dynamics of the pathogen load or the immune response [95]. For example, to study the interactions between target cells T, infected cells I, and virus V, we can use a model similar to the compartmental SIR model described in Equations 3.1. In this case, target cells recruit from some source at rate λ and are infected by virus at rate β, becoming infected cells, which then produce virus at rate p. Virus is cleared at rate c, and target cells and infected cells die at rates d_T and d_I, respectively. Figure 3.3 describes these

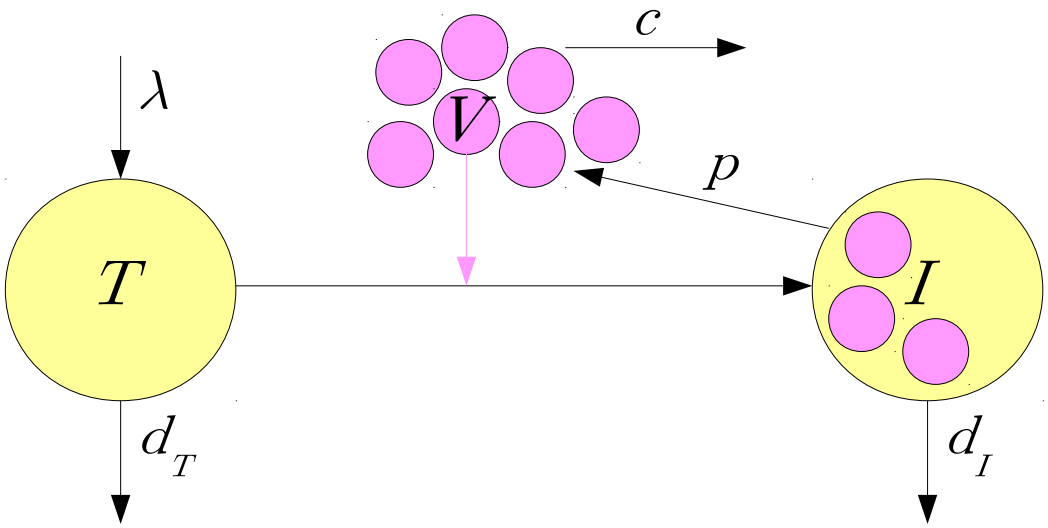

Figure 3.3: **Viral infection model.** A diagram of model (3.4), showing the interactions between target cells (T), infected cells (I), and virus (V).

interactions, which we then can use to obtain the system of differential equations,

$$\begin{aligned} \frac{dT}{dt} &= \lambda - \beta TV - d_T T, \\ \frac{dI}{dt} &= \beta TV - d_I I, \\ \frac{dV}{dt} &= pI - cV. \end{aligned} \tag{3.4}$$

Solving for the equilibria, we find there are two steady states $(\overline{T}, \overline{I}, \overline{V})$,

$$\begin{aligned} A &= \left(\frac{\lambda}{d_T}, 0, 0\right), \\ C &= \left(\frac{cd_I}{\beta p}, \frac{\beta p\lambda - cd_I d_T}{\beta p d_I}, \frac{\beta p\lambda - cd_I d_T}{\beta c d_I}\right). \end{aligned} \tag{3.5}$$

In this case, the steady states can be used to describe A, a short-term acute infection, and

C, a long-term chronic infection. It can be shown that the reproduction number

$$R_0 = \frac{\beta p \lambda}{c d_I d_T}$$

is the average number of virions produced by an infected cell. Thus, if $R_0 < 1$, A will be locally asymptotically stable (and unstable if $R_0 > 1$), meaning the virus will eventually clear from the host. However, if $R_0 > 1$, C will be locally asymptotically stable (and unstable if $R_0 < 1$), meaning a certain number of virus and infected cells will always remain in the body. The goal of drug therapy for chronic infection should thus be to reduce R_0 below this threshold.

One of the most successful uses of this model has been in the context of HIV, due to the abundance of data available, although variations of the model have been used in the context of other infections including hepatitis C, hepatitis B, and influenza [90, 94, 95, 108]. HIV is a chronic infection, which has three main stages of infection: the acute phase, the chronic phase, and the AIDS stage [63]. The above model can account for the first two stages, because during the chronic phase, the virus stays relatively constant, which is known as the set-point viral load [57]. Using the model with minor variations to account for drug therapy, the virus production and clearance rates were determined by comparing the model to patient data. Modeling results found that the half-life of virus was estimated at approximately six hours [96]. Since during the chronic phase, the virus is effectively at steady state, this means the patient must produce virus quickly as well, leading to an average estimate of 10^{10} virions produced daily [96]. Due to the rapid production and clearance of HIV, it could be shown that the virus could easily mutate and become resistant to drugs, if measures were not taken to counteract these effects [95]. Even though this model does not incorporate an immune response, it can still approximate viral dynamics during the first two stages of HIV infection, although the model may need an immune response early in infection during the acute phase to more accurately model this phase of the infection.

For certain infections, an immune system response is required to clear the infection, such

as a T cell or antibody response [95]. For example, a simple model describing T cells may include proliferation, recruitment, and death. Therefore, if T cells E proliferate at rate p_E, recruit from some source s, and die at rate d_E, this can be modeled as

$$\frac{dE}{dt} = s + p_E E - d_E E. \tag{3.6}$$

We can also distinguish between active and resting T cells. The resting T cells E_r recruit from some source s, a proportion a of resting T cells differentiate into active T cells E_a, and a proportion r of active T cells differentiate into resting T cells. Active and resting T cells proliferate and die at rates p_{E_a} and d_{E_a} and p_{E_r} and d_{E_r}, respectively. These interactions can be modeled as

$$\begin{aligned} \frac{dE_r}{dt} &= s + p_{E_r} E_r - d_{E_r} E_r - a E_r + r E_a, \\ \frac{dE_a}{dt} &= p_{E_a} E_a - d_{E_a} E_a + a E_r - r E_a. \end{aligned} \tag{3.7}$$

These models are shown in Figure 3.4, and can be incorporated into the TIV model. Models of T cells have also been used in HIV to clarify its dynamics. Experiments were unclear about whether the drop in T cells during the AIDS phase of HIV was due to high turnover rate of T cells, such that at some point the T cells were not able to sustain their killing rate of the virus [56]; or if it was due to T cell production being lowered [52]. Given that the death rate of T cells can be used as an estimate of the turnover rate of the T cell population, it was shown through estimating the parameters of the model based on experimental data, the proliferation and death rates of T cells were three times the rate of normal levels [79]. Thus, it is strongly suggested that the period of decline of T cells from the chronic phase to the AIDS phase can be described by increased T cell death, and not decreased production rate of T cells [79].

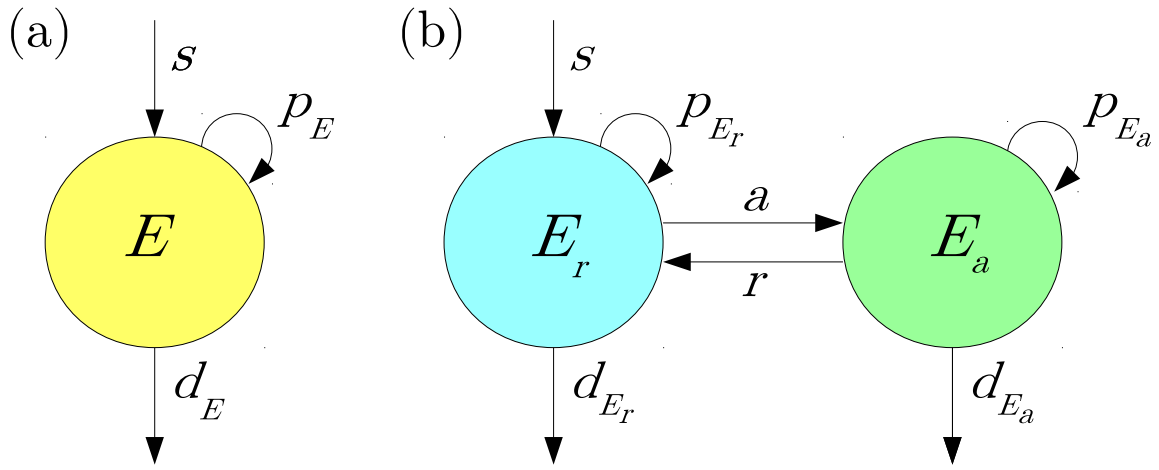

Figure 3.4: **T cell models.** (a) A diagram of model (3.6), showing the proliferation of T cells (E). (b) A diagram of model (3.7), showing the interactions between resting (E_r) and active (E_a) T cells.

3.2.1 Immunological modeling in dengue

Even with controversy over the impact of the immune response on increased disease severity in secondary infection, there have been relatively few attempts modeling the within-host dynamics of dengue. However, there has been an increase in attempts in recent years due to more data becoming available [67]. Results from vaccination studies in the future will hopefully make more data available, which can then be used in models to better understand these impacts [67]. For the models that have been developed, they mostly focus on incorporating at least one type of immune response, whether neutralizing antibodies, non-neutralizing antibodies, or T cells [11, 40, 88]. Due to the early stages of development of these models, there have been contradictory results, and it is unclear whether these are due to different data sets being used or the different models created. For example, studies found that increased disease severity was due to enhancing neutralizing antibodies [40], effects from both T cells and antibodies [11], and non-neutralizing antibody effects [88].

We briefly describe the model that we developed with Dr. Stanca Ciupe below, which incorporates both neutralizing and non-neutralizing antibody effects. This work was published in Mathematical Biosciences [88].

During primary infection, we assume target cells T are uninfected monocytes, which are produced at rate s, die at rate d_T, and become infected by dengue virus V at rate β. Infected monocytes I then die at rate $\delta > d_T$ due to toxicity induced by both the virus and immune response [70, 74]. Virus is produced at rate p and cleared at rate c. Resting B cells B become activated B cells B_a at rate α when encountering virus. Activated B cells become plasma cells P at rate k, also dependent on virus. To account for long-lived plasma cells remaining in the body, we assume plasma cells have logistic growth rate r and carrying capacity K_P. They produce antibodies A at rate N, which in turn then reduce viral infectivity at rate η (neutralizing antibody effects) and enhance viral clearance at rate γ (non-neutralizing antibody effects). Resting B cells, activated B cells, and antibodies die at rates d_B, d_{B_a}, and d_A, respectively.

We model secondary infection similar to primary infection, with the caveat that during secondary infection with a different strain V_2, both strain-specific antibodies A_2 and cross-reactive antibodies A_1 are produced. Under the assumption of antibody dependent enhancement, we model the neutralizing antibody effects by assuming the infectivity rate β_2 of secondary virus is enhanced by the presence of cross-reactive antibody and reduced by strain-specific antibodies at rate η. The non-neutralizing antibody effects of strain-specific antibody are still accounted for, as A_2 enhances viral clearance at rate γ_2. However, we assume that cross-reactive antibody renders the virus unavailable for binding by strain-specific antibody, leading to a reduction of secondary viral clearance at rate $\gamma_E A_1$.

We diagram these interactions of secondary infection in Figure 3.5, with the model equations given below. The model for primary infection can be found by ignoring I_2, V_2, A_2, B_{a_2}, P_2,

and A_2.

$$\begin{aligned}
\frac{dT}{dt} &= s - d_T T - \frac{\beta_1 T V_1}{1+\eta A_1} - \frac{\beta_2 T V_2}{1+\eta A_2}, \\
\frac{dI_i}{dt} &= \frac{\beta_i T V_i}{1+\eta A_i} - \delta I_i, \\
\frac{dV_1}{dt} &= p_1 I_1 - (c + \gamma_1 A_1) V_1, \\
\frac{dV_2}{dt} &= p_2 I_2 - (c + \gamma_2 A_2 - \gamma_E A_1) V_2, \\
\frac{dB}{dt} &= -\alpha B V_1 - \alpha B V_2 - d_B B, \\
\frac{dBa_i}{dt} &= \alpha B V_i - k B_{a_i} V_i - d_{B_a} B_{a_i}, \\
\frac{dP_i}{dt} &= r P_i \left(1 - \frac{P_i}{K_P}\right) + k B_{a_i} V_i, \\
\frac{dA_i}{dt} &= N P_i - d_A A_i,
\end{aligned} \tag{3.8}$$

where $i = 1, 2$.

Using patient data [117], we found that our model was unable to explain the data when assuming enhancement by neutralizing antibodies during secondary infection. Instead, we found that in order to successfully fit the secondary infection model, we must predict a decreased non-neutralizing antibody effect during secondary infection. One possible biological explanation for this result may be that by binding to heterologous virus, cross-reactive antibodies render the virus unavailable for removal by strain-specific antibodies. However, since this non-neutralizing effect accounts for decreased viral clearance and the virus is in quasi-equilibrium with infected cells, we could be accounting for reduced cell killing and the original antigenic sin hypothesis. Due to these results, we thus developed a new model which takes into account the T cell responses, which we describe in chapter four.

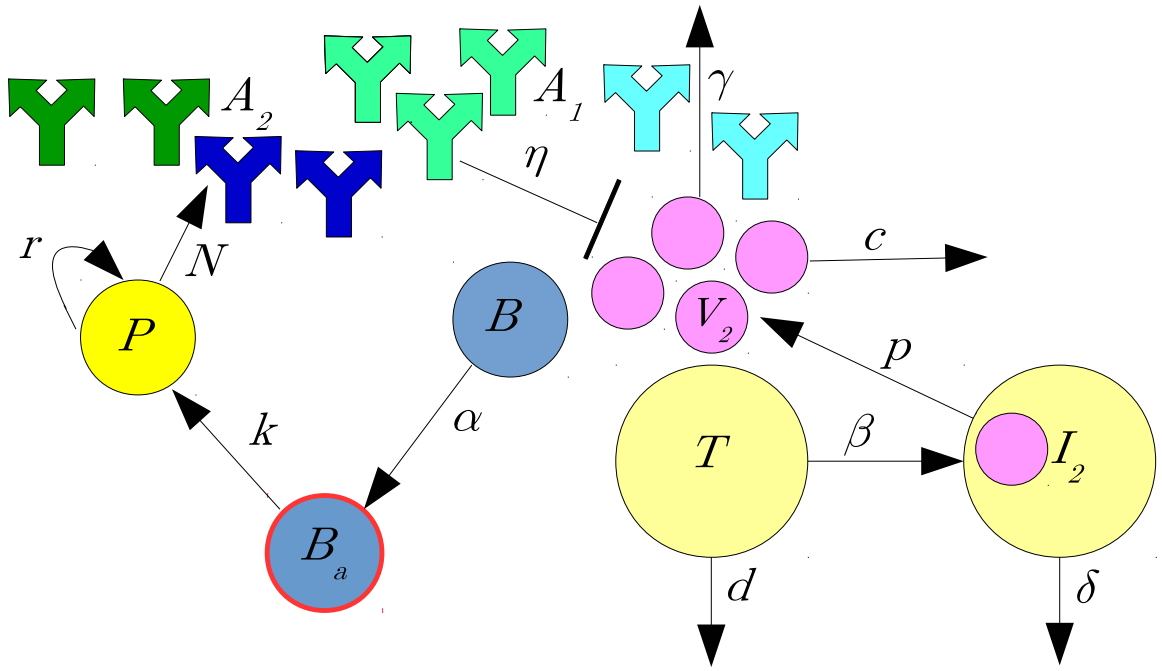

Figure 3.5: **Antibody-dependent enhancement model.** A diagram of model (3.8), showing the interaction between target cells (T), infected cells (I), virus (V), B cells (B), activated B cells (B_a), plasma cells (P), cross-reactive antibodies (A_1), and strain-specific antibodies (A_2). Neutralizing antibodies are dark green (strain-specific) or light green (cross-reactive) and non-neutralizing antibodies are dark blue (strain-specific) or light blue (cross-reactive).

3.3 Multiscale modeling background

While we have previously described models that have studied the impacts of within-host dynamics and population dynamics separately, in reality, the within-host effects often have effects on the population dynamics between hosts [49, 76]. For example, certain drug therapies for influenza have been known to lessen the period of symptoms and decrease viraemia levels [51], which could then lead to lower transmission rates for individuals on the drug therapy [66]. Thus, these drug therapies may have an important role to play in lessening the chances for influenza outbreaks, outcomes which could be tested through modeling [49]. In recent years, there has been increased interest in discovering how the effects at the within-host and between-host scales can be coupled to account for these scales affecting each other.

Within-host and between-host models are usually linked in one of two ways: either the within-host model only impacts the between-host model, or there is some feedback between the two levels. An example of the within-host model only impacting the between-host level may be during an outbreak of HIV or influenza, where the viral load correlates to the transmission rate between hosts, but this in turn does not affect within-host dynamics of getting the disease [49, 102]. Alternatively, modeling a disease transmitted by environmental spores may require feedback between the two levels, assuming the number of spores in the environment changes the inoculum size [103]. Thus, if the within-host dynamics affect the number of spores transmitted, which then affect the number of spores in the environment, which then changes the inoculum size, which then affects the within-host dynamics, both levels have a clear impact on the other [76].

Deciding how the within-host and between-host levels are linked is one of the current challenges in using coupled models. One of the simplest assumptions that can be made is that pathogen load is in some way linked to the rate of transmission, which has been shown in studies of multiple diseases including HIV and dengue viral infection [9, 85]. However, there have been relatively few studies examining whether other aspects such as infection dura-

tion, viral peak, or area under the viral load affects transmission [49]. Incorporating host symptoms may impact levels of infectiousness and shedding within the host, which may thus impact transmission [49].

We diagram an example of a coupled model in Figure 3.6 and show how it can be derived mathematically. We can first assume that the within-host dynamics are modeled by the interactions of target cells, infected cells, and virus as described in Equations (3.4), supposing they are modeled over time τ instead of time t. Using the output of this model, we can define functions $\beta(\tau)$ and $\alpha(\tau)$ that incorporate the solutions $T(\tau)$, $I(\tau)$, and/or $V(\tau)$. We then develop a between-host SI model over time t describing the interaction between susceptible individuals $S(t)$ and infected individuals $i(\tau, t)$ at time t that have been infected for time τ. We can thus use our function $\beta(\tau)$ as the transmission rate and $\alpha(\tau)$ as the loss rate of infected individuals, whether that occurs through natural mortality, disease-induced morality, or recovery. Susceptibles are birthed at rate Λ and die at rate μ. We thus write the between-host model as

$$\begin{aligned} \frac{dS(t)}{dt} &= \Lambda - \mu S(t) - S(t)\int_0^\infty \beta(\tau) i(\tau, t)\, d\tau, \\ \frac{\partial i(\tau, t)}{\partial t} &= -\frac{\partial i(\tau, t)}{\partial \tau} - \alpha(\tau) i(\tau, t), \\ i(0, t) &= S(t)\int_0^\infty \beta(\tau) i(\tau, t)\, d\tau. \end{aligned} \tag{3.9}$$

New insights can be gained into different epidemiological effects by using models similar to the one described above. Ganusov and Antia showed that making the simplifying assumption to treat recovery rate as an independent parameter may not account for all its effects, especially during vaccination [37]. While vaccination may increase recovery rate, it can also induce an immune response that can change the impact of transmission and virulence, resulting in a different evolution of disease spread than increasing recovery rate alone [37]. Other models which incorporate multiple strains of a pathogen have analyzed how within-host fitness and competition between strains within hosts can affect the overall evolution of strains [22, 69].

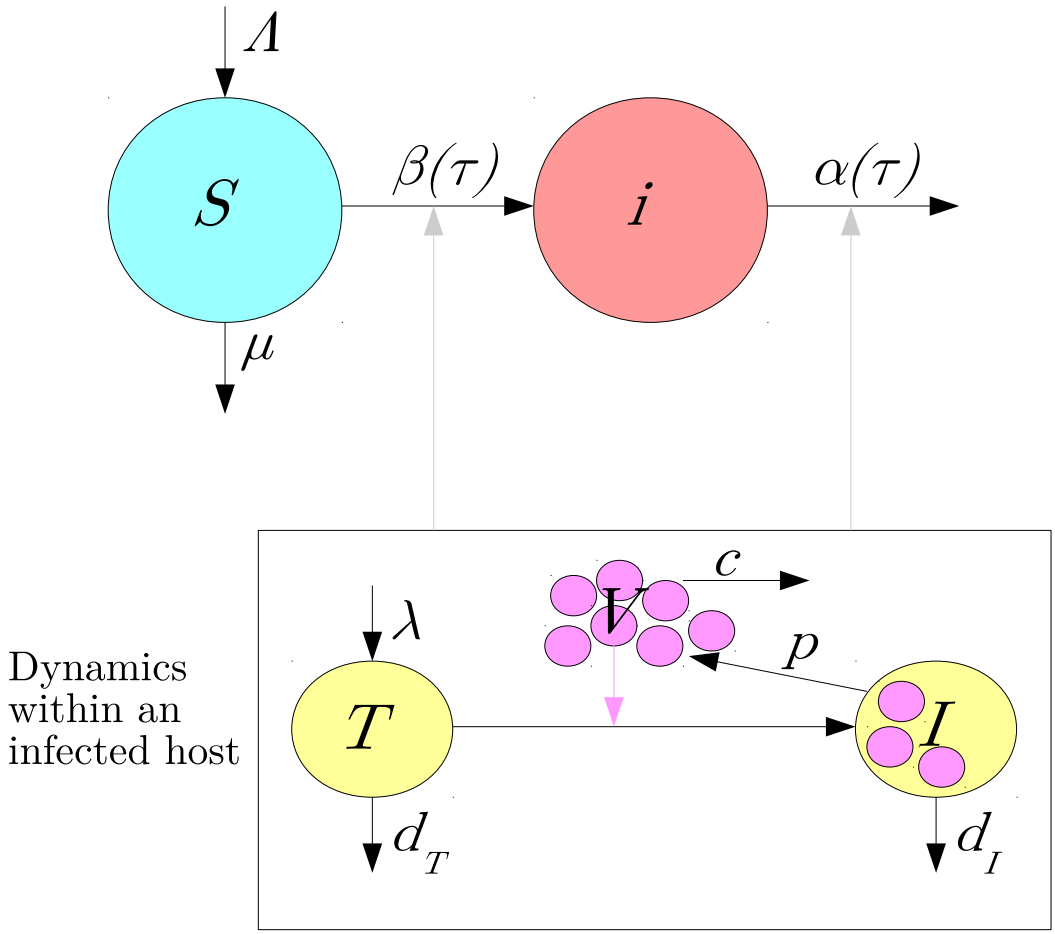

Figure 3.6: **Multiscale model.** A diagram of model (3.9), showing the interaction between susceptible (S) and infected (i) individuals. The transmission and recovery rates may depend on a model of within-host dynamics, which describes the interactions between target cells (T), infected cells (I), and virus (V).

Using results from our within-host dengue models described in Section 3.2.1 and Chapter 4, we incorporate these within-host dynamics into an epidemiological model of dengue in Chapter 5. We study the effects of within-host dynamics on the spread of dengue fever and dengue hemorrhagic fever.

3.3.1 Review of multiscale modeling in HIV

To further understand the different types of multiscale modeling used, we conducted a review of these types of models in the context of HIV with Dr. Narges Dorratoltaj, Dr. Stanca Ciupe, Dr. Stephen Eubank, and Dr. Kaja Abbas. Dr. Dorratoltaj, Dr. Abbas, and I collaborated on writing the paper; Dr. Dorratoltaj and I analyzed and reviewed the papers and created figures and tables; and Dr. Ciupe and Dr. Eubank helped in final revisions of the paper. This work has been published in PeerJ [30]. We summarize some of the results from the paper below and in Table 3.1.

Linking mechanisms

The potential for transmission between HIV+ individuals to susceptibles is affected by the viral load of infected hosts [9]. In all the models that we analyzed in this review, the transmission rate between hosts is dependent on the within-host viral load. We categorize the models into those where the transmission rate is a function of viral load and those where the equilibria of the within-host model are used to determine the transmission rate.

The within-host and between-host scales of HIV immunoepidemiological models are coupled by basing the transmission rate on the time-varying viral load since infection. The viral load (and thus the transmission rate) is high during the acute and AIDS stages of HIV infection while being low during the chronic stage [57, 26]. Unlike the basic SI epidemiological model that assumes constant transmission rate β, the between-host model assigns time-varying transmission rate, which is dependent on the non-linear viral immune dynamics of HIV in

the within-host model.

In some models, the transmission rate depends on the viral load continuously over time [105, 72, 102]. Saenz and Bonhoeffer also distinguished between drug-resistant and drug-sensitive strains and their corresponding impact on the transmission rate [102]. Martcheva and Li made the death of infected individuals depend on the viral load over time, since the AIDS stage is associated with high viral load [72].

In the context of HIV evolution, while the transmission rate varies through time depending on the viral load, the viral load is also modeled to distinguish between different strains [29, 69]. The transmission rate depends on a predefined infectivity profile which changes depending on the stage of infection, and the frequency of the different viral strains in an infected population. Doekes et al made the transmission rate depend on the frequency of viral strains that were only in actively infected CD4+ T cells [29].

The within-host viral load can be used to individualize the transmission rate over time [125, 107]. The CD4+ T cell count can also be used to determine the stage of infection [125].

Another method of linking the within-host and between-host scales is to use the within-host model to determine an equilibrium for the viral load. This equilibrium can then be used as a constant parameter in the between-host model, which can then be analyzed further by differing the parameters of the within-host model [75, 24]. Cuadros and García-Ramos accounted for the amplified viral load due to co-infection and the corresponding increase in HIV transmission rate [24]. Metzger et al determined the differing viral loads associated with HIV and therapeutic infecting particles, and their effect on the transmission probabilities between infected populations [75].

Clinical and public health implications

Clinical studies have shown that HIV has evolved an intermediate level of virulence at the within-host level that optimizes the transmission potential of the virus at the population

level [35]. However, at the within-host level, HIV can evolve quickly [63], virulence increases during the course of the infection [60], and infections with higher replicative capacities have higher virulence [60]. Replicative capacities also increase over the course of infection, albeit slowly [60]. Because of this behavior of HIV at the within-host level, it might be expected that HIV would evolve a high virulence at the within-host level, even if it did not optimize the transmission potential at the population level. To understand these seemingly contradictory results, immunoepidemiological models were used, which incorporated these behaviors of HIV at the within-host level [69, 29]. The model developed by Lythgoe et al found that small rates of within-host evolution optimize the transmission potential at the population level, whereas higher rates of within-host evolution lead to high levels of virulence, but lower transmission potential [69]. Lythgoe et al suggest that the clinical observations seen in HIV may be a result of a within-host fitness landscape that is complex to traverse, since this leads to smaller rates of within-host evolution [69]. They also suggest the effect of the adaptive immune response may play a role in explaining the observed behavior [69]. Based off the results from Lythgoe et al, a similar model was constructed by Doekes et al, which included a latent reservoir of CD4+ T cells at the within-host level [29]. They found that this latent reservoir may be responsible for delaying the evolutionary dynamics at the within-host level, which then leads to the transmission potential being optimized [29].

While there is uncertainty over the timing of initiating antiretroviral therapy (ART), some studies have suggested there may be benefits to beginning treatment early [121, 21]. Experimental studies also suggest that because ART reduces transmissibility, increasing coverage levels may reduce the prevalence of HIV [21]. However, drug-resistant strains can emerge, which can lead to treatment failure [58, 48]. Immunoepidemiological models were used to understand these effects of ART, focusing on treatment timing [107, 125], coverage levels [105], and drug resistance [102, 107]. The models showed that in general, initiating treatment early [125, 107], increasing coverage [105, 102], and increasing effectiveness of ART [105, 102] reduces the prevalence of HIV.

However, in certain cases, increases in the prevalence of HIV may occur even with early

treatment initiation, increased coverage, and increased effectiveness of ART to drug-sensitive strains. Models showed that as ART coverage levels increase, the prevalence of drug-resistant strains increase, which cause an increase in HIV prevalence [102]. Prevalence can also increase if drug-resistant strains cause the drug efficacy to decrease significantly [107]. These results imply that there may be an optimal therapy coverage level that will minimize the number of infections [102]. Therefore, in these cases, the models suggest that HIV prevalence can be reduced by focusing efforts on decreasing the risk of drug resistance emergence [102].

Clinical studies have observed that under certain conditions, the prevalence of HIV increases when ART coverage levels increase [126]. Zaidi et al hypothesize that since ART reduces viral load, patients may live longer, and thus have the ability to infect more people [126]. Immunoepidemiolgical models also observed this effect [105], including a model of super-infection [72]. Both model outcomes are consistent with the hypothesis of Zaidi et al, since the models find that the increased prevalence is due solely to decreases in viral load [105, 72]. The model developed by Shen et al found that this effect can be minimized if drug effectiveness is high [105].

Clinical trials have shown that therapeutic interfering particles (TIPs) have the potential to reduce within-host viral load [64] and transmit between hosts [1]. Experimental studies have also shown that HIV transmission rates between hosts depend on the within-host viral load [35]. Based on these assumptions, an immunoepidemiological model is developed, which deploys TIPs to a small proportion (1%) of the population [75]. The effect on HIV prevalence due to deploying TIPs is compared to deploying ART and to deploying a hypothetical HIV vaccine. When TIPs have the ability to transmit between hosts, the model shows deploying TIPs reduces HIV prevalence to lower levels than deploying ART therapy or deploying vaccines. However, the model shows that if TIPs do not have the ability to transmit between hosts, then there is minimal effect on the reduction of HIV prevalence [75]. While more study of TIPs is needed, TIPs have the potential to be an effective therapy than either ART or vaccines.

Experimental studies suggest that co-infection may be responsible for increases seen in set-point viral load (spVL) at the within-host level over time [78]. These increases due to co-infection vary substantially within-host [61]. Also, the concentrations of co-infection in high-risk groups versus low-risk groups may affect how HIV spreads in the general population [2]. To study the mechanisms responsible for these effects of co-infection, an immunoepidemiological model was developed [24]. They found that populations with higher spVL lead to higher increases in viral load due to co-infection, whereas populations with lower spVL leads to lower increases in viral load due to co-infection. This leads to a greater chance of co-infection increasing the prevalence of HIV in populations with high average spVL [24]. Therefore, the effects of co-infection may be mitigated by identifying the viral factors that can reduce the spVL in the population.

Table 3.1: **Characteristics of HIV multiscale modeling studies.** The study topic, objective, model implementation, linking mechanism between within-host and between-host models, and inferences of the studies included in the review are summarized.

Study	Topic	Objective	Implementation	Linking Mechanism	Inferences
[72]	Super-infection	How does HIV super-infection affect population dynamics?	Partial differential equations	Transmission rate between hosts and death rate of individuals depend on viral load within host over time.	In certain cases, decreasing viral load can cause higher prevalence of HIV since infected individuals may live longer; oscillations at population level do not occur in superinfection, contrasting previous studies that did not use linked models.
[102]	Drug resistance	How do the dynamics of drug-sensitive and drug-resistant HIV strains within hosts affect the prevalence of drug-resistant strains in the population?	Partial differential equations	Transmission rate between hosts depends on viral load within host over time.	Increasing early initiation and coverage decreases total prevalence upto an optimal treatment coverage level but increases incidence and prevalence of drug resistant infections; above the optimal treatment coverage level, number of infections may not decrease in the long term and can even increase.

Study	Topic	Objective	Implementation	Linking Mechanism	Inferences
[69]	Evolution	How does competition between strains within-host affect evolution of HIV virulence?	Integro-differential equations with delay	Strain-specific infectivity rate between hosts depends on frequency of strains within-host.	Small rates of within-host evolution modestly increase HIV virulence while maximizing transmission potential; high rates of within-host evolution largely increase HIV virulence but lower transmission potential.
[29]	Evolution	How does latent reservoir of infected CD4+ T cells affect the types of strains of HIV that will evolve within and between hosts?	Integro-differential equations with delay	Strain-specific infectivity rate between hosts depends on frequency of strain in actively infected CD4+ T cells within-host.	Relatively large latent reservoirs cause delay to within-host evolutionary processes, which select for moderately virulent strains that optimize transmission at the population level; with no reservoir, highly virulent strains are selected for within-host that do not optimize transmission at the population level.
[24]	Co-infection	How does co-infection affect the HIV replication capacity?	Ordinary differential equations	Transmission rate between hosts depends on steady-state of viral load within host.	Impact of co-infection increases as average set-point viral load of population increases.
[125]	ART	How does the timing of antiretroviral therapy (ART) in individuals affect the spread of HIV?	Individual-based model	Transmission rate to each susceptible partner depends on viral load of infected individual.	Beginning ART during acute infection is most effective for reducing spread of HIV.
[105]	ART	How does antiretroviral therapy (ART) affect HIV prevalence?	Partial differential equations	Transmission rate depends on saturated viral load within-host, and varies between stages of infection.	While ART decreases the viral load and infectiousness of each infected host, in certain cases, this can lead to higher spread of HIV throughout the population because these infected individuals live longer; HIV can still be controlled in these cases if drug effectiveness is high.
[107]	ART	How does antiretroviral therapy (ART) affect HIV prevalence?	Individual-based model	Transmission rate to each susceptible partner depends on viral load of infected individual.	Initiating ART early causes lower transmission of HIV in population; however, when ART efficacy decreases with emergence of drug resistance, early treatment leads to higher HIV spread in the population because the prevalence of drug resistant strains increases rapidly.

Study	Topic	Objective	Implementation	Linking Mechanism	Inferences
[75]	TIPs	How does introduction of therapeutic interfering particles (TIPs) affect HIV prevalence?	Ordinary differential equations	Transmission rate between hosts depends on steady-states of TIP and HIV viral loads within-host.	Deploying TIPs in even small numbers of infected individuals reduces the prevalence of HIV to low levels due to TIPs' ability to transmit between hosts and target high-risk groups; using TIPs reduces challenges of antiretroviral therapy and vaccines, and complements them.

Chapter 4

Modeling Original Antigenic Sin in Dengue Viral Infection

In previous work, further described in Section 3.2.1, we developed a within-host model of dengue viral infection, using ordinary differential equations, for the interactions between target cells, infected cells, virus, B cells, plasma cells, and antibodies [88]. We included both neutralizing antibody effects, which reduce viral infectivity, and non-neutralizing antibody effects, which enhance the clearance of the virus. We first determined parameters which allowed the model to match the dynamics of dengue primary infection, and then used clinical data [117] to parameterize the changes between primary and secondary infections. We found that in order to fit the secondary infection model to data, we must predict a decreased non-neutralizing antibody effect during secondary infection. Since this effect accounts for decreased viral clearance and the virus is in quasi-equilibrium with infected cells, we could be accounting for reduced cell killing and the original antigenic sin hypothesis. We thus developed a new model which takes into account the T cell responses.

This work was done under the guidance of Dr. Stanca Ciupe and has been published in Mathematical Medicine and Biology [89]. Parts of the manuscript have been modified for this dissertation.

4.1 Abstract

Cross-reactive T cell responses induced by a primary dengue virus infection may contribute to increased disease severity following heterologous infections with a different virus serotype in a phenomenon known as the original antigenic sin. In this study, we developed and analyzed in-host models of T cell responses compared to primary and secondary dengue virus infections that considered the effect of T cell cross-reactivity in disease enhancement. We fit the models to published patient data and showed that the overall infected cell killing is similar in dengue heterologous infections, resulting in dengue fever and dengue hemorrhagic fever. The contribution to overall killing, however, is dominated by non-specific T cell responses during the majority of secondary dengue hemorrhagic fever cases. By contrast, more than half of secondary dengue fever cases have predominant strain-specific T cell responses with high avidity. These results support the hypothesis that cross-reactive T cell responses occur mainly during severe disease cases of heterologous dengue virus infections.

4.2 Introduction

There are currently two competing hypotheses for the mechanisms behind increased disease severity during secondary heterologous infections: the antibody dependent enhancement (ADE) and the original antigenic sin (OAS). The ADE hypothesis proposes that, during secondary heterologous infections, antibodies specific to the primary infection bind to the secondary virus but cannot neutralize it [122, 42, 81, 46, 116, 23]. Instead, phagocytes recruited to clear the virus-antibody immune complexes internalize non-neutralized virus and become infected in the process [114, 122, 98]. This leads to increased infectivity and, potentially, to increased disease severity.

The OAS hypothesis proposes that cross-reactive CD4 and CD8 T cells specific to the original virus serotype dominate the overall T cell immune responses during secondary heterologous

virus infections [120, 47, 70, 74, 80, 101]. These lower avidity cross-reactive T cells, inefficient in removing infected cells, outcompete the higher avidity T cells specific to the new serotype. Their function is altered with an increased production of pro-inflammatory cytokines contributing to severe dengue pathogenesis [80]. Moreover, the observed disease enhancement due to OAS in the adult population [77] is correlated with weak patient and HLA-specific T cell responses [118, 120]. The OAS hypothesis, however, is contradicted by several studies. It has been shown that T cell responses can offer protection in the general population [118], that heterologous T cell responses are not needed for disease enhancement in children [86], and that peak CD8 T cell responses do not correlate with capillary leakage in children with DHF [31].

To address the role of T cells during secondary heterologous infections we develop, analyze and compare to data mathematical models of T cell responses during primary and secondary dengue infections. Mathematical models of dengue infections have focused on the efficacy of the dengue vaccine [55, 23] on the transmission and severity of heterologous infections at the population levels [84] and on the role of antibody dependent enhancement at the in-host level [88, 20, 11, 91]. To address the role of ADE, we recently developed an in-host model of both neutralizing and non-neutralizing antibody responses during heterologous dengue virus infections. We found that, during secondary heterologous infections, cross-reactive non-neutralizing antibodies bind the heterologous virus and render it unavailable for binding and subsequent removal by strain-specific antibodies through antibody-dependent cell-mediated viral inhibition (ADCVI) and/or antibody-dependent cell-mediated cytotoxicity (ADCC) [88]. Such a decrease in the non-neutralizing effects during secondary infections may, in fact, be attributed to a decrease in the strength of T cell responses during secondary infections due to OAS. In this study, we investigate this hypothesis by developing mathematical models of T cell responses during primary and secondary dengue infections. By comparing our models to published DF and DHF adult patient data [20, 117], we predict that T cell responses are delayed and non-specific during the majority of DHF cases, but strain-specific in more than half of the DF cases, suggesting that the original antigenic sin may correlate with disease

severity.

The paper is structured as follows. In Section 4.3, we develop models of T cell responses to primary and secondary heterologous dengue virus infection, which includes both strain-specific and cross-reactive T cells. In Section 4.4, we present analytical results regarding the stability of our models and numerical results from fitting the models to published adult primary DF, secondary DF and secondary DHF patient data. In particular, we use the estimates to determine the role of cross-reactive T cell responses in disease enhancement. We conclude in Section 4.5 with a discussion.

4.3 Model development

4.3.1 Primary infections

We model T cell mediated immune responses to the primary dengue virus infection as follows. We assume that the virus strain, V, interacts with susceptible monocytes, T, at rate β, producing infected monocytes, I. Infected cells produce p virions per day, die daily at rate δ, and are killed by T cells, E, at rate μ. In the absence of infection, there are s_E/d_E dengue specific T cells available, with s_E being the source (from thymus) and d_E being the per capita death rate. When a naive T cell population encounters infected cells I, it starts expanding at rate ϕ to produce effector cells specific to the virus, E. We assume that the expansion is delayed τ days and model this by the term $\phi E(t-\tau)I(t-\tau)$. The delay of τ days accounts for the length of time it takes naive T cells before they become dengue specific, E. Finally, virus has a natural decay rate of c. These interactions are modeled by the following system

of delay differential equations.

$$\begin{aligned}
\frac{dT}{dt} &= -\beta TV, \\
\frac{dE}{dt} &= s_E + \phi E(t-\tau)I(t-\tau) - d_E E, \\
\frac{dI}{dt} &= \beta TV - \mu EI - \delta I, \\
\frac{dV}{dt} &= pI - cV,
\end{aligned} \tag{4.1}$$

with constant history for the initial conditions

$$T(0) = T_0 > 0, E(t) = E_0 > 0, I(t) = I_0 > 0, V(0) = V_0 > 0, \tag{4.2}$$

where $-\tau \leq t \leq 0$ and $E_0 = \frac{s_E}{d_E}$. We refer to time $t = 0$ as the time of virus detection.

4.3.2 Secondary infections

During secondary infections, heterologous virus, V_2, infects target monocytes, T, at the same rate β, giving rise to infected monocytes, I_2. Population I_2 produces p virions per day, dies at per capita rate δ, and is removed through killing. During heterologous infections, it has been reported that non-specific, cross reactive T cells respond faster to secondary infections than strain-specific T cells, but they are less efficient in removing the infected cells [101]. We assume that there are both non-specific and strain-specific T cell responses against the heterologous strain, namely E_1, the non-specific response generated in the primary infection (previously the E variable), and the V_2-specific T cell response, E_2. We model them as follows. We assume that both non-specific and strain-specific T cells, E_1 and E_2, are at levels s_E/d_E in the absence of infection, with s_E being the source and d_E the per capita death rate. We model this by assuming the expansion of the effector population E_2 at rate $\phi_2 I_2(t-\tau_1)E_2(t-\tau_1)$, τ_1 days after the interaction between infected cells I_2 and E_2. Moreover, the population E_1 expands at rate $\phi_1 I_2(t-\tau_2)E_1(t-\tau_2)$, τ_2 days after the interaction between

infected cells I_2 and E_1. Here, $\phi_2 \neq \phi_1$. Thus, cross-reactive T cells respond faster to secondary infections if $\phi_1 > \phi_2$. For mathematical simplicity, we assume $\tau_1 = \tau_2 = \tau$. Moreover, non-specific and strain-specific T cells remove I_2 at rates $\eta I_2 E_1$ and $\mu I_2 E_2$, with $\eta \neq \mu$. If non-specific T cell responses are dominant and inefficient, we would expect that $\phi_1 > \phi_2$ and $\eta < \mu$. Finally, V_2 has a natural decay rate of c as in (4.1). We can ignore populations I_1 and V_1, representing the infected cells and virus associated with primary infection, which we assume are cleared at the time of secondary heterologous infection. Because of this, we also assume that target cells have rebounded to their pre-infection levels at the start of secondary infection. The model describing this is:

$$\begin{aligned}
\frac{dT}{dt} &= -\beta T V_2, \\
\frac{dE_1}{dt} &= s_E + \phi_1 E_1(t-\tau) I_2(t-\tau) - d_E E_1, \\
\frac{dE_2}{dt} &= s_E + \phi_2 E_2(t-\tau) I_2(t-\tau) - d_E E_2, \\
\frac{dI_2}{dt} &= \beta T V_2 - \mu E_2 I_2 - \eta E_1 I_2 - \delta I_2, \\
\frac{dV_2}{dt} &= p I_2 - c V_2,
\end{aligned} \tag{4.3}$$

with constant history for the initial conditions

$$T(0) = T_0 > 0, E_1(t) = E_0 > 0, E_2(t) = E_0 > 0, I_2(t) = I_0 > 0, V_2(0) = V_0 > 0, \tag{4.4}$$

where $-\tau \leq t \leq 0$, $E_0 = \dfrac{s_E}{d_E}$, and $t = 0$ is the time of detection of heterologous virus strain V_2.

4.4 Results

Analytical results show that both models (4.1) and (4.3) have viral clearance hyperplanes of steady states:

$$S_1 = \left(\overline{T}, \frac{s_E}{d_E}, 0, 0\right), \tag{4.5}$$

and

$$S_2 = \left(\overline{T}, \frac{s_E}{d_E}, \frac{s_E}{d_E}, 0, 0\right), \tag{4.6}$$

respectively, where $\overline{T}$ can be any positive number. These states are globally asymptotically stable for any delay τ, which we prove below. We will then use these models and temporal viral data from primary and secondary infected patients to numerically investigate virus and T cell dynamics for specific dengue cases.

4.4.1 Analysis of the primary infection model

We perform global stability analysis of the system (4.1) for $\tau = 0$ and $\tau > 0$. System (4.1) has a viral clearance hyperplane of steady states:

$$S_1 = \left(\overline{T}, \frac{s_E}{d_E}, 0, 0\right), \tag{4.7}$$

where $\overline{T}$ can be any positive number.

Proposition 4.4.1. *For system (4.1) with $\tau = 0$, the hyperplane S_1 is globally attracting.*

Proof. As in [27, 18, 93], we consider the following Lyapunov functional:

$$W(t) = \frac{\phi}{\mu}\int_{\overline{T}}^{T(t)} dr + \int_{s_E/d_E}^{E(t)} \left(1 - \frac{s_E}{d_E r}\right) dr + \frac{\phi}{\mu}\int_0^{I(t)} dr + \frac{\delta\phi}{p\mu}\int_0^{V(t)} dr. \tag{4.8}$$

Since all parameters and variables are positive, $W(t) \geq 0$ and $W(t) = 0$ if and only if

$T(t) = \overline{T}$, $E(t) = \dfrac{s_E}{d_E}$, $I(t) = 0$ and $V(t) = 0$. For notational simplicity, we assume T, E, I, and V are functions of t such that $T = T(t)$, $E = E(t)$, $I = I(t)$, and $V = V(t)$. Moreover,

$$\begin{aligned}\frac{dW}{dt} &= \frac{\phi}{\mu}\left(\frac{dT}{dt}\right) + \left(1 - \frac{s_E}{d_E E}\right)\left(\frac{dE}{dt}\right) + \frac{\phi}{\mu}\left(\frac{dI}{dt}\right) + \frac{\delta\phi}{p\mu}\left(\frac{dV}{dt}\right) \\ &= -\frac{\phi s_E}{d_E} I - \frac{c\delta\phi}{\mu p} V - \left(\frac{s_E}{d_E E} - 1\right)^2 d_E E \leq 0,\end{aligned} \tag{4.9}$$

and $\dfrac{dW}{dt} = 0$ if and only if $(T, E, I, V) = \left(\overline{T}, \frac{s_E}{d_E}, 0, 0\right)$. Therefore, $\{S_1\}$ is the maximal invariant set where $\dfrac{dW}{dt} = 0$ and, by LaSalle's invariance principle, S_1 is globally attracting.

□

Proposition 4.4.2. *For system (4.1) with $\tau > 0$, the hyperplane S_1 is globally attracting.*

Proof. Consider the Lyapunov functional:

$$\begin{aligned}W(t) = \frac{\phi}{\mu}\int_{\overline{T}}^{T(t)} dr + \int_{s_E/d_E}^{E(t)} \left(1 - \frac{s_E}{d_E r}\right) dr + \frac{\phi}{\mu}\int_0^{I(t)} dr \\ + \frac{\delta\phi}{p\mu}\int_0^{V(t)} dr + \phi\int_{t-\tau}^{t} E(r)I(r)\, dr.\end{aligned} \tag{4.10}$$

Note that since all parameters and variables are positive, we have $W(t) \geq 0$. Also, $W(t) = 0$ if and only if $T(t) = \overline{T}$, $E(t) = \dfrac{s_E}{d_E}$, $I(t) = 0$ and $V(t) = 0$. For notational simplicity, we write $T = T(t)$, $E = E(t)$, $I = I(t)$, and $V = V(t)$. Moreover,

$$\begin{aligned}\frac{dW}{dt} &= \frac{\phi}{\mu}\left(\frac{dT}{dt}\right) + \left(1 - \frac{s_E}{d_E E}\right)\left(\frac{dE}{dt}\right) + \frac{\phi}{\mu}\left(\frac{dI}{dt}\right) + \frac{\delta\phi}{p\mu}\left(\frac{dV}{dt}\right) \\ &\quad + \phi(E(t)I(t) - E(t-\tau)I(t-\tau)) \\ &= -\frac{\phi s_E}{d_E}\frac{E(t-\tau)I(t-\tau)}{E} - \frac{c\delta\phi}{\mu p} V - \left(\frac{s_E}{d_E E} - 1\right)^2 d_E E \leq 0,\end{aligned} \tag{4.11}$$

for all $t \geq 0$ and $\dfrac{dW}{dt} = 0$ if and only if $(T, E, I, V) = \left(\overline{T}, \frac{s_E}{d_E}, 0, 0\right)$. Therefore, $\{S_1\}$ is the maximal invariant set where $\dfrac{dW}{dt} = 0$ and, by LaSalle's invariance principle, S_1 is globally

attracting. □

4.4.2 Analysis of the secondary infection model

We perform global stability analysis of the system (4.3) for $\tau = 0$ and $\tau > 0$. System (4.1) Since all parameters and variables are positive, we are only interested in the asymptotic stability of the clearance hyperplane

$$S_2 = \left(\overline{T}, \frac{s_E}{d_E}, \frac{s_E}{d_E}, 0, 0\right), \tag{4.12}$$

where $\overline{T}$ can be any positive number.

Proposition 4.4.3. *For system (4.3) with $\tau = 0$, the hyperplane S_2 is globally attracting.*

Proof. Consider the following Lyapunov functional:

$$\begin{aligned} W(t) = \frac{\phi_1\phi_2(\mu+\eta)}{\mu\eta}\int_{\overline{T}}^{T(t)} dr + \phi_2\int_{s_E/d_E}^{E_1(t)}\left(1-\frac{s_E}{d_E r}\right)dr + \phi_1\int_{s_E/d_E}^{E_2(t)}\left(1-\frac{s_E}{d_E r}\right)dr \\ + \frac{\phi_1\phi_2(\mu+\eta)}{\mu\eta}\int_0^{I_2(t)} dr + \frac{\phi_1\phi_2\delta}{p\mu}\int_0^{V_2(t)} dr. \end{aligned} \tag{4.13}$$

For notational simplicity, we let $T = T(t)$, $E_1 = E_1(t)$, $E_2 = E_2(t)$, $I_2 = I_2(t)$, and $V_2 = V_2(t)$. Note that $W(t) = 0$ if and only if $(T, E_1, E_2, I_2, V_2) = \left(\overline{T}, \frac{s_E}{d_E}, \frac{s_E}{d_E}, 0, 0\right)$ and $W(t) > 0$ otherwise since all parameters and variables are positive. Moreover,

$$\begin{aligned} \frac{dW}{dt} &= \frac{\phi_1\phi_2(\mu+\eta)}{\mu\eta}\left(\frac{dT}{dt}\right) + \phi_2\left(1-\frac{s_E}{d_E E_1}\right)\left(\frac{dE_1}{dt}\right) + \phi_1\left(1-\frac{s_E}{d_E E_2}\right)\left(\frac{dE_2}{dt}\right) \\ &\quad + \frac{\phi_1\phi_2(\mu_+\eta)}{\mu\eta}\left(\frac{dI_2}{dt}\right) + \frac{\phi_1\phi_2\delta}{p\mu}\left(\frac{dV_2}{dt}\right) \\ &= -2\frac{\phi_1\phi_2 s_E}{d_E}I_2 - \frac{\phi_1\phi_2\eta}{\mu}E_1I_2 - \frac{\phi_1\phi_2\mu}{\eta}E_2I_2 - \frac{\phi_1\phi_2 s_E}{d_E}I_2 - \frac{\phi_1\phi_2\delta}{\eta}I_2 \\ &\quad - \frac{\phi_1\phi_2 c\delta}{p\mu}V_2 - \phi_1\left(\frac{s_E}{d_E E_2}-1\right)^2 d_E E_2 - \phi_2\left(\frac{s_E}{d_E E_1}-1\right)^2 d_E E_1 \leq 0 \end{aligned} \tag{4.14}$$

and $\dfrac{dW}{dt} = 0$ if and only if $(T, E_1, E_2, I_2, V_2) = \left(\overline{T}, \dfrac{s_E}{d_E}, \dfrac{s_E}{d_E}, 0, 0\right)$. Then $\{S_2\}$ is the maximal invariant set where $\dfrac{dW}{dt} = 0$ and, by LaSalle's invariance principle, S_2 is globally attracting.

□

Proposition 4.4.4. *For system (4.3) with $\tau > 0$, the hyperplane S_2 is globally attracting.*

Proof. Consider the following Lyapunov functional:

$$\begin{aligned} W(t) = {} & \frac{\phi_1\phi_2(\mu+\eta)}{\mu\eta}\int_{\overline{T}}^{T(t)} dr + \phi_2\int_{s_E/d_E}^{E_1(t)}\left(1-\frac{s_E}{d_E r}\right)dr + \phi_1\int_{s_E/d_E}^{E_2(t)}\left(1-\frac{s_E}{d_E r}\right)dr \\ & + \frac{\phi_1\phi_2(\mu+\eta)}{\mu\eta}\int_0^{I_2(t)} dr + \frac{\phi_1\phi_2\delta}{p\mu}\int_0^{V_2(t)} dr \\ & + \phi_1\phi_2\int_{t-\tau}^{t}(E_1(r)I_2(r) + E_2(r)I_2(r))\,dr. \end{aligned} \tag{4.15}$$

For notational simplicity, we let $T = T(t)$, $E_1 = E_1(t)$, $E_2 = E_2(t)$, $I_2 = I_2(t)$, and $V_2 = V_2(t)$. Note that $W(t) = 0$ if and only if $(T, E_1, E_2, I_2, V_2) = \left(\overline{T}, \dfrac{s_E}{d_E}, \dfrac{s_E}{d_E}, 0, 0\right)$ and $W(t) > 0$ otherwise since all parameters and variables are positive. Moreover,

$$\begin{aligned} \frac{dW}{dt} = {} & \frac{\phi_1\phi_2(\mu+\eta)}{\mu\eta}\left(\frac{dT}{dt}\right) + \phi_2\left(1-\frac{s_E}{d_E E_1}\right)\left(\frac{dE_1}{dt}\right) + \phi_1\left(1-\frac{s_E}{d_E E_2}\right)\left(\frac{dE_2}{dt}\right) \\ & + \frac{\phi_1\phi_2(\mu+\eta)}{\mu\eta}\left(\frac{dI_2}{dt}\right) + \frac{\phi_1\phi_2\delta}{p\mu}\left(\frac{dV_2}{dt}\right) + \phi_1\phi_2(E_1(t)I_2(t) + E_2(t)I_2(t)) \\ & - \phi_1\phi_2(E_1(t-\tau)I_2(t-\tau) + E_2(t-\tau)I_2(t-\tau)) \\ = {} & -\frac{\phi_1\phi_2\eta}{\mu}E_1I_2 - \frac{\phi_1\phi_2\mu}{\eta}E_2I_2 - \frac{\phi_1\phi_2\delta}{\eta}I_2 - \frac{\phi_1\phi_2 c\delta}{p\mu}V_2 \\ & - \frac{\phi_1\phi_2 s_E}{d_E}\left(\frac{E_1(t-\tau)}{E_1} + \frac{E_2(t-\tau)}{E_2}\right)I_2(t-\tau) \\ & - \phi_1\left(\frac{s_E}{d_E E_2} - 1\right)^2 d_E E_2 - \phi_2\left(\frac{s_E}{d_E E_1} - 1\right)^2 d_E E_1 \le 0 \end{aligned} \tag{4.16}$$

and $\dfrac{dW}{dt} = 0$ if and only if $(T, E_1, E_2, I_2, V_2) = \left(\overline{T}, \dfrac{s_E}{d_E}, \dfrac{s_E}{d_E}, 0, 0\right)$. Then $\{S_2\}$ is the maximal invariant set where $\dfrac{dW}{dt} = 0$ and, by LaSalle's invariance principle, S_2 is globally attracting.

□

4.4.3 Parameter values

We assume that $t = 0$ corresponds to the day of virus detection. Initially, there are $T_0 = 10^7$ uninfected monocytes per ml [20], $V_0 = 357$ virus RNA per ml [117], $E_0 = 60$ T cells per ml [19] and $I_0 = 1$ infected monocyte per ml. Monocytes get infected at rate $\beta = 1.72 \times 10^{-10}$ ml per RNA per day [20]. Infected monocytes die at rate $\delta = 0.14$ per day [20]. Dengue virus is produced at rate $p = 10^4$ per day [20] and has a natural decay rate of $c = 3.48$ per day [20]. T cells die at per capita rate $d_E = 0.5$ per day [19] and are at steady-state before virus detection. Thus, $s_E = E_0 d_E = 30$ cells per ml per day. These fixed parameter values are summarized in Table 4.1.

We assume that specific and non-specific T cell killing rates (μ and η), proliferation rates (ϕ_1 and ϕ_2), and the delay τ are unknown and we estimate them by comparing virus population given by models (4.1) and (4.3) to temporal patient virus data.

We use published temporal viral load data from patients with primary DF infections induced by the DENV-2 serotype [20] and patients with secondary DF and DHF infections induced by the DENV-2 serotype [117, 20] after having been previously infected with one of the other three serotypes. We obtained the data by examining the publications and their supplementary material. We first define a common time course between our models and the two data sets [117, 20]. Virus detection time ($t = 0$ in our models), occurs 5.8 days prior to the first data point reported in [20] (corresponding to symptom onset) and 9.8 days prior to the first data point reported in [117] (corresponding to two days before the fever onset). To align the model and the two data sets, we add 5.8 days to the time vector in [20] and 9.8 days to the time vector in [117].

4.4.4 T cell responses during primary infections

We estimate parameters μ, ϕ, and τ by fitting $V(t)$ given by model (4.1) with initial conditions (4.2) to temporal patient data. We use temporal viral load from five patients with primary DF infections induced by the DENV-2 serotype published in [20] (patient ID: 21, 24, 25, 63, and 83). We align the data to the common time course as described in Section 4.4.3, set all other parameters at the values in Table 4.1, and estimate $\{\mu, \phi, \tau\}$ using the Nelder-Mead simplex method, programmed using 'fminsearch' in Matlab [62]. From an initial n-dimensional vector $\mathbf{x}_0$, the Nelder-Mead simplex method creates a simplex of $n+1$ points. The $n+1$ points are found by calculating $\mathbf{x}_0$+$0.05x_0(i)$ for $i = 1, 2, ..., n$, along with the initial vector $\mathbf{x}_0$. It then calculates the function values for each of these points, and orders them from lowest to highest. At each iteration, it discards the point associated with the highest function value, and calculates a new point. Under certain conditions, it keeps only the point with the smallest function value and calculates n new points. The algorithm stops when both the new calculated point and its function value are within a specified tolerance of all of the other points and their function values [62]. In our case, we use the criterion

$$\sum_{i=1}^{n}[\log(y(t_i)) - \log(v(t_i))]$$

where $y(t_i)$ is the data at time t_i and $v(t_i)$ is the viral load from the output of the model at time t_i. We use the Nelder-Mead simplex method since it is used for unconstrained optimization and does not need to consider the differentiablility of the function to be minimized [62].

We find that patient 63's estimate for ϕ is two orders of magnitude lower than the estimates for the other patients. We consider it an outlier, and we exclude it from our analysis. For the remaining patients, we compute parameter averages, 95% confidence intervals using bootstrapping, and inter-patient ranges (see Table 4.2). We predict an average delay of 20 hours in the activation of T cells following recognition of infection.

We use the inter-patient average parameter estimates to characterize the dynamics of the virus and T cell responses during primary infection (see Figure 4.1). We predict that virus reaches a maximum concentration, of 1.04×10^{10} RNA per ml, 6.24 days after viral detection (of 357 RNA per ml). Following peak viremia, the virus decays below the limit of detection by day 11.3. These results are consistent with clinical reports [110, 113, 38].

We are interested in the role of T cell responses in clearing the virus through cell-cell mediated killing of infected cells. We define the cumulative infected cell loss due to T cell mediated killing on the interval $0 \leq t \leq \gamma$ to be

$$L(\gamma) = \int_0^\gamma \mu E(t) I(t)\, dt, \tag{4.17}$$

and the average daily viral concentration on interval $0 \leq t \leq \gamma$ to be

$$A_V(\gamma) = \frac{1}{\gamma} \int_0^\gamma V(t)\, dt. \tag{4.18}$$

Moreover, we define the viral and infected cell clearance times, t_{VC} and t_{IC}, to be the times when $V(t) < 1$ RNA per ml and $I(t) < 1$ cell per ml, respectively. We define the difference between the time of viral clearance and the time of infected cell clearance to be

$$D = t_{VC} - t_{IC}. \tag{4.19}$$

For each patient, we quantified the temporal changes in $L(\gamma)$ for $0 \leq \gamma \leq t_{IC}$, $A_V(\gamma)$ for $0 \leq \gamma \leq t_{VC}$ and D. We found that the inter-patient average for $A_V(t_{VC})$ is 9.43×10^8 RNA per ml per day, for D is 4.56 days, and for $L(t_{IC})$ is 6.40×10^6 cells per ml. Individual patient graphs showing the cumulative infected cell loss due to T cell mediated killing $L(\gamma)$ over time for $0 \leq \gamma \leq 15$ are shown in Figure 4.2. Among the patients, the cumulative infected cell loss increases sharply for the first 6.57 days after virus detection (on average 1.88 days before the time of infected cell clearance).

Table 4.1: Fixed parameters and initial conditions.

Initial Condition	Description	Value	Units	Reference
T_0	Initial uninfected monocytes	10^7	cells/ml	[20]
E_0	Initial T cells	60	cells/ml	[19]
I_0	Initial infected monocytes	1	cells/ml	-
V_0	Initial virus	357	RNA/ml	[117]
Parameter	Description	Value	Units	Reference
β	Infectivity rate	1.72×10^{-10}	ml/RNA $\cdot$ day	[20]
s_E	Effector cell production rate	30	cells/ml $\cdot$ day	[19]
d_E	Effector cell death rate	0.5	per day	[19]
δ	Infected monocytes death rate	0.14	per day	[20]
p	Virus production rate	10^4	RNA/ml $\cdot$ cells $\cdot$ day	[20]
c	Virus clearance rate	3.48	per day	[20]

Table 4.2: Estimated parameters obtained by fitting model (4.1) to primary DF data.

Parameter	Mean	Confidence Intervals	Range
μ	1.04×10^{-5}	$[9.05 \times 10^{-6}, 1.18 \times 10^{-5}]$	$[9.15 \times 10^{-6}, 1.14 \times 10^{-5}]$
ϕ	4.44×10^{-4}	$[3.27 \times 10^{-4}, 5.59 \times 10^{-4}]$	$[3.61 \times 10^{-4}, 5.48 \times 10^{-4}]$
τ	0.83	$[0.34, 1.31]$	$[0.41, 1.19]$

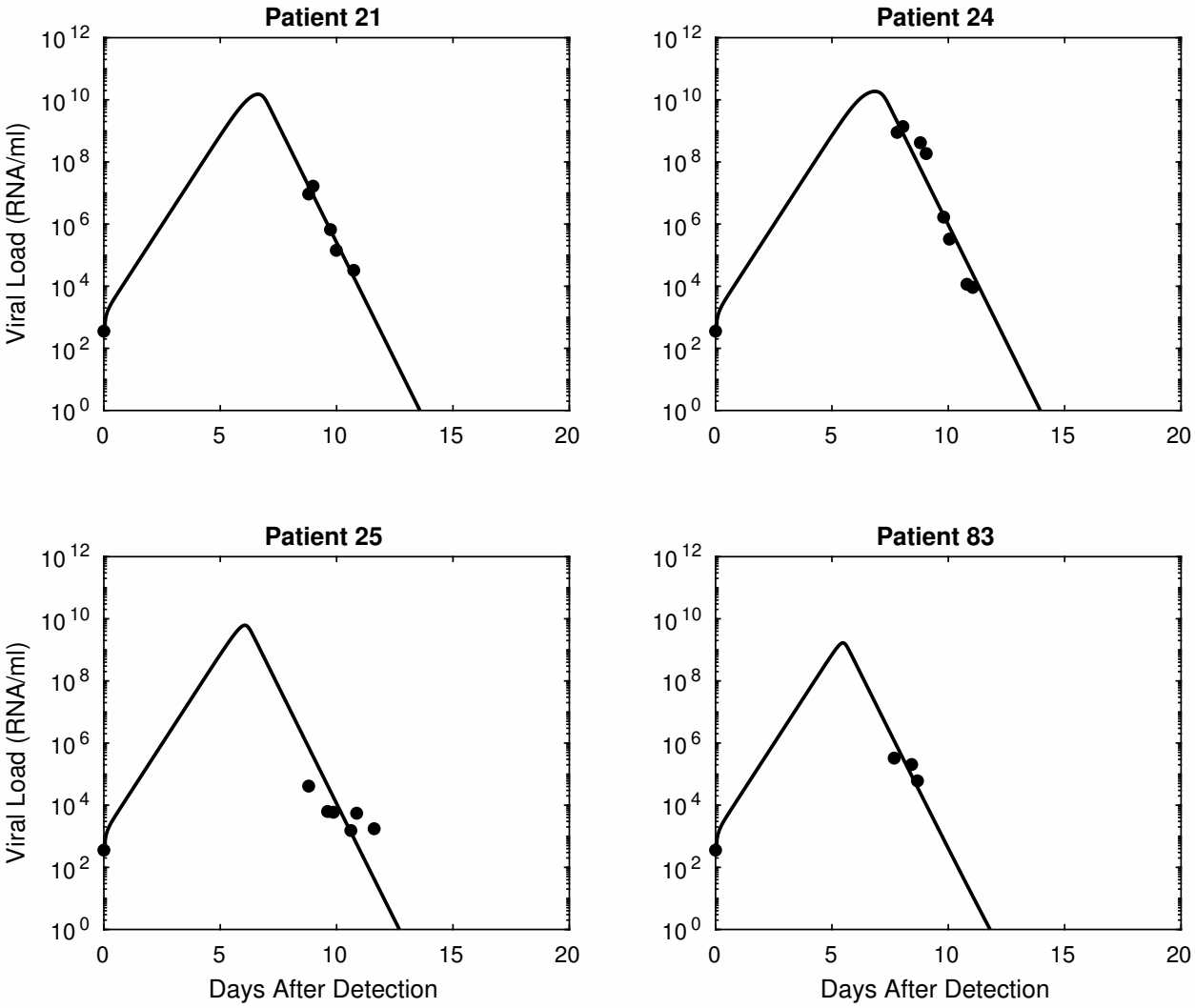

Figure 4.1: **Virus dynamics during primary infections.** Virus RNA per ml as given by model (4.1) (solid lines) versus patient viral load data from primary DF infection with DENV-2 serotype (solid dots).

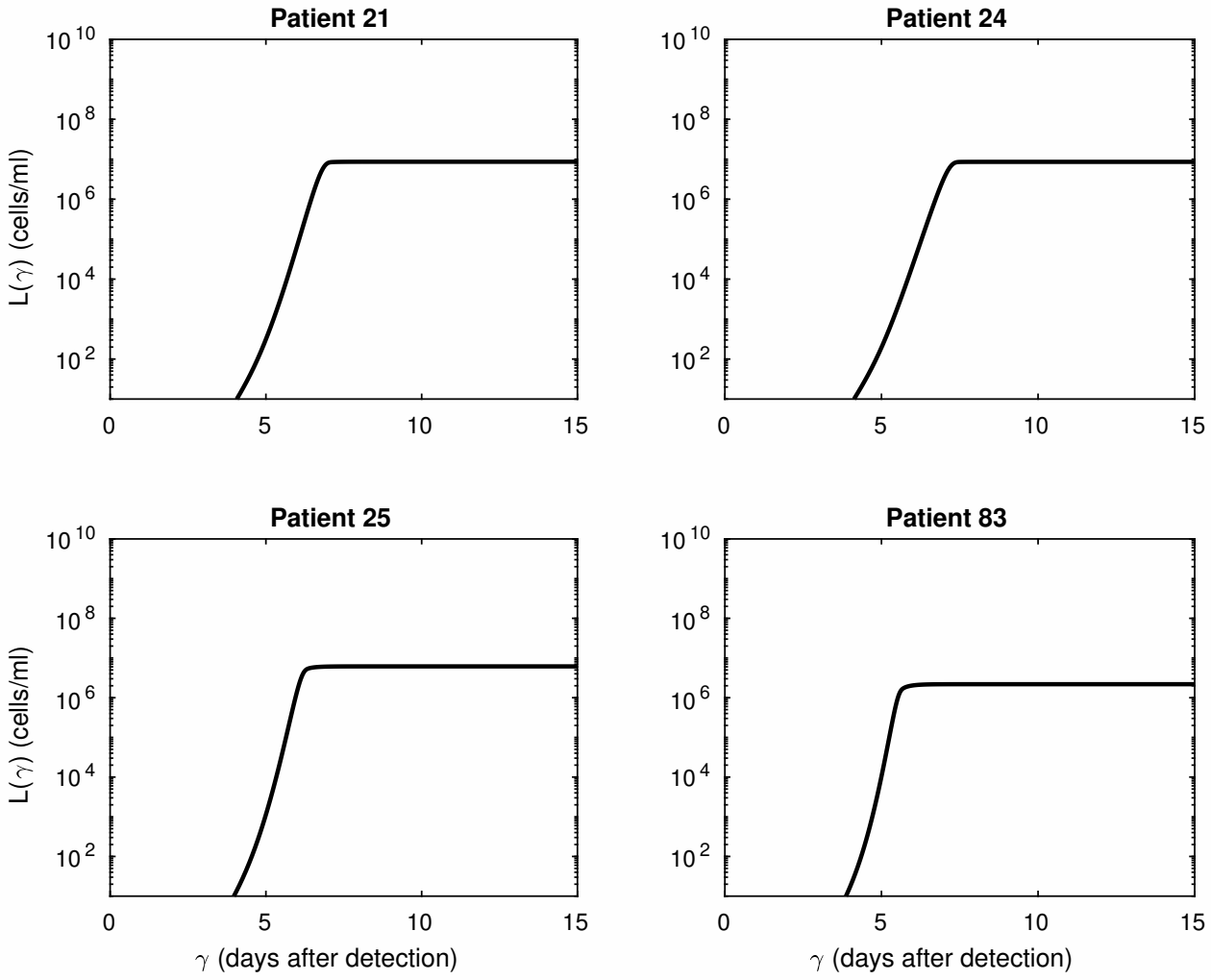

Figure 4.2: **T cell mediated killing during primary infections.** Cumulative infected cell loss at time γ due to T cell mediated killing in primary DF infections as given by equation (4.17).

4.4.5 T cell responses during secondary infections

We examine the possible changes in the virus and the T cell dynamics in patients with secondary heterologous dengue infections as given by the model (4.3) as follows. We use temporal virus data from 21 DF and 20 DHF patients infected with the DENV-2 serotype [117, 20]. We align the data to a common time course as described in Section 4.4.3 and fix parameters to the values given in Table 4.1. We assume the number of target cells have

returned to their original state, which allows us to use the same number of initial target cells T_0. Moreover, we assume that parameters μ, ϕ_1, and τ are the mean values in Table 4.2. We estimate the remaining parameters η (the killing rate of non-specific T cells) and ϕ_2 (the proliferation rate of strain-specific T cells) by fitting $V_2(t)$ as given by model (4.3) with initial conditions (4.4) to individual patient virus data using the Nelder-Mead simplex method, programmed using 'fminsearch' in Matlab [62]. The best fits for individual patients with secondary infections resulting in DF and DHF cases are presented in Figures 4.3 and 4.4, respectively. Inter-patient average and 95% confidence intervals for each estimated parameter are presented in Tables 4.3 and 4.4 for DF and DHF infections, respectively.

Table 4.3: Estimated parameters obtained by fitting model (4.3) to secondary DF data.

Parameter	Mean	Confidence Intervals	Range
η	2.77×10^{-6}	$[-1.01 \times 10^{-6}, 6.54 \times 10^{-6}]$	$[1.47 \times 10^{-12}, 3.79 \times 10^{-5}]$
ϕ_2	1.53×10^{-3}	$[5.02 \times 10^{-4}, 2.56 \times 10^{-3}]$	$[4.97 \times 10^{-7}, 7.34 \times 10^{-3}]$

Table 4.4: Estimated parameters obtained by fitting model (4.3) to secondary DHF data.

Parameter	Mean	Confidence Intervals	Range
η	3.06×10^{-6}	$[-4.27 \times 10^{-7}, 6.54 \times 10^{-6}]$	$[1.06 \times 10^{-12}, 3.24 \times 10^{-5}]$
ϕ_2	3.09×10^{-4}	$[-2.83 \times 10^{-4}, 9.00 \times 10^{-4}]$	$[5.18 \times 10^{-9}, 5.52 \times 10^{-3}]$

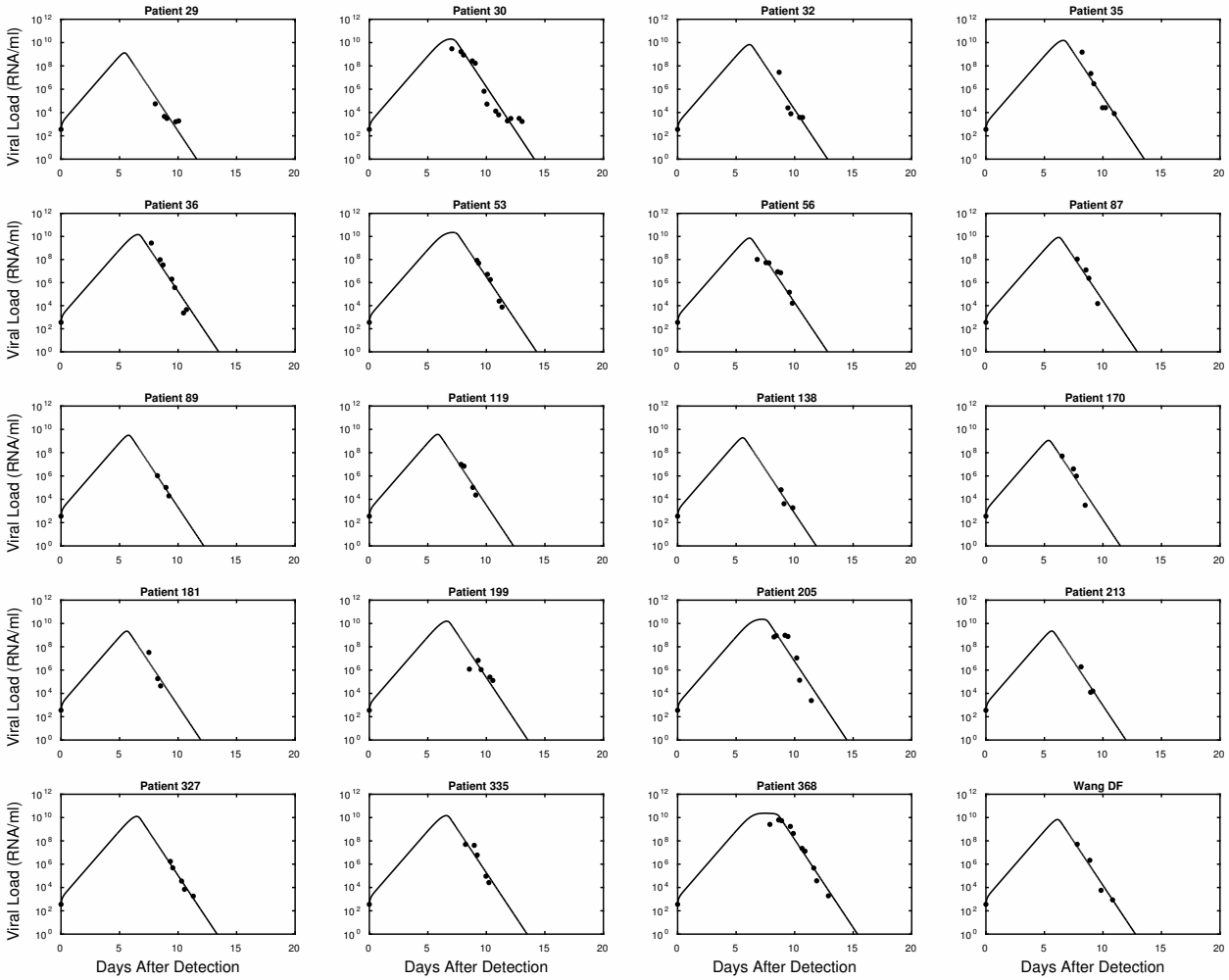

Figure 4.3: **Virus dynamics during secondary DF infections.** Virus RNA per ml as given by model (4.3) (solid lines) versus patient viral load data from secondary DF infections with DENV-2 serotype (solid dots). (Patient 388 data not shown.)

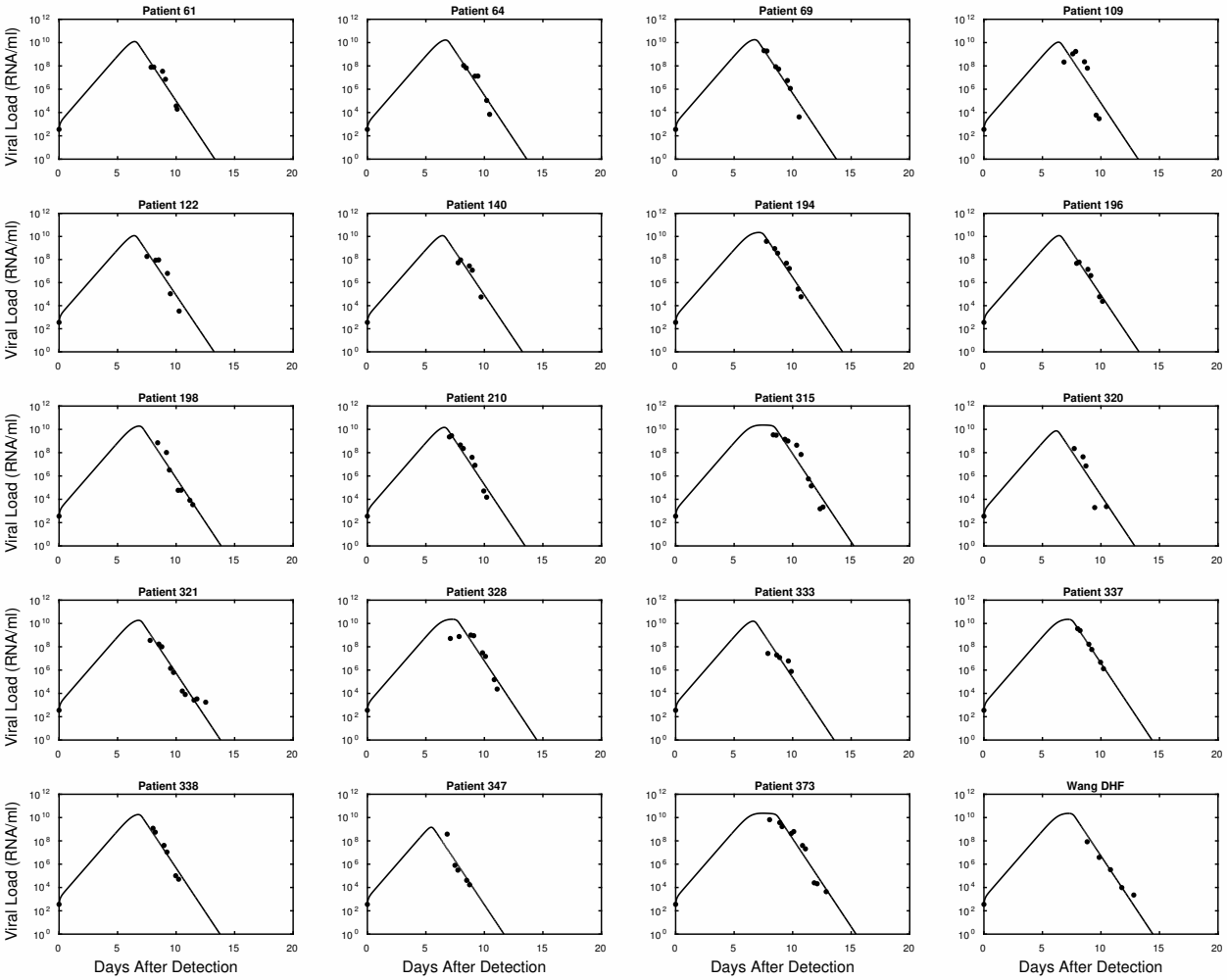

Figure 4.4: **Virus dynamics during secondary DHF infections.** Virus RNA per ml as given by model (4.3) (solid lines) versus patient viral load data from secondary DHF cases with DENV-2 serotype (solid dots).

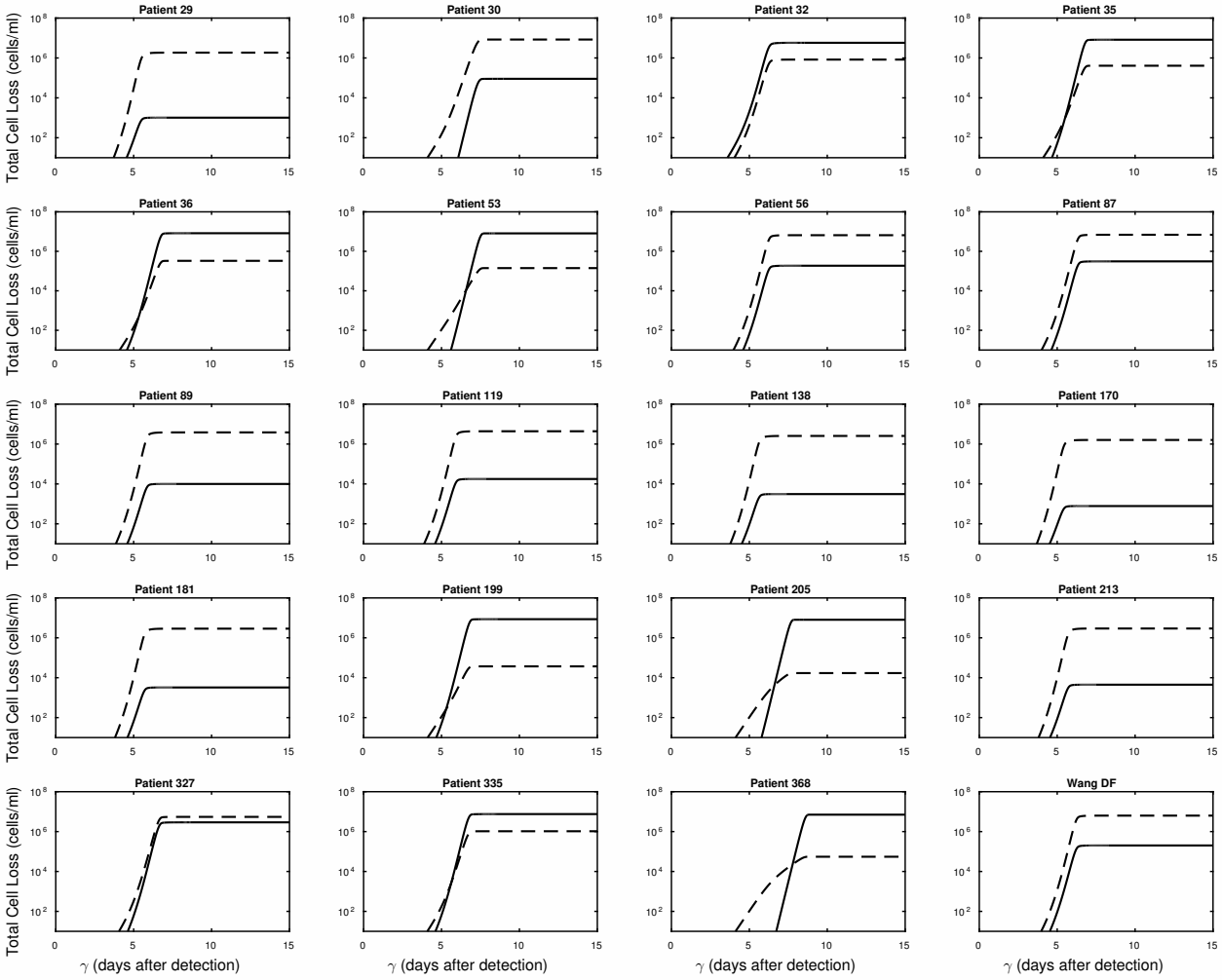

Figure 4.5: **T cell mediated killing during secondary DF infections.** Cumulative infected cell loss at time γ due to non-specific (solid lines) and strain-specific (dashed lines) T cell mediated killing in secondary DF infections as given by equation (4.20).

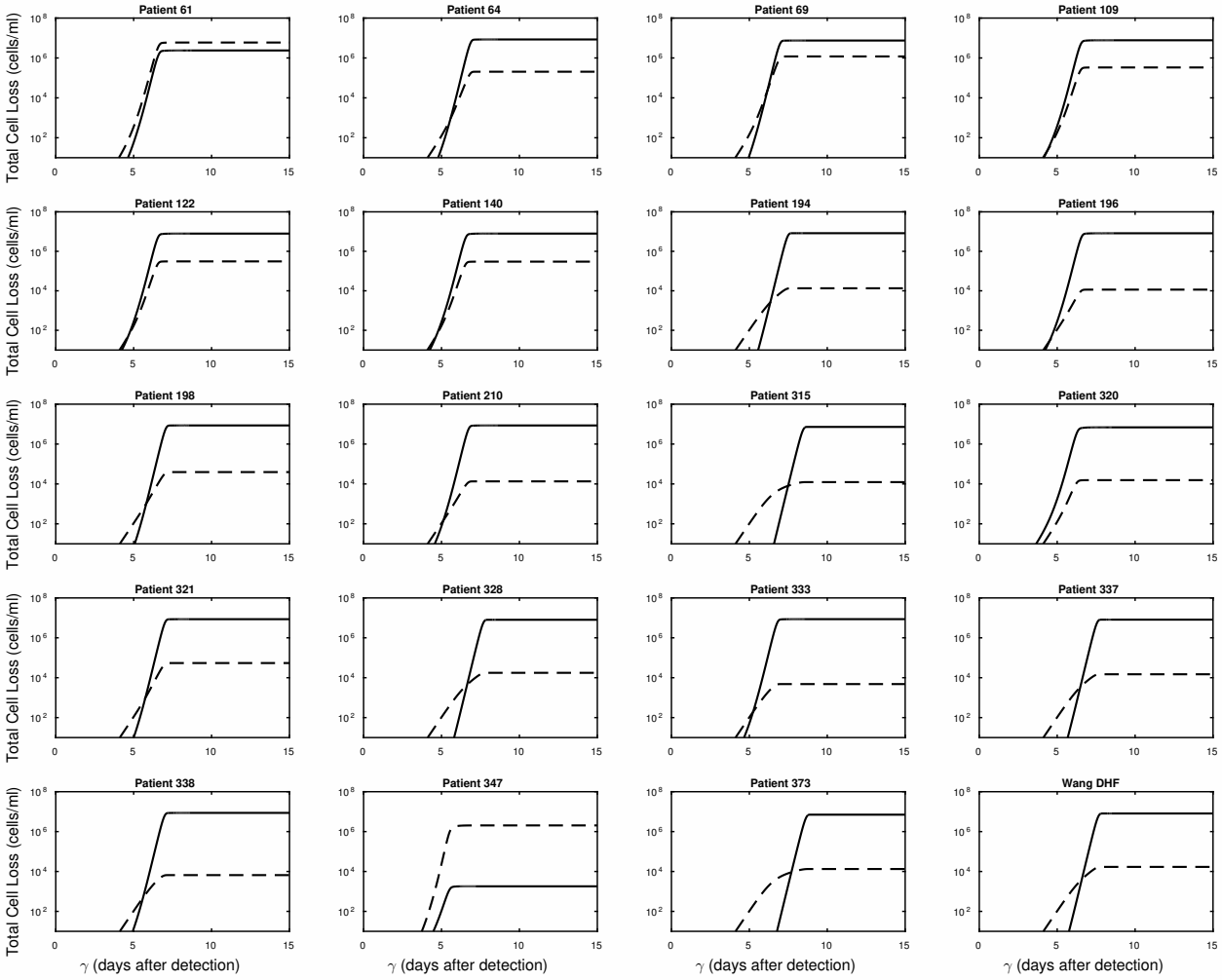

Figure 4.6: **T cell mediated killing during secondary DHF infections.** Cumulative infected cell loss at time γ due to non-specific (solid lines) and strain-specific (dashed lines) T cell mediated killing in secondary DHF infections as given by equation (4.20).

As in the primary infections, we quantify the role of T cell responses in enhancing disease severity. For $i = 1, 2$, we define the cumulative loss of infected cells due to T cell mediated killing during the time interval $0 \leq t \leq \gamma$ to be

$$L_i(\gamma) = \int_0^\gamma \kappa_i I_2(t)\, dt, \tag{4.20}$$

where $\kappa_1 = \eta E_1(t)$ and $\kappa_2 = \mu E_2(t)$ correspond to non-specific and strain-specific T cell

responses, and $E_1(t)$ and $E_2(t)$ are given by the model (4.3). The total cumulative infected cell loss in secondary infections during time period $0 \leq t \leq \gamma$ is

$$L(\gamma) = L_1(\gamma) + L_2(\gamma). \tag{4.21}$$

As before, we calculate the values $L(t_{IC})$ (Equation 4.21), $A_V(t_{VC})$ (Equation 4.18 where in this case $V(t) = V_2(t)$), and D (Equation 4.19) for each individual patient experiencing secondary DF and DHF infections, where t_{IC} is the time of infected cell clearance and t_{VC} is the time of virus clearance. In order to make the distinction between infections where infected cell killing is induced by strain-specific or non-specific T cells, we define

$$P = \frac{L_1(t_{IC})}{L_1(t_{IC}) + L_2(t_{IC})}, \tag{4.22}$$

to be the percentage of non-specific killing and $1 - P$ to be the percentage of strain-specific killing of infected cells between the time of viral detection and the time of infected cell clearance.

We investigate the differences in virus and T cell dynamics between the primary and secondary infections as given by models (4.1) and (4.3). When secondary infections result in DF cases, we predict a virus peak of 1.06×10^{10} RNA per ml, occurring 6.29 days after viral detection, and decaying below detection 5.16 days later. These results are similar to those from primary DF infection. By contrast, when secondary infections result in DHF cases, a virus peak of 1.62×10^{10} RNA per ml occurs 6.72 days after detection and decays below detection 5.38 days later. The peak virus concentration is 1.6-times higher than in primary infection, as observed experimentally [113]. The timing of peak and decay, however, is not significantly different than the timings of the primary and secondary DF infections.

During secondary DF infections, model (4.3) predicts that the proliferation rate of strain-specific T cells is 3.4 times larger than that of non-specific T cells, $\phi_2 = 1.53 \times 10^{-3}$ compared to $\phi_1 = 4.44 \times 10^{-4}$ per cell per day. The killing rate of the non-specific T cells is 3.8 times

smaller than that of strain-specific T cells, $\eta = 2.77 \times 10^{-6}$ compared to $\mu = 1.04 \times 10^{-5}$ per cell per day.

During secondary DHF infections, model (4.3) predicts that the proliferation rate of strain-specific T cells is 1.4 times smaller than that of non-specific T cells, $\phi_2 = 3.09 \times 10^{-4}$ compared to $\phi_1 = 4.44 \times 10^{-4}$ per cell per day. The killing rate of non-specific T cells is 3.4 times smaller than that of strain-specific T cells, $\eta = 3.06 \times 10^{-6}$ compared to $\mu = 1.04 \times 10^{-5}$ per cell per day. These results are summarized in Figure 4.7.

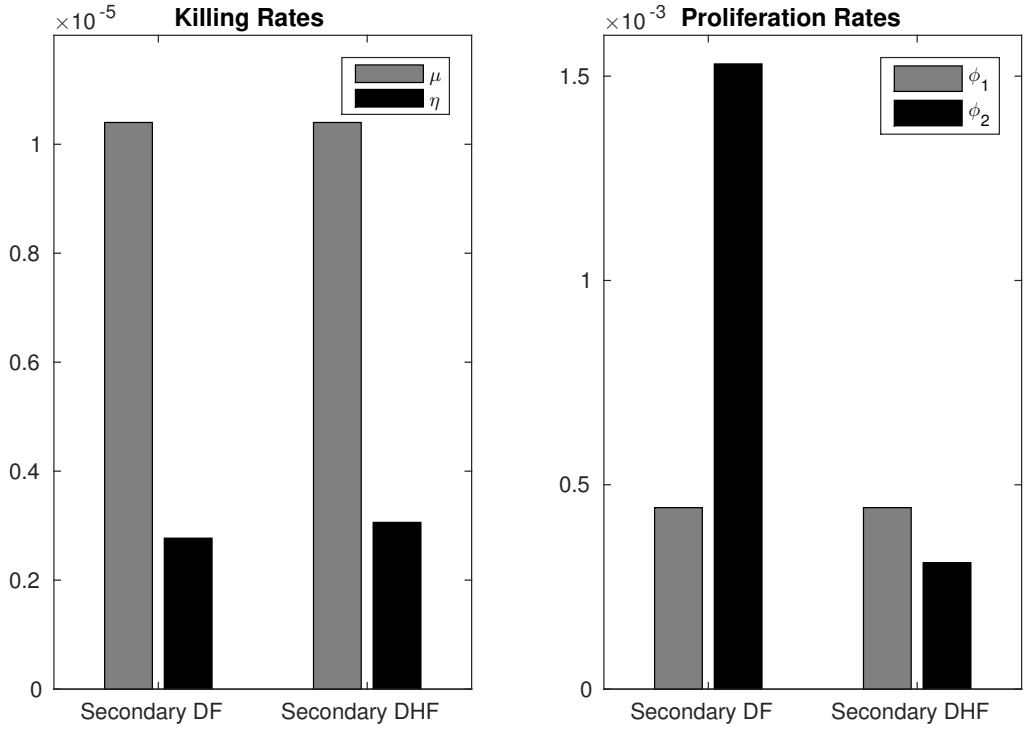

Figure 4.7: **Comparing killing and proliferation rates in secondary DF and DHF infections.** The left figure compares μ (killing rate of strain-specific T cells) and η (killing rate of non-specific T cells) in both secondary DF and DHF infections. The right figure compares ϕ_1 (proliferation rate of non-specific T cells) and ϕ_2 (proliferation rate of strain-specific T cells) in both secondary DF and DHF infections.

These results alone do not support the idea of OAS during secondary infections as $\eta < \mu$ in both DF and DHF cases, but $\phi_1 > \phi_2$ in secondary DF cases and $\phi_2 < \phi_1$ in secondary

DHF cases. To further determine the role of strain-specific and non-specific T cell responses we calculate the average values of $L(t_{IC})$ (Equation 4.21), $A_V(t_{VC})$ (Equation 4.18 where $V(t) = V_2(t)$) and D (Equation 4.19) as given by the best fit of the model (4.3) to data from patients experiencing DF and DHF secondary infections.

Inter-patient averages for the average daily virus loads $A_V(t_{VC})$ are 9.43×10^8, 1.06×10^9 and 1.69×10^9 RNA per ml during primary DF, secondary DF and secondary DHF infections, respectively. The inter-patient average D values are 4.56, 4.81 and 5.18 days in primary DF, secondary DF and secondary DHF infections. While the average viral load is higher and time between virus and infected cell clearance are longer during DHF secondary infections, the differences are not significant. Similarly, the inter-patient averages for the cumulative cell loss $L(t_{IC})$ are similar during primary DF, secondary DF and secondary DHF infections, changing from 6.40×10^6 to 6.22×10^6 to 7.87×10^6 cells per ml, respectively. Therefore the overall infected cell loss due to T cell mediated killing does not correlate with disease severity. These results are summarized in Figure 4.8.

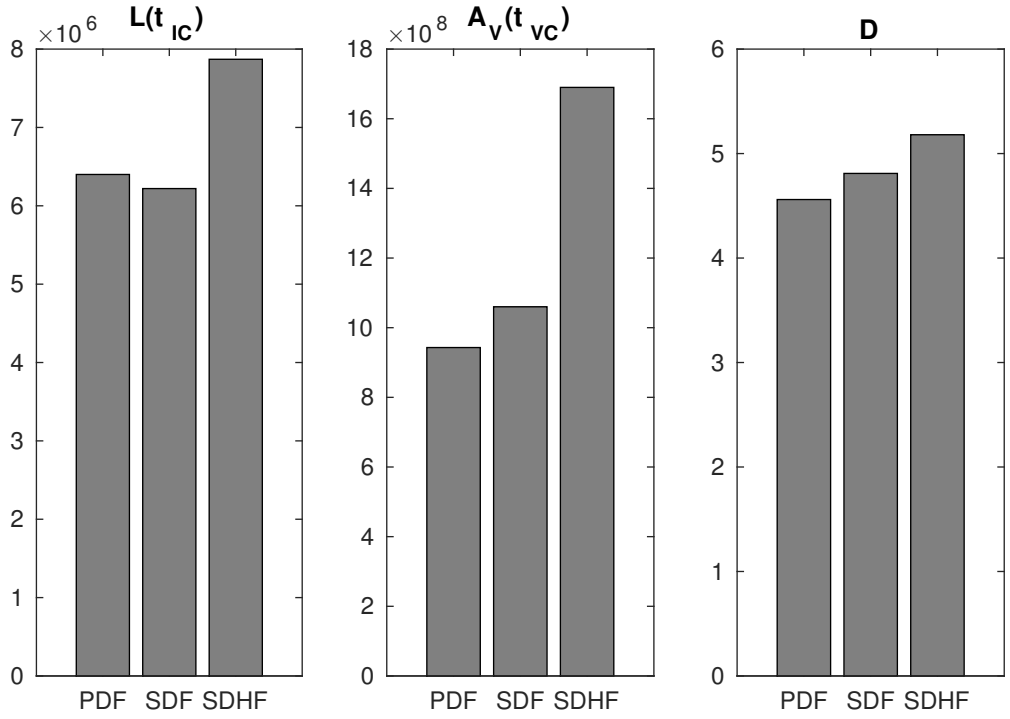

Figure 4.8: **Comparing loss, average viral load and difference in clearance in primary DF (PDF), secondary DF (SDF), and secondary DHF (SDHF) infections.** A comparison of $L(t_{IC})$ (Equations 4.17 and 4.21, the total infected cell loss at time of infected cell clearance), $A_V(t_{VC})$ (Equation 4.18, the average viral load between time of virus detection and time of viral clearance), and D (Equation 4.19, the difference between the time of viral clearance and the time of infected cell clearance) between primary, secondary DF, and secondary DHF infections.

We next investigate whether specific and non-specific T cell mediated killing as given by model (4.3) is different among secondary DF and DHF cases. For each patient with secondary DF and DHF infections, we graphed $L_1(\gamma)$ and $L_2(\gamma)$ for $0 \leq \gamma \leq 15$ (see Figures 4.5 and 4.6, respectively). We also calculated P (Equation 4.22) and $1 - P$, which are defined as the percentage of infected cell loss due to non-specific T cell responses and the percentage of infected cell loss due to strain-specific T cell responses, respectively. We found that during secondary DF infections, 57% of patients (12 out of 21) had strain-specific T cell responses that were responsible for an average of 96.1% of infected cell loss. The other 43% of the patients (9 out of 21) had non-specific T cell responses which were responsible for 94.2%

of infected cell loss. For secondary DHF infections, 90% of the patients (18 out of 20) had non-specific T cell killing responsible for 98.3% infected cell loss while the remaining 10% (2 out of 20) of the patients had strain-specific T cell responses responsible for 85.7% infected cell loss. These results are summarized in Figure 4.9. We infer from these results that more severe secondary DHF cases have mainly non-specific T cell responses. By contrast, more than half of secondary DF cases have predominant strain-specific, high avidity, T cell responses. These results support the OAS hypothesis that cross-reactive T cell responses occur mainly during severe disease cases of heterologous dengue virus infections.

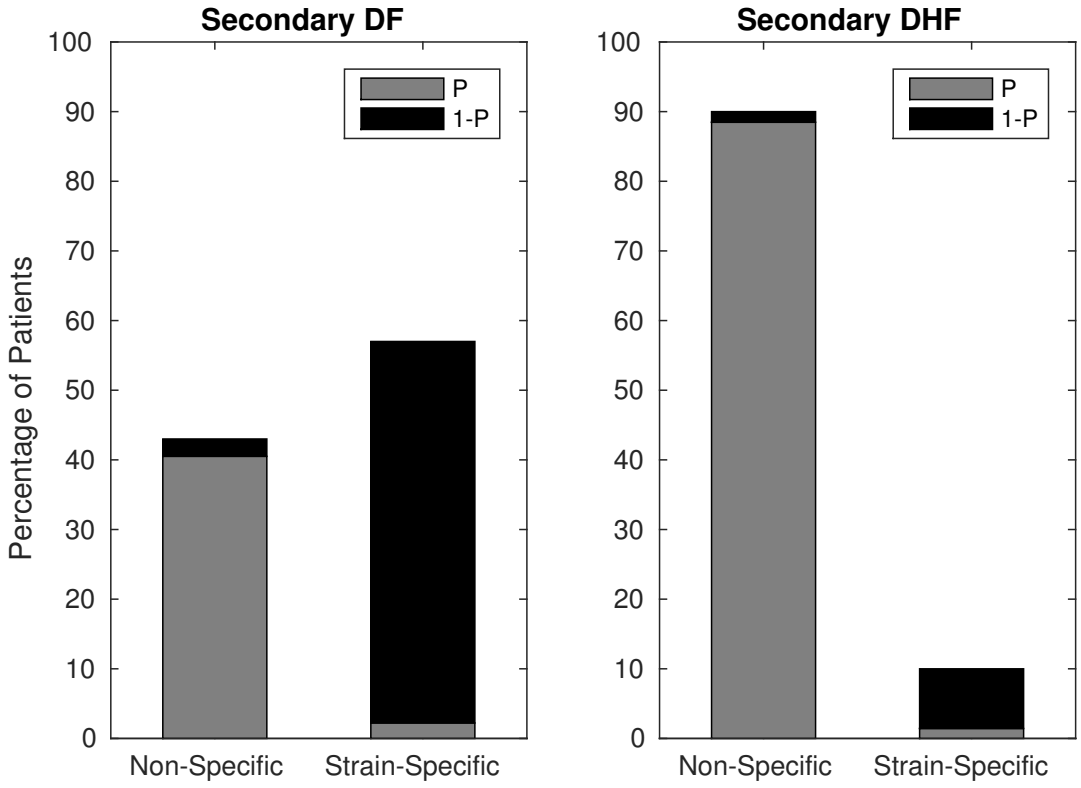

Figure 4.9: **Comparing infected cell loss in secondary DF and DHF infections.** A comparison between P (Equation 4.22, the percentage of killing done by non-specific T cells) and $1 - P$ (the percentage of killing done by strain-specific T cells) in both secondary DF and DHF infections. The percentage of secondary DF and DHF infections caused by either non-specific or strain-specific T cell responses is also compared.

4.5 Discussion

We developed a mathematical model of T cell responses to dengue primary infections. We fitted the model to temporal dengue virus data [20], and we used it to evaluate parameters for T cell expansion and killing capacity. We determined that an average of 20 hours delay in immune cell expansion is needed to adequately capture the initial viral concentration and the times of viral peak and viral clearance, as seen in primary infection data and other clinical reports [38, 114, 110, 20]. For the estimated parameters our model predicted a sharp increase in cumulative cell loss due to T cell mediated killing for the first week following virus detection, followed by a slow decrease corresponding to infected cell removal.

We investigated the mechanisms behind disease enhancement during secondary infections with heterologous virus strains. Several hypotheses have been proposed for the increase in disease severity experienced during DHF and DSS cases, such as the antibody dependent enhancement [122, 42, 81, 46] and the original antigenic sin [114, 122, 98]. We have previously examined the effect of ADE using an in-host modeling approach [88] and predicted that cross-reactive non-neutralizing antibodies may explain the increased virus concentration and time to clearance seen in DHF cases.

Fewer studies and data have been generated on the possible role of T cell responses during heterologous dengue infections. As with B cell responses [98], a secondary infection may be dominated by cross-reactive memory T cells that are reactivated during heterologous challenge, yet have less avidity for the current infecting serotype, and may limit the development of strain-specific T cell populations through competition for space and signal [101, 36, 119, 120]. To determine whether non-specific T cell clones with less avidity for new infections are predominant during heterologous infections, we adapted the T cell model to secondary heterologous dengue virus infections. We considered that both strain-specific and non-specific T cell populations are produced, and we investigated their individual contribution to disease outcome by fitting the model to temporal secondary infections dengue virus data [20, 117]. We evaluated parameters for strain-specific and non-specific T cell expansion,

as well as killing capacity.

We found that while both non-specific and strain-specific T cell responses are developed during heterologous infections, their roles in the removal of infected cells differ during DF and DHF cases. During heterologous DF cases, we predict that 12 out of 21 patients have a predominantly strain-specific T cell response. By contrast, during DHF cases, 18 out of 20 patients have a non-specific T cell response. We did not predict any difference in overall infected cell death due to T cell mediated killing during primary DF, secondary DF and secondary DHF cases. However, the overall T cell response during DHF is higher than in DF cases, suggesting that other T cell functions, such as cytokine production, may correlate with disease severity. Further investigation is needed to determine the exact role of pro-inflammatory cytokines.

In conclusion, we developed and analyzed in-host models of dengue viral infections that considered the contributions of T cells to disease severity. We fitted the models to published patient data and showed that the overall infected cell killing is similar in dengue secondary infections resulting in DF and DHF cases. The contribution to overall killing, however, is dominated by non-specific, less efficacious, T cell responses during secondary DHF cases compared with strain-specific, high avidity T cell responses in at least half of secondary DF cases. Therefore, the cross-reactive cellular immune responses, as described in the hypothesis of original antigenic sin, may be present and responsible for the disease enhancement during heterologous infections.

Chapter 5

Unraveling Within-Host Signatures of Dengue Infection at the Population Level

Based on the results from our previous within-host models, we developed a model that describes how the within-host behavior of dengue viral infection affects epidemiological outcomes. This was joint work done with Dr. Julie Blackwood, Dr. Lauren Childs, and Dr. Stanca Ciupe. I developed the analytical results, Dr. Childs and Dr. Blackwood developed the numerical scheme, and we all wrote and revised the manuscript and created the figures together. We have modified parts of the manuscript for this dissertation. The manuscript has been accepted by the Journal of Theoretical Biology, and is in the process of publication [87].

5.1 Abstract

Dengue virus causes worldwide concern with nearly 100 million infected cases reported annually. The within-host dynamics differ between primary and secondary infections, where secondary infections with a different virus serotype typically last longer, produce higher viral loads, and induce more severe disease. We build upon the variable within-host virus dynamics during infections resulting in mild dengue fever and severe dengue hemorrhagic fever. We couple these within-host virus dynamics to a population-level model through a system of partial differential equations creating an immunoepidemiological model. The resulting multiscale model examines the dynamics of between-host infections in the presence of two circulating virus strains that involves feedback from the within-host and between-hosts interactions, encompassing multiple scales. We analytically determine the relationship between the model parameters and the characteristics of the model's solutions, and find an analytical threshold under which infections persist in the population. Furthermore, we develop and implement a full numerical scheme for our immunoepidemiological model, allowing the simulation of population dynamics under variable parameter conditions.

5.2 Introduction

Mathematical models have been used to determine the mechanisms behind the differences in virus dynamics observed during primary and secondary infections, and during mild and severe cases [8, 12, 20, 40, 88, 89, 91]. Virologically, disease severity translates to higher viral loads that last for longer periods of time [65, 110]. In particular, during infections resulting in dengue fever (denoted by F), virus has a lower delayed peak and a shorter time to clearance. By contrast, during infections resulting in dengue hemorrhagic fever (denoted by H), virus has a higher peak and a longer time to clearance [65, 110]. However, such virus profiles alone are not indicators of disease severity, since there exists intra-patient immunological variability. Mathematical models have examined the interplay between virus and host in

the disease enhancement seen during secondary infections, in particular antibody dependent enhancement [20, 88] and original antigenic sin [89]. Calibration of such models to data from patients with mild and severe infections [20, 117] strongly supported original antigenic sin, rather than antibody dependent enhancement, as the driver of increased disease severity [89].

In this study, we investigate the relationship between individual virus-immune profiles and the dynamics of dengue infection at the population level. In particular, we are interested in the relationship between the type of disease (F versus H) during primary infection and enhancement in susceptibility and transmissibility at the population level during secondary infections with a heterologous serotype. Previous modeling work has reported both reduced [4, 5] and enhanced transmission [14, 16, 25, 104] during secondary heterologous infections, as well as enhanced susceptibility [3, 99] and cross-immunity between serotypes [15, 84].

We investigate the role of disease severity (F versus H) of primary and secondary infections with two co-circulating dengue serotypes on the incidence and persistence of the strains in the population. We first develop a time-since-infection immunoepidemiological model which couples the within-host virus dynamics with the population-level transmission dynamics of two dengue serotypes. We then investigate the model analytically and find conditions for the extinction and persistence of one or both serotypes in the population. Finally, we numerically approximate the model to determine how disease severity during primary and secondary infections affects transmission, susceptibility, and the persistence of strains in the population. The novelty of our approach consists of assessing how the severity of the in-host infection translates into the disease persistence in the population.

5.3 Materials and methods

5.3.1 Time-since-infection multiscale model

We develop a time-since-infection multiscale partial differential equation (PDE) model of dengue infection. At the population level, our model considers the dynamics of two different virus serotypes that are co-circulating in the population. We ignore explicit vector transmission and assume that infection acts like direct contact (i.e. people become infected, which will infect a certain number of mosquitoes, which will then infect a certain number of other people). Although there are four dengue serotypes, we make the simplifying assumption that there are only two serotypes present in the population at one time. Lastly, we model population densities and assume that the population size is fixed at the initial population size, defined as the birth rate divided by the *per capita* mortality rate, Λ/m_0.

For each serotype, we assume that individuals can either be susceptible (S), infected (I), or recovered (R) from infection. At a given time t, we denote the population density of individuals susceptible to both serotypes by $N_{SS}(t)$, recovered from a primary infection by $N_{RS}(t)$ or $N_{SR}(t)$, and recovered from infections with both strains by $N_{RR}(t)$ (the subscripts in our notation refer to the infection status with strain 1 and 2, respectively). Since infection with one strain typically induces immunity against repeated infections with the same strain [77, 100], we only consider primary-secondary infection events caused by two different virus strains. Although the dynamics of these populations can be described by ordinary differential equations (ODEs), we additionally track the time-since-infection τ for infected individuals. Therefore, the infected classes depend on two independent variables, t and τ, and are described by PDEs. To distinguish variables that depend on time versus those that depend on both time and time-since-infection, we denote the former using capital letters and the latter using lowercase letters. In particular, we denote the population density of individuals who have been infected with a primary infection for τ days at time t by $n_{IS}(\tau, t)$ or $n_{SI}(\tau, t)$. Similarly, the population density of individuals who have been infected with a

second heterologous virus for τ days at time t is $n_{RI}(\tau, t)$ or $n_{IR}(\tau, t)$. We assume that the outbreak occurs in a region of negligible disease mortality [39].

Both primary and secondary infections occur through contact with infected individuals at rate $bV_{i,j}(\tau)$ where b is a constant of proportionality that relates the viral load to the between-host transmission rate, i denotes the strain ($i \in \{1, 2\}$) and j denotes the infection order ($j \in \{prim, sec\}$). While the relationship between transmission rate and viral load is assumed to be linear in this case, we discuss other possibilities for this relationship in Section 4. The dependence of $V_{i,j}$ on τ accounts for the differences in between-host transmissibility depending on an individual's time-since-infection, which we define explicitly in Section 5.3.2. We assume that the recovery rate, $r_{i,j}$, can depend on both strain i and infection order ($j \in \{prim, sec\}$). In our analysis, we assume the recovery rate $r_{i,j}$ and the virus profile $V_{i,j}$ are independent of each other. However, the recovery rate $r_{i,j}$ and the virus profile $V_{i,j}$ are related to each other in our simulations. For example, we assume the recovery rate is one over the length of infection. See Table 5.1 for a summary of all parameters and variables. A schematic representation of the model is provided in Figure 5.1.

Here, we present the complete mathematical representation of the system. The ODEs for

Table 5.1: Variables and parameters of the between-host model.

Variable	Definition	Notes
t	time	$t \in [0, \infty)$
τ	time-since-infection	$\tau \in [0, \infty)$
$N_{xy}(t), n_{xy}(\tau, t)$	population size with status x (for strain 1) and y (for strain 2)	$x, y \in \{S, I, R\}$
N_T	total population size	

Parameter	Definition	Notes
Λ	fixed birth rate	
m_0	*per capita* mortality rate	
b	proportionality constant relating viral load to transmission rate	
$r_{i,j}$	recovery rate for an infection with strain i of order j	$i \in \{1, 2\}$, $j \in \{prim, sec\}$
$V_{i,j}$	viral load for an infection with strain i of order j	$i \in \{1, 2\}$, $j \in \{prim, sec\}$

the population densities in disease-free states are given by

$$\begin{aligned}
\frac{dN_{SS}(t)}{dt} &= \Lambda - m_0 N_{SS}(t) - \frac{N_{SS}(t)}{N_T(t)} \int_0^\infty \Big[bV_{1,prim}(\tau) n_{IS}(\tau, t) + bV_{2,prim}(\tau) n_{SI}(\tau, t) \\
&\qquad + bV_{1,sec}(\tau) n_{IR}(\tau, t) + bV_{2,sec}(\tau) n_{RI}(\tau, t) \Big] d\tau, \\
\frac{dN_{SR}(t)}{dt} &= -m_0 N_{SR}(t) - \frac{N_{SR}(t)}{N_T(t)} \int_0^\infty \Big[bV_{1,prim}(\tau) n_{IS}(\tau, t) + bV_{1,sec}(\tau) n_{IR}(\tau, t) \Big] d\tau \\
&\qquad + \int_0^\infty r_{2,prim} n_{SI}(\tau, t)\, d\tau, \\
\frac{dN_{RS}(t)}{dt} &= -m_0 N_{RS}(t) - \frac{N_{RS}(t)}{N_T(t)} \int_0^\infty \Big[bV_{2,prim}(\tau) n_{SI}(\tau, t) + bV_{2,sec}(\tau) n_{RI}(\tau, t) \Big] d\tau \\
&\qquad + \int_0^\infty r_{1,prim} n_{IS}(\tau, t)\, d\tau, \\
\frac{dN_{RR}(t)}{dt} &= -m_0 N_{RR}(t) + \int_0^\infty \Big(r_{1,sec} n_{IR}(\tau, t) + r_{2,sec} n_{RI}(\tau, t) \Big) d\tau.
\end{aligned} \tag{5.1}$$

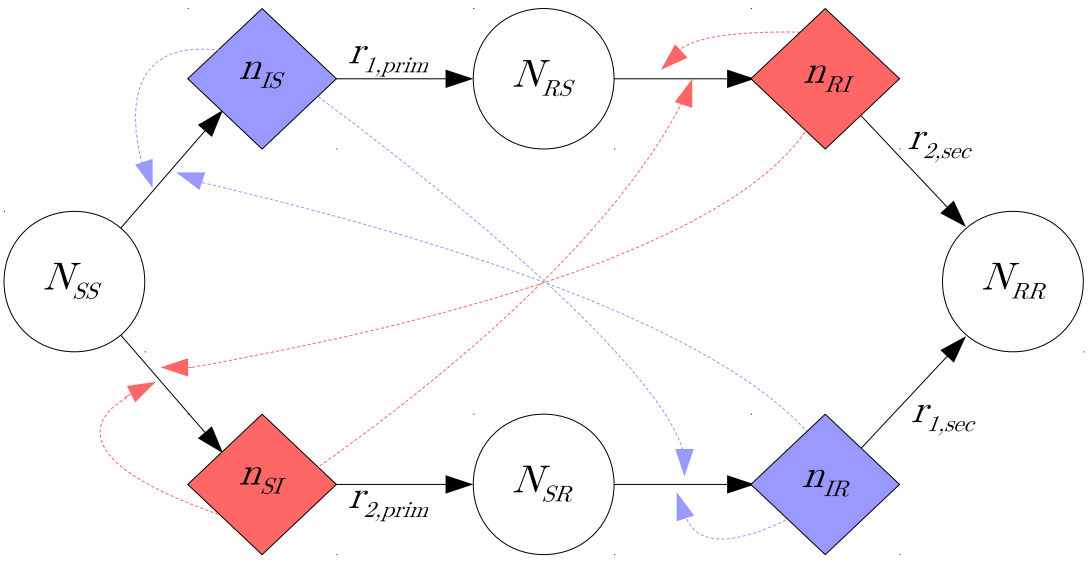

Figure 5.1: **Schematic diagram of two-strain between-host dengue infection.** Shaded diamonds indicate infected states with strain 1 (blue) and strain 2 (red). Corresponding colored arrows demonstrate infection of susceptible individuals by strain 1 (blue) and strain 2 (red). Subscripts i, j indicate the disease status for strain 1 (first subscript) or strain 2 (second subscript) with $\{i, j\} \in \{S, I, R\}$.

The PDEs for the infection states are given by

$$\begin{aligned}
\frac{\partial n_{SI}(\tau,t)}{\partial \tau} + \frac{\partial n_{SI}(\tau,t)}{\partial t} &= -m_0 n_{SI}(\tau,t) - r_{2,prim} n_{SI}(\tau,t), \\
\frac{\partial n_{IS}(\tau,t)}{\partial \tau} + \frac{\partial n_{IS}(\tau,t)}{\partial t} &= -m_0 n_{IS}(\tau,t) - r_{1,prim} n_{IS}(\tau,t), \\
\frac{\partial n_{RI}(\tau,t)}{\partial \tau} + \frac{\partial n_{RI}(\tau,t)}{\partial t} &= -m_0 n_{RI}(\tau,t) - r_{2,sec} n_{RI}(\tau,t), \\
\frac{\partial n_{IR}(\tau,t)}{\partial \tau} + \frac{\partial n_{IR}(\tau,t)}{\partial t} &= -m_0 n_{IR}(\tau,t) - r_{1,sec} n_{IR}(\tau,t),
\end{aligned}$$

with boundary conditions

$$\begin{aligned}
n_{SI}(0,t) &= \frac{N_{SS}(t)}{N_T(t)} \int_0^\infty \Big[bV_{2,prim}(\tau) n_{SI}(\tau,t) + bV_{2,sec}(\tau) n_{RI}(\tau,t) \Big] d\tau, \\
n_{IS}(0,t) &= \frac{N_{SS}(t)}{N_T(t)} \int_0^\infty \Big[bV_{1,prim}(\tau) n_{IS}(\tau,t) + bV_{1,sec}(\tau) n_{IR}(\tau,t) \Big] d\tau, \\
n_{RI}(0,t) &= \frac{N_{RS}(t)}{N_T(t)} \int_0^\infty \Big[bV_{2,prim}(\tau) n_{SI}(\tau,t) + bV_{2,sec}(\tau) n_{RI}(\tau,t) \Big] d\tau, \\
n_{IR}(0,t) &= \frac{N_{SR}(t)}{N_T(t)} \int_0^\infty \Big[bV_{1,prim}(\tau) n_{IS}(\tau,t) + bV_{1,sec}(\tau) n_{IR}(\tau,t) \Big] d\tau.
\end{aligned}$$

The initial conditions for our system are given by

$$\begin{aligned}
N_{SS}(0) &= N_{SS0}, & N_{SI}(0) &= \int_0^\infty n_{SI0}(\tau) d\tau, \\
N_{SR}(0) &= N_{SR0}, & N_{IS}(0) &= \int_0^\infty n_{IS0}(\tau) d\tau, \\
N_{RS}(0) &= N_{RS0}, & N_{RI}(0) &= \int_0^\infty n_{RI0}(\tau) d\tau, \\
N_{RR}(0) &= N_{RR0}, & N_{IR}(0) &= \int_0^\infty n_{IR0}(\tau) d\tau.
\end{aligned}$$

where

$$N_x(t) = \int_0^\infty n_x(\tau,t) d\tau \text{ for } x \in \{SI, IS, RI, IR\}. \tag{5.2}$$

Finally, the total population at each time t is given by

$$\begin{aligned}
N_T(t) = N_{SS}(t) + N_{SR}(t) + N_{RS}(t) + N_{RR}(t) \\
+ \int_0^\infty \Big(n_{SI}(\tau,t) + n_{IS}(\tau,t) + n_{RI}(\tau,t) + n_{IR}(\tau,t) \Big) d\tau.
\end{aligned} \tag{5.3}$$

Since the system is closed, $N_T(t) = \dfrac{\Lambda}{m_0}$ for all t.

We refer to our model formulation collectively as system (5.1). We aim to determine under what conditions one or both viruses establish as endemic in the population. We first investigate this analytically, by determining the equilibria of system (5.1) and their stability.

5.3.2 Within-host virus dynamics

As described in Section 5.3.1, we assume that the transmission rate of dengue virus between individuals is proportional to the viral load within infected individuals which, in turn, directly depends on the time since infection (τ) [85]. While the profile of a viral load as τ varies is subject to variability based on an individual's immune characteristics [88, 89], the virus profile across all infected individuals can be approximated by a triangular-like distribution [20, 88, 89, 117]. Models of ordinary differential equations were used to describe the interaction between primary and secondary virus, the host target cells, and the host immune responses [88, 89]. Fitting of these models to human viral load data [20, 117] generated virus profiles which were roughly triangular in nature when viewed on a log scale. Here, we approximate the dynamics of virus profiles by triangular distributions which follow the average virus profiles described in [88, 89]. We consider two virus profiles: one describing dengue fever (F); and one describing dengue hemorrhagic fever (H) based on data from [20, 117] (see Figure 5.2). In the case of dengue fever, virus peaks at a lower value and earlier in infection (see Figure 5.2, solid line) and, in the case of dengue hemorrhagic fever, virus has a higher peak and persists for a longer time before clearance (see Figure 5.2, dashed line).

5.4 Analytical results

Here, we provide an asymptotic stability analysis of the model which is based on the methods described in [71] (pp. 333-343). First, define

$$\begin{aligned}
\Gamma_{1,prim} &= \int_0^\infty bV_{1,prim}(\tau)e^{-(m_0+r_{1,prim})\tau}\,d\tau,\\
\Gamma_{2,prim} &= \int_0^\infty bV_{2,prim}(\tau)e^{-(m_0+r_{2,prim})\tau}\,d\tau,\\
\Gamma_{1,sec} &= \int_0^\infty bV_{1,sec}(\tau)e^{-(m_0+r_{1,sec})\tau}\,d\tau,\\
\Gamma_{2,sec} &= \int_0^\infty bV_{2,sec}(\tau)e^{-(m_0+r_{2,sec})\tau}\,d\tau.
\end{aligned}$$

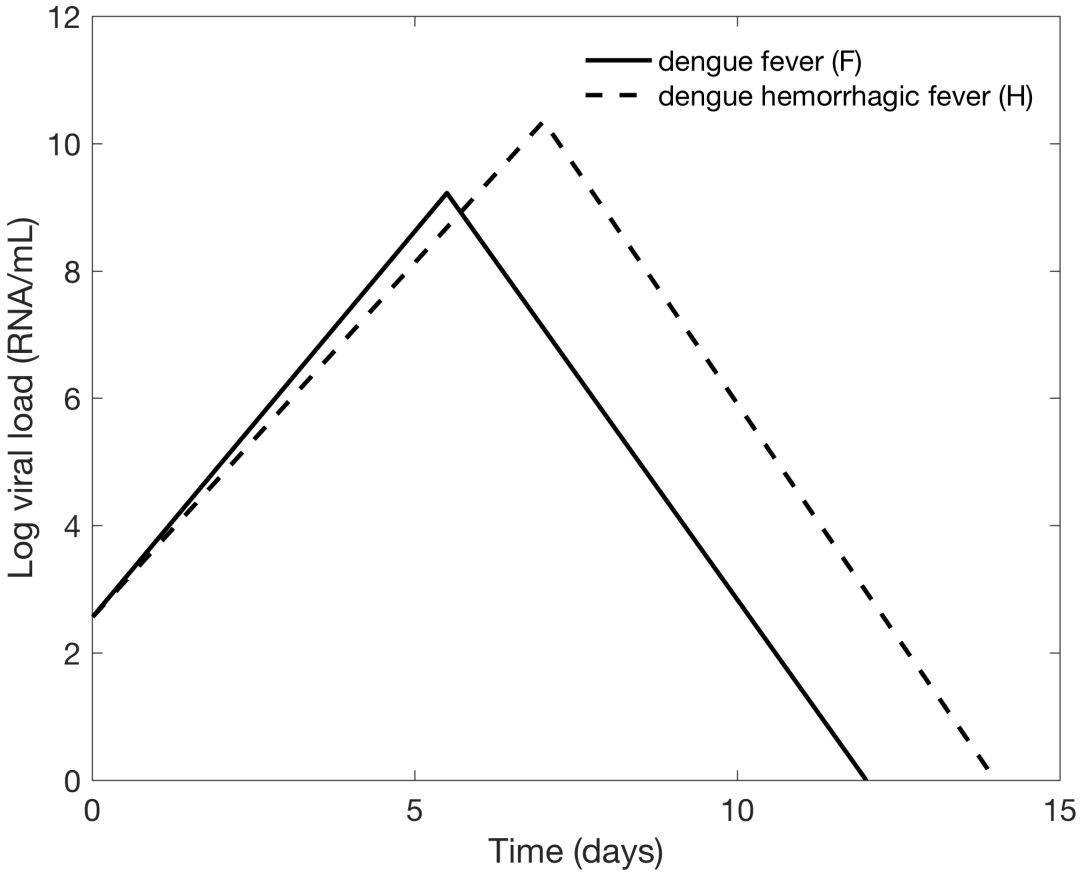

Figure 5.2: **Within-host viral load.** The average virus profile for individuals from [20, 117] as fitted in [88, 89] follows a triangular distribution when viewed on a log scale. Solid line for dengue fever (F) and dashed line for dengue hemorrhagic fever (H).

These equations capture the total force of infection of a given infection type (e.g. $\Gamma_{1,prim}$ represents primary infection with strain 1) over an infectious period. For analytical purposes, we do not assume anything about the nature of the virus profiles. We can first show that the solutions of system (5.1) are bounded.

5.4.1 Boundedness

Proposition 5.4.1. *The solutions of System (5.1) are bounded.*

Proof. Note that based on the definitions (5.2), $N_T(t)$ as defined in (5.3) is thus

$$N_T(t) = N_{SS}(t) + N_{SR}(t) + N_{RS}(t) + N_{RR}(t) + N_{SI}(t) + N_{IS}(t) + N_{RI}(t) + N_{IR}(t). \quad (5.4)$$

Since patients will eventually die if infected long enough, we can assume that for all t,

$$\lim_{\tau\to\infty} n_{SI}(\tau, t) = 0.$$

Now consider integrating the partial differential equation associated with $n_{SI}(\tau, t)$ in System (5.1) with respect to τ.

Thus, we have

$$\begin{aligned}
\frac{\partial n_{SI}(\tau,t)}{\partial \tau} + \frac{\partial n_{SI}(\tau,t)}{\partial t} &= -m_0 n_{SI}(\tau,t) - r_{2,prim} n_{SI}(\tau,t)\, d\tau \\
\int_0^\infty \left(\frac{\partial n_{SI}(\tau,t)}{\partial \tau} + \frac{\partial n_{SI}(\tau,t)}{\partial t} \right) d\tau &= \int_0^\infty \Big(- m_0 n_{SI}(\tau,t) - r_{2,prim} n_{SI}(\tau,t) \Big)\, d\tau \\
\lim_{s\to\infty} n_{SI}(s,t)\Big|_0^s + \frac{d\Big(\int_0^\infty n_{SI}(\tau,t)\, d\tau \Big)}{dt} &= -(m_0 + r_{2,prim}) \int_0^\infty n_{SI}(\tau,t)\, d\tau \\
-n_{SI}(0,t) + \frac{dN_{SI}(t)}{dt} &= -(m_0 + r_{2,prim}) N_{SI}(t) \\
\frac{dN_{SI}(t)}{dt} &= n_{SI}(0,t) - (m_0 + r_{2,prim}) N_{SI}(t).
\end{aligned}$$

We can find similar results for $n_{IS}(\tau,t)$, $n_{RI}(\tau,t)$, and $n_{IR}(\tau,t)$.

In summary, we have

$$\begin{aligned}
\frac{dN_{SI}(t)}{dt} &= n_{SI}(0,t) - (m_0 + r_{2,prim})N_{SI}(t),\\
\frac{dN_{IS}(t)}{dt} &= n_{IS}(0,t) - (m_0 + r_{1,prim})N_{IS}(t),\\
\frac{dN_{RI}(t)}{dt} &= n_{RI}(0,t) - (m_0 + r_{2,sec})N_{RI}(t),\\
\frac{dN_{IR}(t)}{dt} &= n_{IR}(0,t) - (m_0 + r_{1,sec})N_{IR}(t).
\end{aligned} \tag{5.5}$$

Using the boundary conditions from System (5.1), the equations (5.5), and the definitions (5.2), we write the equations of System (5.1) as

$$\begin{aligned}
\frac{dN_{SS}(t)}{dt} &= \Lambda - m_0 N_{SS}(t) - n_{SI}(0,t) - n_{IS}(0,t),\\
\frac{dN_{SR}(t)}{dt} &= -m_0 N_{SR}(t) - n_{IR}(0,t) + r_{2,prim}N_{SI}(t),\\
\frac{dN_{RS}(t)}{dt} &= -m_0 N_{RS}(t) - n_{RI}(0,t) + r_{1,prim}N_{IS}(t),\\
\frac{dN_{RR}(t)}{dt} &= -m_0 N_{RR}(t) + r_{2,sec}N_{RI}(t) + r_{1,sec}N_{IR}(t),\\
\frac{dN_{SI}(t)}{dt} &= n_{SI}(0,t) - (m_0 + r_{2,prim})N_{SI}(t),\\
\frac{dN_{IS}(t)}{dt} &= n_{IS}(0,t) - (m_0 + r_{1,prim})N_{IS}(t),\\
\frac{dN_{RI}(t)}{dt} &= n_{RI}(0,t) - (m_0 + r_{2,sec})N_{RI}(t),\\
\frac{dN_{IR}(t)}{dt} &= n_{IR}(0,t) - (m_0 + r_{1,sec})N_{IR}(t).
\end{aligned} \tag{5.6}$$

Adding together the equations in (5.6) and using the definition of $N_T(t)$ in (5.4), we find that

$$\frac{dN_T(t)}{dt} = \Lambda - m_0 N_T(t).$$

Thus,

$$N_T(t) = \frac{\Lambda}{m_0} + Ce^{-m_0 t} \leq \frac{\Lambda}{m_0} + C$$

for some constant C.

Thus, the solutions of System (5.1) are bounded. □

5.4.2 Determining generic equilibrium

We look for equilibria of System (5.1) by looking for time-independent solutions that satisfy System (5.1) with the time derivatives equal to zero.

The equilibria

$$\left(N^*_{SS}, N^*_{SR}, N^*_{RS}, N^*_{RR}, n^*_{SI}(\tau), n^*_{IS}(\tau), n^*_{RI}(\tau), n^*_{IR}(\tau)\right)$$

of system (5.1) are given by

$$\begin{aligned}
N^*_{SS} &= \frac{\Lambda - n^*_{SI}(0) - n^*_{IS}(0)}{m_0}, \\
N^*_{SR} &= \frac{r_{2,prim} n^*_{SI}(0) - (m_0 + r_{2,prim}) n^*_{IR}(0)}{m_0(m_0 + r_{2,prim})}, \\
N^*_{RS} &= \frac{r_{1,prim} n^*_{IS}(0) - (m_0 + r_{1,prim}) n^*_{RI}(0)}{m_0(m_0 + r_{1,prim})}, \\
N^*_{RR} &= \frac{1}{m_0}\left(\frac{r_{1,sec} n^*_{IR}(0)}{m_0 + r_{1,sec}} + \frac{r_{2,sec} n^*_{RI}(0)}{m_0 + r_{2,sec}}\right), \\
n^*_{SI}(\tau) &= n^*_{SI}(0) e^{-(m_0 + r_{2,prim})\tau}, \\
n^*_{IS}(\tau) &= n^*_{IS}(0) e^{-(m_0 + r_{1,prim})\tau}, \\
n^*_{RI}(\tau) &= n^*_{RI}(0) e^{-(m_0 + r_{2,sec})\tau}, \\
n^*_{IR}(\tau) &= n^*_{IR}(0) e^{-(m_0 + r_{1,sec})\tau},
\end{aligned} \tag{5.7}$$

where $\big(n^*_{SI}(0), n^*_{IS}(0), n^*_{RI}(0), n^*_{IR}(0)\big)$ are solutions of system (5.8)

$$\begin{aligned}
n^*_{SI}(0) &= \frac{1}{\Lambda}\Big(\Lambda - n^*_{SI}(0) - n^*_{IS}(0)\Big)\Big(n^*_{SI}(0)\Gamma_{2,prim} + n^*_{RI}(0)\Gamma_{2,sec}\Big),\\
n^*_{IS}(0) &= \frac{1}{\Lambda}\Big(\Lambda - n^*_{SI}(0) - n^*_{IS}(0)\Big)\Big(n^*_{IS}(0)\Gamma_{1,prim} + n^*_{IR}(0)\Gamma_{1,sec}\Big),\\
n^*_{RI}(0) &= \frac{1}{\Lambda(m_0 + r_{1,prim})}\Big(r_{1,prim}n^*_{IS}(0) - (m_0 + r_{1,prim})n^*_{RI}(0)\Big)\Big(n^*_{SI}(0)\Gamma_{2,prim} + n^*_{RI}(0)\Gamma_{2,sec}\Big),\\
n^*_{IR}(0) &= \frac{1}{\Lambda(m_0 + r_{2,prim})}\Big(r_{2,prim}n^*_{SI}(0) - (m_0 + r_{2,prim})n^*_{IR}(0)\Big)\Big(n^*_{IS}(0)\Gamma_{1,prim} + n^*_{IR}(0)\Gamma_{1,sec}\Big).
\end{aligned} \tag{5.8}$$

Note that the total equilibrium population remains constant as

$$N^*_T = N^*_{SS} + N^*_{SR} + N^*_{RS} + N^*_{RR} + \int_0^\infty \Big(n^*_{SI}(\tau) + n^*_{IS}(\tau) + n^*_{RI}(\tau) + n^*_{IR}(\tau)\Big)d\tau = \frac{\Lambda}{m_0}.$$

Proposition 5.4.2. *The solutions of System (5.8) can be used to determine the generic equilibrium, as written in Equations (5.7).*

Proof. We look for time-independent solutions

$$\Big(N^*_{SS}, N^*_{SR}, N^*_{RS}, N^*_{RR}, n^*_{SI}(\tau), n^*_{IS}(\tau), n^*_{RI}(\tau), n^*_{IR}(\tau)\Big)$$

that satisfy System (5.1) with the time derivatives equal to zero. Thus, System (5.1) becomes

$$\begin{aligned}
\Lambda - m_0 N^*_{SS} - \frac{N^*_{SS}}{N^*_T}\int_0^\infty \Big[& bV_{1,prim}(\tau)n^*_{IS}(\tau) + bV_{2,prim}(\tau)n^*_{SI}(\tau) \\
& + bV_{1,sec}(\tau)n^*_{IR}(\tau) + bV_{2,sec}(\tau)n^*_{RI}(\tau)\Big]\, d\tau = 0, \\
-m_0 N^*_{SR} - \frac{N^*_{SR}}{N^*_T}\int_0^\infty \Big[& bV_{1,prim}(\tau)n^*_{IS}(\tau) + bV_{1,sec}(\tau)n^*_{IR}(\tau)\Big]\, d\tau \\
& + \int_0^\infty r_{2,prim}n^*_{SI}(\tau)\, d\tau = 0, \\
-m_0 N^*_{RS} - \frac{N^*_{RS}}{N^*_T}\int_0^\infty \Big[& bV_{2,prim}(\tau)n^*_{SI}(\tau) + bV_{2,sec}(\tau)n^*_{RI}(\tau)\Big]\, d\tau \\
& + \int_0^\infty r_{1,prim}n^*_{IS}(\tau)\, d\tau = 0, \\
-m_0 N^*_{RR} + \int_0^\infty & \Big(r_{1,sec}n^*_{IR}(\tau) + r_{2,sec}n^*_{RI}(\tau)\Big) d\tau = 0, \qquad (5.9)
\end{aligned}$$

$$\begin{aligned}
\frac{dn^*_{SI}(\tau)}{d\tau} &= -m_0 n^*_{SI}(\tau) - r_{2,prim}n^*_{SI}(\tau), \\
\frac{dn^*_{IS}(\tau)}{d\tau} &= -m_0 n^*_{IS}(\tau) - r_{1,prim}n^*_{IS}(\tau), \\
\frac{dn^*_{RI}(\tau)}{d\tau} &= -m_0 n^*_{RI}(\tau) - r_{2,sec}n^*_{RI}(\tau), \\
\frac{dn^*_{IR}(\tau)}{d\tau} &= -m_0 n^*_{IR}(\tau) - r_{1,sec}n^*_{IR}(\tau), \qquad (5.10)
\end{aligned}$$

where equations (5.10) have initial conditions

$$\begin{aligned}
n^*_{SI}(0) &= \frac{N^*_{SS}}{N^*_T}\int_0^\infty \Big[bV_{2,prim}(\tau)n^*_{SI}(\tau) + bV_{2,sec}(\tau)n^*_{RI}(\tau)\Big]d\tau,\\
n^*_{IS}(0) &= \frac{N^*_{SS}}{N^*_T}\int_0^\infty \Big[bV_{1,prim}(\tau)n^*_{IS}(\tau) + bV_{1,sec}(\tau)n^*_{IR}(\tau)\Big]d\tau,\\
n^*_{RI}(0) &= \frac{N^*_{RS}}{N^*_T}\int_0^\infty \Big[bV_{2,prim}(\tau)n^*_{SI}(\tau) + bV_{2,sec}(\tau)n^*_{RI}(\tau)\Big]d\tau,\\
n^*_{IR}(0) &= \frac{N^*_{SR}}{N^*_T}\int_0^\infty \Big[bV_{1,prim}(\tau)n^*_{IS}(\tau) + bV_{1,sec}(\tau)n^*_{IR}(\tau)\Big]d\tau. \qquad (5.11)
\end{aligned}$$

Consider

$$\frac{dn^*_{SI}(\tau)}{d\tau} = -m_0 n^*_{SI}(\tau) - r_{2,prim}n^*_{SI}(\tau) \qquad (5.12)$$

with initial condition in τ (i.e. from our boundary conditions of System (5.1))

$$n^*_{SI}(0) = \frac{N^*_{SS}}{N^*_T}\int_0^\infty \Big[bV_{2,prim}(\tau)n^*_{SI}(\tau) + bV_{2,sec}(\tau)n^*_{RI}(\tau)\Big]d\tau. \qquad (5.13)$$

Solving the differential equation in (5.12) we have

$$n^*_{SI}(\tau) = n^*_{SI}(0)e^{-(m_0+r_{2,prim})\tau}. \qquad (5.14)$$

However, note this is not an explicit solution since $n^*_{SI}(0)$ depends on $n^*_{SI}(\tau)$, as can be seen in equation (5.13). We can solve for $n^*_{IS}(\tau)$, $n^*_{RI}(\tau)$, and $n^*_{IR}(\tau)$ similarly.

Thus, in summary, we have

$$\begin{aligned} n^*_{SI}(\tau) &= n^*_{SI}(0)e^{-(m_0+r_{2,prim})\tau}, \\ n^*_{IS}(\tau) &= n^*_{IS}(0)e^{-(m_0+r_{1,prim})\tau}, \\ n^*_{RI}(\tau) &= n^*_{RI}(0)e^{-(m_0+r_{2,sec})\tau}, \\ n^*_{IR}(\tau) &= n^*_{IR}(0)e^{-(m_0+r_{1,sec})\tau}. \end{aligned} \tag{5.15}$$

Substituting the solutions (5.15) into our initial conditions (5.11), we find

$$\begin{aligned} n^*_{SI}(0) &= \frac{N^*_{SS}}{N^*_T}\int_0^\infty \left[bV_{2,prim}(\tau)n^*_{SI}(0)e^{-(m_0+r_{2,prim})\tau} + bV_{2,sec}(\tau)n^*_{RI}(0)e^{-(m_0+r_{2,sec})\tau}\right]d\tau, \\ n^*_{IS}(0) &= \frac{N^*_{SS}}{N^*_T}\int_0^\infty \left[bV_{1,prim}(\tau)n^*_{IS}(0)e^{-(m_0+r_{1,prim})\tau} + bV_{1,sec}(\tau)n^*_{IR}(0)e^{-(m_0+r_{1,sec})\tau}\right]d\tau, \\ n^*_{RI}(0) &= \frac{N^*_{RS}}{N^*_T}\int_0^\infty \left[bV_{2,prim}(\tau)n^*_{SI}(0)e^{-(m_0+r_{2,prim})\tau} + bV_{2,sec}(\tau)n^*_{RI}(0)e^{-(m_0+r_{2,sec})\tau}\right]d\tau, \\ n^*_{IR}(0) &= \frac{N^*_{SR}}{N^*_T}\int_0^\infty \left[bV_{1,prim}(\tau)n^*_{IS}(0)e^{-(m_0+r_{1,prim})\tau} + bV_{1,sec}(\tau)n^*_{IR}(0)e^{-(m_0+r_{1,sec})\tau}\right]d\tau. \end{aligned} \tag{5.16}$$

Using the above definitions (5.16), we can write the other four equations (5.9) as

$$\begin{aligned} \Lambda - m_0N^*_{SS} - n^*_{SI}(0) - n^*_{IS}(0) &= 0, \\ -m_0N^*_{SR} - n^*_{IR}(0) + \int_0^\infty r_{2,prim}n^*_{SI}(0)e^{-(m_0+r_{2,prim})\tau}\,d\tau &= 0, \\ -m_0N^*_{RS} - n^*_{RI}(0) + \int_0^\infty r_{1,prim}n^*_{IS}(0)e^{-(m_0+r_{1,prim})\tau}\,d\tau &= 0, \\ -m_0N^*_{RR} + \int_0^\infty r_{1,sec}n^*_{IR}(0)e^{-(m_0+r_{1,sec})\tau} + r_{2,sec}n^*_{RI}(0)e^{-(m_0+r_{2,sec})\tau}\,d\tau &= 0. \end{aligned} \tag{5.17}$$

Note for $a > 0$, we have

$$\int_0^\infty e^{-a\tau}\,d\tau = \frac{1}{a}.$$

We operate under the assumption that all parameters are positive.

Thus, we can write equations (5.17) as

$$\begin{aligned}
\Lambda - m_0 N^*_{SS} - n^*_{SI}(0) - n^*_{IS}(0) &= 0,\\
-m_0 N^*_{SR} - n^*_{IR}(0) + \frac{r_{2,prim} n^*_{SI}(0)}{m_0 + r_{2,prim}} &= 0,\\
-m_0 N^*_{RS} - n^*_{RI}(0) + \frac{r_{1,prim} n^*_{IS}(0)}{m_0 + r_{1,prim}} &= 0,\\
-m_0 N^*_{RR} + \frac{r_{1,sec} n^*_{IR}(0)}{m_0 + r_{1,sec}} + \frac{r_{2,sec} n^*_{RI}(0)}{m_0 + r_{2,sec}} &= 0.
\end{aligned}$$

Solving these equations for N^*_{SS}, N^*_{SR}, N^*_{RS}, and N^*_{RR}, we have

$$\begin{aligned}
N^*_{SS} &= \frac{\Lambda - n^*_{SI}(0) - n^*_{IS}(0)}{m_0},\\
N^*_{SR} &= \frac{r_{2,prim} n^*_{SI}(0) - (m_0 + r_{2,prim}) n^*_{IR}(0)}{m_0(m_0 + r_{2,prim})},\\
N^*_{RS} &= \frac{r_{1,prim} n^*_{IS}(0) - (m_0 + r_{1,prim}) n^*_{RI}(0)}{m_0(m_0 + r_{1,prim})},\\
N^*_{RR} &= \frac{1}{m_0}\left(\frac{r_{1,sec} n^*_{IR}(0)}{m_0 + r_{1,sec}} + \frac{r_{2,sec} n^*_{RI}(0)}{m_0 + r_{2,sec}}\right).
\end{aligned} \tag{5.18}$$

At this point, we can write the generic equilibrium

$$\Big(N^*_{SS}, N^*_{SR}, N^*_{RS}, N^*_{RR}, n^*_{SI}(\tau), n^*_{IS}(\tau), n^*_{RI}(\tau), n^*_{IR}(\tau)\Big)$$

using the equations in (5.15) and (5.18).

However, these equations still depend on the variables

$$\Big(n^*_{SI}(0), n^*_{IS}(0), n^*_{RI}(0), n^*_{IR}(0)\Big).$$

Thus, we need to derive a system of these variables such that they can be solved for.

Using the equations (5.15), (5.18), and the definition of N_T^*, it can be shown that

$$N_T^* = \frac{\Lambda}{m_0}. \tag{5.19}$$

Substituting the equations (5.18) and (5.19) into equations (5.16), we have

$$\begin{aligned}
n_{SI}^*(0) &= \frac{\Lambda - n_{SI}^*(0) - n_{IS}^*(0)}{\Lambda} \int_0^\infty \Big[bV_{2,prim}(\tau) n_{SI}^*(0) e^{-(m_0+r_{2,prim})\tau} \\
&\qquad + bV_{2,sec}(\tau) n_{RI}^*(0) e^{-(m_0+r_{2,sec})\tau} \Big] d\tau, \\
n_{IS}^*(0) &= \frac{\Lambda - n_{SI}^*(0) - n_{IS}^*(0)}{\Lambda} \int_0^\infty \Big[bV_{1,prim}(\tau) n_{IS}^*(0) e^{-(m_0+r_{1,prim})\tau} \\
&\qquad + bV_{1,sec}(\tau) n_{IR}^*(0) e^{-(m_0+r_{1,sec})\tau} \Big] d\tau, \\
n_{RI}^*(0) &= \frac{r_{2,prim} n_{SI}^*(0) - (m_0 + r_{2,prim}) n_{IR}^*(0)}{\Lambda(m_0 + r_{2,prim})} \int_0^\infty \Big[bV_{2,prim}(\tau) n_{SI}^*(0) e^{-(m_0+r_{2,prim})\tau} \\
&\qquad + bV_{2,sec}(\tau) n_{RI}^*(0) e^{-(m_0+r_{2,sec})\tau} \Big] d\tau, \\
n_{IR}^*(0) &= \frac{r_{1,prim} n_{IS}^*(0) - (m_0 + r_{1,prim}) n_{RI}^*(0)}{\Lambda(m_0 + r_{1,prim})} \int_0^\infty \Big[bV_{1,prim}(\tau) n_{IS}^*(0) e^{-(m_0+r_{1,prim})\tau} \\
&\qquad + bV_{1,sec}(\tau) n_{IR}^*(0) e^{-(m_0+r_{1,sec})\tau} \Big] d\tau.
\end{aligned} \tag{5.20}$$

Using the definitions of $\Gamma_{1,prim}$, $\Gamma_{2,prim}$, $\Gamma_{1,sec}$, and $\Gamma_{2,sec}$, we can write equations (5.20) as

$$\begin{aligned}
n_{SI}^*(0) &= \frac{1}{\Lambda}\Big(\Lambda - n_{SI}^*(0) - n_{IS}^*(0)\Big)\Big(n_{SI}^*(0)\Gamma_{2,prim} + n_{RI}^*(0)\Gamma_{2,sec}\Big), \\
n_{IS}^*(0) &= \frac{1}{\Lambda}\Big(\Lambda - n_{SI}^*(0) - n_{IS}^*(0)\Big)\Big(n_{IS}^*(0)\Gamma_{1,prim} + n_{IR}^*(0)\Gamma_{1,sec}\Big), \\
n_{RI}^*(0) &= \frac{1}{\Lambda(m_0 + r_{1,prim})}\Big(r_{1,prim} n_{IS}^*(0) - (m_0 + r_{1,prim}) n_{RI}^*(0)\Big)\Big(n_{SI}^*(0)\Gamma_{2,prim} + n_{RI}^*(0)\Gamma_{2,sec}\Big), \\
n_{IR}^*(0) &= \frac{1}{\Lambda(m_0 + r_{2,prim})}\Big(r_{2,prim} n_{SI}^*(0) - (m_0 + r_{2,prim}) n_{IR}^*(0)\Big)\Big(n_{IS}^*(0)\Gamma_{1,prim} + n_{IR}^*(0)\Gamma_{1,sec}\Big).
\end{aligned} \tag{5.21}$$

In summary, we now have a system of the variables

$$\Big(n^*_{SI}(0), n^*_{IS}(0), n^*_{RI}(0), n^*_{IR}(0)\Big)$$

that can be solved for. We note the system in (5.21) is the same as System (5.8).

Using the solutions to System (5.8), we can thus write the generic equilibrium

$$\Big(N^*_{SS}, N^*_{SR}, N^*_{RS}, N^*_{RR}, n^*_{SI}(\tau), n^*_{IS}(\tau), n^*_{RI}(\tau), n^*_{IR}(\tau)\Big)$$

using the definitions described in equations (5.15) and (5.18). We note these equations are the same as the ones described in Equations (5.7).

Thus, the proposition is proved. □

The solutions of system (5.8) result in four possible equilibria. We first list the equilibria.

5.4.3 Extinction equilibrium

Proposition 5.4.3. *The extinction equilibrium is*

$$\begin{aligned}&\Big(N^*_{SS}, N^*_{SR}, N^*_{RS}, N^*_{RR}, n^*_{SI}(\tau), n^*_{IS}(\tau), n^*_{RI}(\tau), n^*_{IR}(\tau)\Big)\\ =&\Big(\frac{\Lambda}{m_0}, 0, 0, 0, 0, 0, 0, 0\Big).\end{aligned} \tag{5.22}$$

Proof. Trivially, we see that one solution of System (5.8) is

$$\Big(n^*_{SI}(0), n^*_{IS}(0), n^*_{RI}(0), n^*_{IR}(0)\Big) = (0, 0, 0, 0).$$

Thus, plugging these values into Equations (5.7), we find this equilibrium is

$$\Big(\frac{\Lambda}{m_0}, 0, 0, 0, 0, 0, 0, 0\Big).$$

We denote this equilibrium as the extinction equilibrium. □

5.4.4 Strain 1 equilibrium

Proposition 5.4.4. *The equilibrium where only strain 1 persists is*

$$\begin{aligned}&\Big(N^*_{SS}, N^*_{SR}, N^*_{RS}, N^*_{RR}, n^*_{SI}(\tau), n^*_{IS}(\tau), n^*_{RI}(\tau), n^*_{IR}(\tau)\Big)\\ =&\Big(\frac{\Lambda}{\Gamma_{1,prim}}, 0, \frac{\Lambda r_{1,prim}(\Gamma_{1,prim}-1)}{m_0(m_0+r_{1,prim}\Gamma_{1,prim})}, 0, 0, \frac{\Lambda(\Gamma_{1,prim}-1)}{\Gamma_{1,prim}}e^{-(m_0+r_{1,prim})\tau}, 0, 0\Big). \qquad (5.23)\end{aligned}$$

Proof. To find a non-trivial solution to System (5.8), we first assume that $n^*_{IR}(0) = 0$ and $n^*_{RI}(0) = 0$. We also assume that $n^*_{IS}(0)$ is nonzero.

Thus, the second equation from System (5.8) becomes

$$n^*_{IS}(0) - \frac{1}{\Lambda}\Big(\Lambda - n^*_{SI}(0) - n^*_{IS}(0)\Big)\Big(n^*_{IS}(0)\Gamma_{1,prim}\Big) = 0,$$

which implies

$$n^*_{IS}(0)\Big(\Lambda(1-\Gamma_{1,prim}) + \Gamma_{1,prim}n^*_{IS}(0) + \Gamma_{1,prim}n^*_{SI}(0)\Big) = 0.$$

Since $n^*_{IS}(0)$ is nonzero,

$$\Lambda(1-\Gamma_{1,prim}) + \Gamma_{1,prim}n^*_{IS}(0) + \Gamma_{1,prim}n^*_{SI}(0) = 0,$$

which implies

$$n^*_{IS}(0) = \frac{\Lambda(\Gamma_{1,prim}-1) - \Gamma_{1,prim}n^*_{SI}(0)}{\Gamma_{1,prim}}. \qquad (5.24)$$

Because $n^*_{RI}(0) = 0$, the third equation in System (5.8) becomes

$$\frac{1}{\Lambda(m_0 + r_{1,prim})}\Big(r_{1,prim} n^*_{IS}(0)\Big)\Big(n^*_{SI}(0)\Gamma_{2,prim}\Big) = 0.$$

Since $n^*_{IS}(0)$ is nonzero, we thus have that $n^*_{SI}(0) = 0$.

Thus, equation (5.24) becomes

$$n^*_{IS}(0) = \frac{\Lambda(\Gamma_{1,prim} - 1)}{\Gamma_{1,prim}}.$$

In summary, a solution to System (5.8) is

$$\Big(n^*_{SI}(0), n^*_{IS}(0), n^*_{RI}(0), n^*_{IR}(0)\Big) = \Big(0, \frac{\Lambda(\Gamma_{1,prim} - 1)}{\Gamma_{1,prim}}, 0, 0\Big).$$

Thus, plugging these values into Equations (5.7), we find this equilibrium is

$$\begin{aligned}&\Big(N^*_{SS}, N^*_{SR}, N^*_{RS}, N^*_{RR}, n^*_{SI}(\tau), n^*_{IS}(\tau), n^*_{RI}(\tau), n^*_{IR}(\tau)\Big)\\ =&\Big(\frac{\Lambda}{\Gamma_{1,prim}}, 0, \frac{\Lambda r_{1,prim}(\Gamma_{1,prim} - 1)}{m_0(m_0 + r_{1,prim}\Gamma_{1,prim})}, 0, 0, \frac{\Lambda(\Gamma_{1,prim} - 1)}{\Gamma_{1,prim}} e^{-(m_0 + r_{1,prim})\tau}, 0, 0\Big).\end{aligned}$$

We denote this as the equilibrium where only strain 1 persists. □

5.4.5 Strain 2 equilibrium

Proposition 5.4.5. *The equilibrium where only strain 2 persists is*

$$\begin{aligned}&\Big(N^*_{SS}, N^*_{SR}, N^*_{RS}, N^*_{RR}, n^*_{SI}(\tau), n^*_{IS}(\tau), n^*_{RI}(\tau), n^*_{IR}(\tau)\Big)\\ =&\Big(\frac{\Lambda}{\Gamma_{2,prim}}, \frac{\Lambda r_{2,prim}(\Gamma_{2,prim} - 1)}{m_0(m_0 + r_{2,prim}\Gamma_{2,prim})}, 0, 0, \frac{\Lambda(\Gamma_{2,prim} - 1)}{\Gamma_{2,prim}} e^{-(m_0 + r_{2,prim})\tau}, 0, 0, 0\Big). \qquad (5.25)\end{aligned}$$

Proof. The proposition is proved similar to Proposition 5.4.4 by interchanging $n^*_{IS}(0)$ with $n^*_{SI}(0)$.

Also, the first equation from System (5.8) is used instead of the second equation.

In summary, a solution to System (5.8) is

$$\left(n^*_{SI}(0), n^*_{IS}(0), n^*_{RI}(0), n^*_{IR}(0)\right) = \left(\frac{\Lambda(\Gamma_{2,prim}-1)}{\Gamma_{2,prim}}, 0, 0, 0\right).$$

Thus, plugging these values into Equations (5.7), we find this equilibrium is

$$\begin{aligned}&\left(N^*_{SS}, N^*_{SR}, N^*_{RS}, N^*_{RR}, n^*_{SI}(\tau), n^*_{IS}(\tau), n^*_{RI}(\tau), n^*_{IR}(\tau)\right)\\ =&\left(\frac{\Lambda}{\Gamma_{2,prim}}, \frac{\Lambda r_{2,prim}(\Gamma_{2,prim}-1)}{m_0(m_0+r_{2,prim}\Gamma_{2,prim})}, 0, 0, \frac{\Lambda(\Gamma_{2,prim}-1)}{\Gamma_{2,prim}}e^{-(m_0+r_{2,prim})\tau}, 0, 0, 0\right).\end{aligned}$$

We denote this as the equilibrium where only strain 2 persists. □

5.4.6 Coexistence equilibrium

Remark 5.4.1. *There are two coexistence equilibria.*

Using Mathematica, we find that there exist two solutions to System (5.8) such that the terms

$$\left(n^*_{SI}(0), n^*_{IS}(0), n^*_{RI}(0), n^*_{IR}(0)\right)$$

are all nonzero.

Assuming all positive parameters, we find that at most one of the solutions has all positive terms.

Thus, plugging these values back into Equations (5.7), we find two distinct coexistence equilibria, where at most one coexistence equilibrium is positive.

However, they are difficult to write explicitly for general parameters.

Therefore, using specific parameters, we solve for the equilibria numerically using System (5.8) and Equations (5.7).

5.4.7 Determining generic stability

We now determine the stability for a generic equilibrium. We can then use these results to determine the stability of our equilibria.

Define C_1, C_2, $\Gamma_{1,prim,\lambda}$, $\Gamma_{2,prim,\lambda}$, $\Gamma_{1,sec,\lambda}$, and $\Gamma_{2,sec,\lambda}$ as

$$\begin{aligned}
C_1 &= \frac{m_0}{\Lambda}\int_0^\infty \left(bV_{1,prim}(\tau)n^*_{IS}(\tau) + bV_{1,sec}(\tau)n^*_{IR}(\tau)\right)d\tau,\\
C_2 &= \frac{m_0}{\Lambda}\int_0^\infty \left(bV_{2,prim}(\tau)n^*_{SI}(\tau) + bV_{2,sec}(\tau)n^*_{RI}(\tau)\right)d\tau,\\
\Gamma_{1,prim,\lambda} &= \frac{m_0}{\Lambda}\int_0^\infty bV_{1,prim}(\tau)e^{-(m_0+r_{1,prim}+\lambda)\tau}\,d\tau,\\
\Gamma_{2,prim,\lambda} &= \frac{m_0}{\Lambda}\int_0^\infty bV_{2,prim}(\tau)e^{-(m_0+r_{2,prim}+\lambda)\tau}\,d\tau,\\
\Gamma_{1,sec,\lambda} &= \frac{m_0}{\Lambda}\int_0^\infty bV_{1,sec}(\tau)e^{-(m_0+r_{1,sec}+\lambda)\tau}\,d\tau,\\
\Gamma_{2,sec,\lambda} &= \frac{m_0}{\Lambda}\int_0^\infty bV_{2,sec}(\tau)e^{-(m_0+r_{2,sec}+\lambda)\tau}\,d\tau.
\end{aligned}$$

Proposition 5.4.6. *Consider the generic equilibrium*

$$\Big(N^*_{SS}, N^*_{SR}, N^*_{RS}, N^*_{RR}, n^*_{SI}(\tau), n^*_{IS}(\tau), n^*_{RI}(\tau), n^*_{IR}(\tau)\Big).$$

Assume

$$N_T(t) = \frac{\Lambda}{m_0}.$$

Using the matrix definition $M_\lambda =$

$$\begin{pmatrix} \lambda+m_0 & 0 & 0 & 1 & 1 & 0 & 0 \\ 0 & \lambda+m_0 & 0 & \frac{-r_{2,prim}}{\lambda+m_0+r_{2,prim}} & 0 & 0 & 1 \\ 0 & 0 & \lambda+m_0 & 0 & \frac{-r_{1,prim}}{\lambda+m_0+r_{1,prim}} & 1 & 0 \\ -C_2 & 0 & 0 & 1-N^*_{SS}\Gamma_{2,prim,\lambda} & 0 & -N^*_{SS}\Gamma_{2,sec,\lambda} & 0 \\ -C_1 & 0 & 0 & 0 & 1-N^*_{SS}\Gamma_{1,prim,\lambda} & 0 & -N^*_{SS}\Gamma_{1,sec,\lambda} \\ 0 & 0 & -C_2 & -N^*_{RS}\Gamma_{2,prim,\lambda} & 0 & 1-N^*_{RS}\Gamma_{2,sec,\lambda} & 0 \\ 0 & -C_1 & 0 & 0 & -N^*_{SR}\Gamma_{1,prim,\lambda} & 0 & 1-N^*_{SR}\Gamma_{1,sec,\lambda} \end{pmatrix}, \quad (5.26)$$

the stability of the equilibrium can be found by analyzing the solutions to the equation

$$\det(M_\lambda) = 0.$$

If all the solutions have negative real parts, then the generic equilibrium is locally asymptotically stable. If at least one of the solutions has positive real parts, then the generic equilibrium is unstable.

Proof. Consider the generic equilibrium

$$\Big(N^*_{SS}, N^*_{SR}, N^*_{RS}, N^*_{RR}, n^*_{SI}(\tau), n^*_{IS}(\tau), n^*_{RI}(\tau), n^*_{IR}(\tau)\Big).$$

To determine the stability of this particular equilibrium of the system, we first linearize System (5.1) around the equilibrium.

We let

$$\begin{aligned}
N_{SS}(t) &= N^*_{SS} + N_{SSp}(t),\\
N_{SR}(t) &= N^*_{SR} + N_{SRp}(t),\\
N_{RS}(t) &= N^*_{RS} + N_{RSp}(t),\\
N_{RR}(t) &= N^*_{RR} + N_{RRp}(t),\\
n_{SI}(\tau,t) &= n^*_{SI}(\tau) + n_{SIp}(\tau,t),\\
n_{IS}(\tau,t) &= n^*_{IS}(\tau) + n_{ISp}(\tau,t),\\
n_{RI}(\tau,t) &= n^*_{RI}(\tau) + n_{RIp}(\tau,t),\\
n_{IR}(\tau,t) &= n^*_{IR}(\tau) + n_{IRp}(\tau,t),
\end{aligned} \tag{5.27}$$

where the functions with subscript p represent perturbations from the equilibrium.

Recall

$$N_T(t) = \frac{\Lambda}{m_0}. \tag{5.28}$$

Plugging in definitions (5.27) and (5.28) into System (5.1) and its boundary conditions, we

have

$$
\begin{aligned}
\frac{d\Big(N^*_{SS}+N_{SSp}(t)\Big)}{dt} &= \Lambda - m_0\Big(N^*_{SS}+N_{SS}(t)\Big)\\
&\quad - \frac{m_0}{\Lambda}\Big(N^*_{SS}+N_{SSp}(t)\Big)\int_0^\infty \Big[bV_{1,prim}(\tau)\Big(n^*_{IS}(\tau)+n_{ISp}(\tau,t)\Big)\\
&\quad + bV_{2,prim}(\tau)\Big(n^*_{SI}(\tau)+n_{SIp}(\tau,t)\Big) + bV_{1,sec}(\tau)\Big(n^*_{IR}(\tau)+n_{IRp}(\tau,t)\Big)\\
&\quad + bV_{2,sec}(\tau)\Big(n^*_{RI}(\tau)+n_{RIp}(\tau,t)\Big)\Big]d\tau,\\
\frac{d\Big(N^*_{SR}+N_{SpR}(t)\Big)}{dt} &= -m_0\Big(N^*_{SR}+N_{SRp}(t)\Big)\\
&\quad - \frac{m_0}{\Lambda}\Big(N^*_{SR}+N_{SRp}(t)\Big)\int_0^\infty \Big[bV_{1,prim}(\tau)\Big(n^*_{IS}(\tau)+n_{ISp}(\tau,t)\Big)\\
&\quad + bV_{1,sec}(\tau)\Big(n^*_{IR}(\tau)+n_{IRp}(\tau,t)\Big)\Big]d\tau + \int_0^\infty r_{2,prim}\Big(n^*_{SI}(\tau)+n_{SIp}(\tau,t)\Big)\,d\tau,\\
\frac{d\Big(N^*_{RS}+N_{RSp}(t)\Big)}{dt} &= -m_0\Big(N^*_{RS}+N_{RSp}(t)\Big)\\
&\quad - \frac{m_0}{\Lambda}\Big(N^*_{RS}+N_{RSp}(t)\Big)\int_0^\infty \Big[bV_{2,prim}(\tau)\Big(n^*_{SI}(\tau)+n_{SIp}(\tau,t)\Big)\\
&\quad + bV_{2,sec}(\tau)\Big(n^*_{RI}(\tau)+n_{RIp}(\tau,t)\Big)\Big]d\tau + \int_0^\infty r_{1,prim}\Big(n^*_{IS}(\tau)+n_{ISp}(\tau,t)\Big)\,d\tau,\\
\frac{d\Big(N^*_{RR}+N_{RRp}(t)\Big)}{dt} &= -m_0\Big(N^*_{RR}+N_{RRp}(t)\Big)\\
&\quad + \int_0^\infty r_{1,sec}\Big(n^*_{IR}(\tau)+n_{IR}(\tau,t)\Big) + r_{2,sec}\Big(n^*_{RI}(\tau)+n_{RI}(\tau,t)\Big)d\tau,
\end{aligned}
$$

$$
\begin{aligned}
\frac{\partial\Big(n^*_{SI}(\tau)+n_{SIp}(\tau,t)\Big)}{\partial\tau} + \frac{\partial\Big(n^*_{SI}(\tau)+n_{SIp}(\tau,t)\Big)}{\partial t} &= -(m_0+r_{2,prim})\Big(n^*_{SI}(\tau)+n_{SIp}(\tau,t)\Big),\\
\frac{\partial\Big(n^*_{IS}(\tau)+n_{ISp}(\tau,t)\Big)}{\partial\tau} + \frac{\partial\Big(n^*_{IS}(\tau)+n_{ISp}(\tau,t)\Big)}{\partial t} &= -(m_0+r_{1,prim})\Big(n^*_{IS}(\tau)+n_{ISp}(\tau,t)\Big),\\
\frac{\partial\Big(n^*_{RI}(\tau)+n_{RIp}(\tau,t)\Big)}{\partial\tau} + \frac{\partial\Big(n^*_{RI}(\tau)+n_{RIp}(\tau,t)\Big)}{\partial t} &= -(m_0+r_{2,sec})\Big(n^*_{RI}(\tau)+n_{RIp}(\tau,t)\Big),\\
\frac{\partial\Big(n^*_{IR}(\tau)+n_{IRp}(\tau,t)\Big)}{\partial\tau} + \frac{\partial\Big(n^*_{IR}(\tau)+n_{IRp}(\tau,t)\Big)}{\partial t} &= -(m_0+r_{1,sec})\Big(n^*_{IR}(\tau)+n_{IRp}(\tau,t)\Big),
\end{aligned}
$$

$$\Big(n^*_{SI}(0)+n_{SIp}(0,t)\Big)=\frac{m_0}{\Lambda}\Big(N^*_{SS}+N_{SSp}(t)\Big)\int_0^\infty\Big[bV_{2,prim}(\tau)\Big(n^*_{SI}(\tau)+n_{SIp}(\tau,t)\Big)$$
$$+bV_{2,sec}(\tau)\Big(n^*_{RI}(\tau)+n_{RIp}(\tau,t)\Big)\Big]d\tau,$$
$$\Big(n^*_{IS}(0)+n_{ISp}(0,t)\Big)=\frac{m_0}{\Lambda}\Big(N^*_{SS}+N_{SSp}(t)\Big)\int_0^\infty\Big[bV_{1,prim}(\tau)\Big(n^*_{IS}(\tau)+n_{ISp}(\tau,t)\Big)$$
$$+bV_{1,sec}(\tau)\Big(n^*_{IR}(\tau)+n_{IRp}(\tau,t)\Big)\Big]d\tau,$$
$$\Big(n^*_{RI}(0)+n_{RIp}(0,t)\Big)=\frac{m_0}{\Lambda}\Big(N^*_{RS}+N_{RSp}(t)\Big)\int_0^\infty\Big[bV_{2,prim}(\tau)\Big(n^*_{SI}(\tau)+n_{SIp}(\tau,t)\Big)$$
$$+bV_{2,sec}(\tau)\Big(n^*_{RI}(\tau)+n_{RIp}(\tau,t)\Big)\Big]d\tau,$$
$$\Big(n^*_{IR}(0)+n_{IRp}(0,t)\Big)=\frac{m_0}{\Lambda}\Big(N^*_{SR}+N_{SRp}(t)\Big)\int_0^\infty\Big[bV_{1,prim}(\tau)\Big(n^*_{IS}(\tau)+n_{ISp}(\tau,t)\Big)$$
$$+bV_{1,sec}(\tau)\Big(n^*_{IR}(\tau)+n_{IRp}(\tau,t)\Big)\Big]d\tau.$$

Through multiplying out and taking derivatives, we have the following system.

$$
\begin{aligned}
\frac{dN_{SSp}(t)}{dt} &= \Lambda - m_0 N^*_{SS} \\
&\quad - \frac{m_0 N^*_{SS}}{\Lambda} \int_0^\infty \Big[bV_{1,prim}(\tau) n^*_{IS}(\tau) + bV_{2,prim}(\tau) n^*_{SI}(\tau) + bV_{1,sec}(\tau) n^*_{IR}(\tau) + bV_{2,sec}(\tau) n^*_{RI}(\tau) \Big] d\tau \\
&\quad - m_0 N_{SSp}(t) \\
&\quad - \frac{m_0 N^*_{SS}}{\Lambda} \int_0^\infty \Big[bV_{1,prim}(\tau) n_{ISp}(\tau,t) + bV_{2,prim}(\tau) n_{SIp}(\tau,t) \\
&\qquad\qquad + bV_{1,sec}(\tau) n_{IRp}(\tau,t) + bV_{2,sec}(\tau) n_{RIp}(\tau,t) \Big] d\tau \\
&\quad - \frac{m_0 N_{SSp}(t)}{\Lambda} \int_0^\infty \Big[bV_{1,prim}(\tau) n^*_{IS}(\tau) + bV_{2,prim}(\tau) n^*_{SI}(\tau) + bV_{1,sec}(\tau) n^*_{IR}(\tau) + bV_{2,sec}(\tau) n^*_{RI}(\tau) \Big] d\tau \\
&\quad - \frac{m_0 N_{SSp}(t)}{\Lambda} \int_0^\infty \Big[bV_{1,prim}(\tau) n_{ISp}(\tau,t) + bV_{2,prim}(\tau) n_{SIp}(\tau,t) \\
&\qquad\qquad + bV_{1,sec}(\tau) n_{IRp}(\tau,t) + bV_{2,sec}(\tau) n_{RIp}(\tau,t) \Big] d\tau, \\
\frac{dN_{SRp}(t)}{dt} &= -m_0 N^*_{SR} - \frac{m_0 N^*_{SR}}{\Lambda} \int_0^\infty \Big[bV_{1,prim}(\tau) n^*_{IS}(\tau) + bV_{1,sec}(\tau) n^*_{IR}(\tau) \Big] d\tau + \int_0^\infty r_{2,prim} n^*_{SI}(\tau)\, d\tau \\
&\quad - m_0 N_{SRp}(t) - \frac{m_0 N^*_{SR}}{\Lambda} \int_0^\infty \Big[bV_{1,prim}(\tau) n_{ISp}(\tau,t) + bV_{1,sec}(\tau) n_{IRp}(\tau,t) \Big] d\tau \\
&\quad - \frac{m_0 N_{SRp}(t)}{\Lambda} \int_0^\infty \Big[bV_{1,prim}(\tau) n^*_{IS}(\tau) + bV_{1,sec}(\tau) n^*_{IR}(\tau) \Big] d\tau + \int_0^\infty r_{2,prim} n_{SIp}(\tau,t)\, d\tau \\
&\quad - \frac{m_0 N_{SRp}(t)}{\Lambda} \int_0^\infty \Big[bV_{1,prim}(\tau) n_{ISp}(\tau,t) + bV_{1,sec}(\tau) n_{IRp}(\tau,t) \Big] d\tau, \\
\frac{dN_{RSp}(t)}{dt} &= -m_0 N^*_{RS} - \frac{m_0 N^*_{RS}}{\Lambda} \int_0^\infty \Big[bV_{2,prim}(\tau) n^*_{SI}(\tau) + bV_{2,sec}(\tau) n^*_{RI}(\tau) \Big] d\tau + \int_0^\infty r_{1,prim} n^*_{IS}(\tau)\, d\tau \\
&\quad - m_0 N_{RSp}(t) - \frac{m_0 N^*_{RS}}{\Lambda} \int_0^\infty \Big[bV_{2,prim}(\tau) n_{SIp}(\tau,t) + bV_{2,sec}(\tau) n_{RIp}(\tau,t) \Big] d\tau \\
&\quad - \frac{m_0 N_{RSp}(t)}{\Lambda} \int_0^\infty \Big[bV_{2,prim}(\tau) n^*_{SI}(\tau) + bV_{2,sec}(\tau) n^*_{RI}(\tau) \Big] d\tau + \int_0^\infty r_{1,prim} n_{ISp}(\tau,t)\, d\tau \\
&\quad - \frac{m_0 N_{RSp}(t)}{\Lambda} \int_0^\infty \Big[bV_{2,prim}(\tau) n_{SIp}(\tau,t) + bV_{2,sec}(\tau) n_{RIp}(\tau,t) \Big] d\tau, \\
\frac{dN_{RRp}(t)}{dt} &= -m_0 N^*_{RR} + \int_0^\infty \Big[r_{2,prim} n^*_{IR}(\tau) + r_{2,sec} n^*_{RI}(\tau) \Big] d\tau \\
&\quad - m_0 N_{RRp}(t) + \int_0^\infty \Big[r_{2,prim} n_{IRp}(\tau,t) + r_{2,sec} n_{RIp}(\tau,t) \Big] d\tau,
\end{aligned}
$$

$$\frac{dn^*_{SI}(\tau)}{d\tau} + \frac{\partial n_{SIp}(\tau,t)}{\partial\tau} + \frac{\partial n_{SIp}(\tau,t)}{\partial t} = -(m_0 + r_{2,prim})n^*_{SI}(\tau) - (m_0 + r_{2,prim})n_{SIp}(\tau,t),$$
$$\frac{dn^*_{IS}(\tau)}{d\tau} + \frac{\partial n_{ISp}(\tau,t)}{\partial\tau} + \frac{\partial n_{ISp}(\tau,t)}{\partial t} = -(m_0 + r_{1,prim})n^*_{IS}(\tau) - (m_0 + r_{1,prim})n_{ISp}(\tau,t),$$
$$\frac{dn^*_{RI}(\tau)}{d\tau} + \frac{\partial n_{RIp}(\tau,t)}{\partial\tau} + \frac{\partial n_{RIp}(\tau,t)}{\partial t} = -(m_0 + r_{2,sec})n^*_{RI}(\tau) - (m_0 + r_{2,sec})n_{RIp}(\tau,t),$$
$$\frac{dn^*_{IR}(\tau)}{d\tau} + \frac{\partial n_{IRp}(\tau,t)}{\partial\tau} + \frac{\partial n_{IRp}(\tau,t)}{\partial t} = -(m_0 + r_{1,sec})n^*_{IR}(\tau) - (m_0 + r_{1,sec})n_{IRp}(\tau,t),$$

$$\begin{aligned}
n^*_{SI}(0) + n_{SIp}(0,t) &= \frac{m_0 N^*_{SS}}{\Lambda}\int_0^\infty \Big[bV_{2,prim}(\tau)n^*_{SI}(\tau) + bV_{2,sec}(\tau)n^*_{RI}(\tau)\Big]d\tau \\
&+ \frac{m_0 N^*_{SS}}{\Lambda}\int_0^\infty \Big[bV_{2,prim}(\tau)n_{SIp}(\tau,t) + bV_{2,sec}(\tau)n_{RIp}(\tau,t)\Big]d\tau \\
&+ \frac{m_0 N_{SSp}(t)}{\Lambda}\int_0^\infty \Big[bV_{2,prim}(\tau)n^*_{SI}(\tau) + bV_{2,sec}(\tau)n^*_{RI}(\tau)\Big]d\tau \\
&+ \frac{m_0 N_{SSp}(t)}{\Lambda}\int_0^\infty \Big[bV_{2,prim}(\tau)n_{SIp}(\tau,t) + bV_{2,sec}(\tau)n_{RIp}(\tau,t)\Big]d\tau, \\
n^*_{IS}(0) + n_{ISp}(0,t) &= \frac{m_0 N^*_{SS}}{\Lambda}\int_0^\infty \Big[bV_{1,prim}(\tau)n^*_{IS}(\tau) + bV_{1,sec}(\tau)n^*_{IR}(\tau)\Big]d\tau \\
&+ \frac{m_0 N^*_{SS}}{\Lambda}\int_0^\infty \Big[bV_{1,prim}(\tau)n_{ISp}(\tau,t) + bV_{1,sec}(\tau)n_{IRp}(\tau,t)\Big]d\tau \\
&+ \frac{m_0 N_{SSp}(t)}{\Lambda}\int_0^\infty \Big[bV_{1,prim}(\tau)n^*_{IS}(\tau) + bV_{1,sec}(\tau)n^*_{IR}(\tau)\Big]d\tau \\
&+ \frac{m_0 N_{SSp}(t)}{\Lambda}\int_0^\infty \Big[bV_{1,prim}(\tau)n_{ISp}(\tau,t) + bV_{1,sec}(\tau)n_{IRp}(\tau,t)\Big]d\tau, \\
n^*_{RI}(0) + n_{RIp}(0,t) &= \frac{m_0 N^*_{RS}}{\Lambda}\int_0^\infty \Big[bV_{2,prim}(\tau)n^*_{SI}(\tau) + bV_{2,sec}(\tau)n^*_{RI}(\tau)\Big]d\tau \\
&+ \frac{m_0 N^*_{RS}}{\Lambda}\int_0^\infty \Big[bV_{2,prim}(\tau)n_{SIp}(\tau,t) + bV_{2,sec}(\tau)n_{RIp}(\tau,t)\Big]d\tau \\
&+ \frac{m_0 N_{RSp}(t)}{\Lambda}\int_0^\infty \Big[bV_{2,prim}(\tau)n^*_{SI}(\tau) + bV_{2,sec}(\tau)n^*_{RI}(\tau)\Big]d\tau \\
&+ \frac{m_0 N_{RSp}(t)}{\Lambda}\int_0^\infty \Big[bV_{2,prim}(\tau)n_{SIp}(\tau,t) + bV_{2,sec}(\tau)n_{RIp}(\tau,t)\Big]d\tau, \\
n^*_{IR}(0) + n_{IRp}(0,t) &= \frac{m_0 N^*_{SR}}{\Lambda}\int_0^\infty \Big[bV_{1,prim}(\tau)n^*_{IS}(\tau) + bV_{1,sec}(\tau)n^*_{IR}(\tau)\Big]d\tau \\
&+ \frac{m_0 N^*_{SR}}{\Lambda}\int_0^\infty \Big[bV_{1,prim}(\tau)n_{ISp}(\tau,t) + bV_{1,sec}(\tau)n_{IRp}(\tau,t)\Big]d\tau \\
&+ \frac{m_0 N_{SRp}(t)}{\Lambda}\int_0^\infty \Big[bV_{1,prim}(\tau)n^*_{IS}(\tau) + bV_{1,sec}(\tau)n^*_{IR}(\tau)\Big]d\tau \\
&+ \frac{m_0 N_{SRp}(t)}{\Lambda}\int_0^\infty \Big[bV_{1,prim}(\tau)n_{ISp}(\tau,t) + bV_{1,sec}(\tau)n_{IRp}(\tau,t)\Big]d\tau. \qquad (5.29)
\end{aligned}$$

At equilibrium, since $N_T^* = \dfrac{\Lambda}{m_0}$, the following equations are satisfied, as described in Equations (5.9), (5.10), and (5.11).

$$\begin{aligned}
\Lambda - m_0 N_{SS}^* - \frac{m_0 N_{SS}^*}{\Lambda}\int_0^\infty \Big[bV_{1,prim}n_{IS}^*(\tau) + bV_{2,prim}(\tau)n_{SI}^*(\tau) + bV_{1,sec}n_{IR}^*(\tau) + bV_{2,sec}(\tau)n_{RI}^*(\tau)\Big]d\tau = 0,\\
-m_0 N_{SR}^* - \frac{m_0 N_{SR}^*}{\Lambda}\int_0^\infty \Big[bV_{1,prim}(\tau)n_{IS}^*(\tau) + bV_{1,sec}(\tau)n_{IR}^*(\tau)\Big]d\tau + \int_0^\infty r_{2,prim}n_{SI}^*(\tau)\,d\tau = 0,\\
-m_0 N_{RS}^* - \frac{m_0 N_{RS}^*}{\Lambda}\int_0^\infty \Big[bV_{2,prim}(\tau)n_{SI}^*(\tau) + bV_{2,sec}(\tau)n_{RI}^*(\tau)\Big]d\tau + \int_0^\infty r_{1,prim}n_{IS}^*(\tau)\,d\tau = 0,\\
-m_0 N_{RR}^* + \int_0^\infty \Big[r_{1,sec}n_{IR}^*(\tau) + r_{2,sec}n_{RI}(\tau)^*\Big]d\tau = 0,
\end{aligned}$$

$$\begin{aligned}
\frac{dn_{SI}^*(\tau)}{d\tau} &= -(m_0 + r_{2,prim})n_{SI}^*(\tau),\\
\frac{dn_{IS}^*(\tau)}{d\tau} &= -(m_0 + r_{1,prim})n_{IS}^*(\tau),\\
\frac{dn_{RI}^*(\tau)}{d\tau} &= -(m_0 + r_{2,sec})n_{RI}^*(\tau),\\
\frac{dn_{IR}^*(\tau)}{d\tau} &= -(m_0 + r_{1,sec})n_{IR}^*(\tau),
\end{aligned}$$

$$\begin{aligned}
n_{SI}^*(0) &= \frac{m_0 N_{SS}^*}{\Lambda}\int_0^\infty \Big[bV_{2,prim}(\tau)n_{SI}^*(\tau) + bV_{2,sec}(\tau)n_{RI}^*(\tau)\Big]d\tau,\\
n_{IS}^*(0) &= \frac{m_0 N_{SS}^*}{\Lambda}\int_0^\infty \Big[bV_{1,prim}(\tau)n_{IS}^*(\tau) + bV_{1,sec}(\tau)n_{IR}^*(\tau)\Big]d\tau,\\
n_{RI}^*(0) &= \frac{m_0 N_{RS}^*}{\Lambda}\int_0^\infty \Big[bV_{2,prim}(\tau)n_{SI}^*(\tau) + bV_{2,sec}(\tau)n_{RI}^*(\tau)\Big]d\tau,\\
n_{IR}^*(0) &= \frac{m_0 N_{SR}^*}{\Lambda}\int_0^\infty \Big[bV_{1,prim}(\tau)n_{IS}^*(\tau) + bV_{1,sec}(\tau)n_{IR}^*(\tau)\Big]d\tau.
\end{aligned} \tag{5.30}$$

Since we assume our perturbations are small, we can ignore any quadratic terms of perturbations. Using the equations (5.30) and ignoring the quadratic terms of perturbations, we

can simplify system (5.29) to the following system.

$$
\begin{aligned}
\frac{dN_{SSp}(t)}{dt} &= -m_0 N_{SSp}(t) \\
&\quad - \frac{m_0 N^*_{SS}}{\Lambda} \int_0^\infty \Big[bV_{1,prim}(\tau) n_{ISp}(\tau,t) + bV_{2,prim}(\tau) n_{SIp}(\tau,t) \\
&\qquad\qquad + bV_{1,sec}(\tau) n_{IRp}(\tau,t) + bV_{2,sec}(\tau) n_{RIp}(\tau,t) \Big] d\tau \\
&\quad - \frac{m_0 N_{SSp}(t)}{\Lambda} \int_0^\infty \Big[bV_{1,prim}(\tau) n^*_{IS}(\tau) + bV_{2,prim}(\tau) n^*_{SI}(\tau) \\
&\qquad\qquad + bV_{1,sec}(\tau) n^*_{IR}(\tau) + bV_{2,sec}(\tau) n^*_{RI}(\tau) \Big] d\tau, \\
\frac{dN_{SRp}(t)}{dt} &= -m_0 N_{SRp}(t) - \frac{m_0 N^*_{SR}}{\Lambda} \int_0^\infty \Big[bV_{1,prim}(\tau) n_{ISp}(\tau,t) + bV_{1,sec}(\tau) n_{IRp}(\tau,t) \Big] d\tau \\
&\quad - \frac{m_0 N_{SRp}(t)}{\Lambda} \int_0^\infty \Big[bV_{1,prim}(\tau) n^*_{IS}(\tau) + bV_{1,sec}(\tau) n^*_{IR}(\tau) \Big] d\tau + \int_0^\infty r_{2,prim} n_{SIp}(\tau,t)\, d\tau, \\
\frac{dN_{RSp}(t)}{dt} &= -m_0 N_{RSp}(t) - \frac{m_0 N^*_{RS}}{\Lambda} \int_0^\infty \Big[bV_{2,prim}(\tau) n_{SIp}(\tau,t) + bV_{2,sec}(\tau) n_{RIp}(\tau,t) \Big] d\tau \\
&\quad - \frac{m_0 N_{RSp}(t)}{\Lambda} \int_0^\infty \Big[bV_{2,prim}(\tau) n^*_{SI}(\tau) + bV_{2,sec}(\tau) n^*_{RI}(\tau) \Big] d\tau + \int_0^\infty r_{1,prim} n_{ISp}(\tau,t)\, d\tau, \\
\frac{dN_{RRp}(t)}{dt} &= -m_0 N_{RRp}(t) + \int_0^\infty \Big[r_{2,prim} n_{IRp}(\tau,t) + r_{2,sec} n_{RIp}(\tau,t) \Big] d\tau,
\end{aligned}
$$

$$
\begin{aligned}
\frac{\partial n_{SIp}(\tau,t)}{\partial \tau} + \frac{\partial n_{SIp}(\tau,t)}{\partial t} &= -(m_0 + r_{2,prim}) n_{SIp}(\tau,t), \\
\frac{\partial n_{ISp}(\tau,t)}{\partial \tau} + \frac{\partial n_{ISp}(\tau,t)}{\partial t} &= -(m_0 + r_{1,prim}) n_{ISp}(\tau,t), \\
\frac{\partial n_{RIp}(\tau,t)}{\partial \tau} + \frac{\partial n_{RIp}(\tau,t)}{\partial t} &= -(m_0 + r_{2,sec}) n_{RIp}(\tau,t), \\
\frac{\partial n_{IRp}(\tau,t)}{\partial \tau} + \frac{\partial n_{IRp}(\tau,t)}{\partial t} &= -(m_0 + r_{1,sec}) n_{IRp}(\tau,t),
\end{aligned}
$$

$$
\begin{aligned}
n_{SIp}(0,t) &= \frac{m_0 N^*_{SS}}{\Lambda}\int_0^\infty \Big[bV_{2,prim}(\tau)n_{SIp}(\tau,t) + bV_{2,sec}(\tau)n_{RIp}(\tau,t)\Big]d\tau \\
&\quad + \frac{m_0 N_{SSp}(t)}{\Lambda}\int_0^\infty \Big[bV_{2,prim}(\tau)n^*_{SI}(\tau) + bV_{2,sec}(\tau)n^*_{RI}(\tau)\Big]d\tau, \\
n_{ISp}(0,t) &= \frac{m_0 N^*_{SS}}{\Lambda}\int_0^\infty \Big[bV_{1,prim}(\tau)n_{ISp}(\tau,t) + bV_{1,sec}(\tau)n_{IRp}(\tau,t)\Big]d\tau \\
&\quad + \frac{m_0 N_{SSp}(t)}{\Lambda}\int_0^\infty \Big[bV_{1,prim}(\tau)n^*_{IS}(\tau) + bV_{1,sec}(\tau)n^*_{IR}(\tau)\Big]d\tau, \\
n_{RIp}(0,t) &= \frac{m_0 N^*_{RS}}{\Lambda}\int_0^\infty \Big[bV_{2,prim}(\tau)n_{SIp}(\tau,t) + bV_{2,sec}(\tau)n_{RIp}(\tau,t)\Big]d\tau \\
&\quad + \frac{m_0 N_{RSp}(t)}{\Lambda}\int_0^\infty \Big[bV_{2,prim}(\tau)n^*_{SI}(\tau) + bV_{2,sec}(\tau)n^*_{RI}(\tau)\Big]d\tau, \\
n_{IRp}(0,t) &= \frac{m_0 N^*_{SR}}{\Lambda}\int_0^\infty \Big[bV_{1,prim}(\tau)n_{ISp}(\tau,t) + bV_{1,sec}(\tau)n_{IRp}(\tau,t)\Big]d\tau \\
&\quad + \frac{m_0 N_{SRp}(t)}{\Lambda}\int_0^\infty \Big[bV_{1,prim}(\tau)n^*_{IS}(\tau) + bV_{1,sec}(\tau)n^*_{IR}(\tau)\Big]d\tau. \qquad (5.31)
\end{aligned}
$$

System (5.31) is a linear system. Thus, we look for solutions of the following forms.

$$
\begin{aligned}
N_{SSp}(t) &= N_{SS0}e^{\lambda t}, \\
N_{SRp}(t) &= N_{SR0}e^{\lambda t}, \\
N_{RSp}(t) &= N_{RS0}e^{\lambda t}, \\
N_{RRp}(t) &= N_{RR0}e^{\lambda t}, \\
n_{SIp}(\tau,t) &= n_{SI0}(\tau)e^{\lambda t}, \\
n_{ISp}(\tau,t) &= n_{IS0}(\tau)e^{\lambda t}, \\
n_{RIp}(\tau,t) &= n_{RI0}(\tau)e^{\lambda t}, \\
n_{IRp}(\tau,t) &= n_{IR0}(\tau)e^{\lambda t}, \qquad (5.32)
\end{aligned}
$$

where $N_{SS0}, N_{SR0}, N_{RS0}, N_{RR0}, n_{SI0}(\tau), n_{IS0}(\tau), n_{RI0}(\tau), n_{IR0}(\tau)$, and λ are nonzero. This ensures we are dealing with a perturbation away from the equilibrium.

Thus, if system (5.31) is solved such that the real parts of λ are negative, then over time, the perturbations get closer to zero, and thus our solutions (5.27) move closer to the equilibrium. In this case, the equilibrium is locally asymptotically stable.

If system (5.31) is solved such that the real parts of λ are positive, then over time, the perturbations get larger, and thus our solutions (5.27) move away from the equilibrium. In this case, the equilibrium is unstable.

Therefore, our goal is to write system (5.31) in such a form such that it can be used to determine whether the system is solved when the real parts of λ are negative or when the real parts of λ are positive.

Substituting the solutions (5.32) into the system (5.31), we obtain

$$
\begin{aligned}
\frac{d\left(N_{SS0}e^{\lambda t}\right)}{dt} &= -m_0 N_{SS0} e^{\lambda t} \\
&\quad - \frac{m_0 N^*_{SS}}{\Lambda} \int_0^\infty \Big[bV_{1,prim}(\tau) n_{IS0}(\tau) e^{\lambda t} + bV_{2,prim}(\tau) n_{SI0}(\tau) e^{\lambda t} \\
&\qquad\qquad + bV_{1,sec}(\tau) n_{IR0}(\tau) e^{\lambda t} + bV_{2,sec}(\tau) n_{RI0}(\tau) e^{\lambda t} \Big] d\tau \\
&\quad - \frac{m_0 N_{SS0} e^{\lambda t}}{\Lambda} \int_0^\infty \Big[bV_{1,prim}(\tau) n^*_{IS}(\tau) + bV_{2,prim}(\tau) n^*_{SI}(\tau) \\
&\qquad\qquad + bV_{1,sec}(\tau) n^*_{IR}(\tau) + bV_{2,sec}(\tau) n^*_{RI}(\tau) \Big] d\tau, \\
\frac{d\left(N_{SR0}e^{\lambda t}\right)}{dt} &= -m_0 N_{SR0} e^{\lambda t} - \frac{m_0 N^*_{SR}}{\Lambda} \int_0^\infty \Big[bV_{1,prim}(\tau) n_{IS0}(\tau) e^{\lambda t} + bV_{1,sec}(\tau) n_{IR0}(\tau) e^{\lambda t} \Big] d\tau \\
&\quad - \frac{m_0 N_{SR0} e^{\lambda t}}{\Lambda} \int_0^\infty \Big[bV_{1,prim}(\tau) n^*_{IS}(\tau) + bV_{1,sec}(\tau) n^*_{IR}(\tau) \Big] d\tau + \int_0^\infty r_{2,prim} n_{SI0}(\tau) e^{\lambda t}\, d\tau, \\
\frac{d\left(N_{RS0}e^{\lambda t}\right)}{dt} &= -m_0 N_{RS0} e^{\lambda t} - \frac{m_0 N^*_{RS}}{\Lambda} \int_0^\infty \Big[bV_{2,prim}(\tau) n_{SI0}(\tau) e^{\lambda t} + bV_{2,sec}(\tau) n_{RI0}(\tau) e^{\lambda t} \Big] d\tau \\
&\quad - \frac{m_0 N_{RS0} e^{\lambda t}}{\Lambda} \int_0^\infty \Big[bV_{2,prim}(\tau) n^*_{SI}(\tau) + bV_{2,sec}(\tau) n^*_{RI}(\tau) \Big] d\tau + \int_0^\infty r_{1,prim} n_{IS0}(\tau) e^{\lambda t}\, d\tau, \\
\frac{d\left(N_{RR0}e^{\lambda t}\right)}{dt} &= -m_0 N_{RR0} e^{\lambda t} + \int_0^\infty \Big[r_{2,prim} n_{IR0}(\tau) e^{\lambda t} + r_{2,sec} n_{RI0}(\tau) e^{\lambda t} \Big] d\tau,
\end{aligned}
$$

$$\frac{\partial\Big(n_{SI0}(\tau)e^{\lambda t}\Big)}{\partial\tau}+\frac{\partial\Big(n_{SI0}(\tau)e^{\lambda t}\Big)}{\partial t}=-(m_0+r_{2,prim})n_{SI0}(\tau)e^{\lambda t},$$
$$\frac{\partial\Big(n_{IS0}(\tau)e^{\lambda t}\Big)}{\partial\tau}+\frac{\partial\Big(n_{IS0}(\tau)e^{\lambda t}\Big)}{\partial t}=-(m_0+r_{1,prim})n_{IS0}(\tau)e^{\lambda t},$$
$$\frac{\partial\Big(n_{RI0}(\tau)e^{\lambda t}\Big)}{\partial\tau}+\frac{\partial\Big(n_{RI0}(\tau)e^{\lambda t}\Big)}{\partial t}=-(m_0+r_{2,sec})n_{RI0}(\tau)e^{\lambda t},$$
$$\frac{\partial\Big(n_{IR0}(\tau)e^{\lambda t}\Big)}{\partial\tau}+\frac{\partial\Big(n_{IR0}(\tau)e^{\lambda t}\Big)}{\partial t}=-(m_0+r_{1,sec})n_{IR0}(\tau)e^{\lambda t},$$

$$\begin{aligned}
n_{SI0}(0)e^{\lambda t}&=\frac{m_0N^*_{SS}}{\Lambda}\int_0^\infty\Big[bV_{2,prim}(\tau)n_{SI0}(\tau)e^{\lambda t}+bV_{2,sec}(\tau)n_{RI0}(\tau)e^{\lambda t}\Big]d\tau\\
&\quad+\frac{m_0N_{SS0}e^{\lambda t}}{\Lambda}\int_0^\infty\Big[bV_{2,prim}(\tau)n^*_{SI}(\tau)+bV_{2,sec}(\tau)n^*_{RI}(\tau)\Big]d\tau,\\
n_{IS0}(0)e^{\lambda t}&=\frac{m_0N^*_{SS}}{\Lambda}\int_0^\infty\Big[bV_{1,prim}(\tau)n_{IS0}(\tau)e^{\lambda t}+bV_{1,sec}(\tau)n_{IR0}(\tau)e^{\lambda t}\Big]d\tau\\
&\quad+\frac{m_0N_{SS0}e^{\lambda t}}{\Lambda}\int_0^\infty\Big[bV_{1,prim}(\tau)n^*_{IS}(\tau)+bV_{1,sec}(\tau)n^*_{IR}(\tau)\Big]d\tau,\\
n_{RI0}(0)e^{\lambda t}&=\frac{m_0N^*_{RS}}{\Lambda}\int_0^\infty\Big[bV_{2,prim}(\tau)n_{SI0}(\tau)e^{\lambda t}+bV_{2,sec}(\tau)n_{RI0}(\tau)e^{\lambda t}\Big]d\tau\\
&\quad+\frac{m_0N_{RS0}e^{\lambda t}}{\Lambda}\int_0^\infty\Big[bV_{2,prim}(\tau)n^*_{SI}(\tau)+bV_{2,sec}(\tau)n^*_{RI}(\tau)\Big]d\tau,\\
n_{IR0}(0)e^{\lambda t}&=\frac{m_0N^*_{SR}}{\Lambda}\int_0^\infty\Big[bV_{1,prim}(\tau)n_{IS0}(\tau)e^{\lambda t}+bV_{1,sec}(\tau)n_{IR0}(\tau)e^{\lambda t}\Big]d\tau\\
&\quad+\frac{m_0N_{SR0}e^{\lambda t}}{\Lambda}\int_0^\infty\Big[bV_{1,prim}(\tau)n^*_{IS}(\tau)+bV_{1,sec}(\tau)n^*_{IR}(\tau)\Big]d\tau.
\end{aligned}\tag{5.33}$$

Note from taking derivatives, we have

$$\begin{aligned}
\frac{d\Big(N_{SS0}e^{\lambda t}\Big)}{dt}&=\lambda N_{SS0}e^{\lambda t},\\
\frac{d\Big(N_{SR0}e^{\lambda t}\Big)}{dt}&=\lambda N_{SR0}e^{\lambda t},\\
\frac{d\Big(N_{RS0}e^{\lambda t}\Big)}{dt}&=\lambda N_{RS0}e^{\lambda t},\\
\frac{d\Big(N_{RR0}e^{\lambda t}\Big)}{dt}&=\lambda N_{RR0}e^{\lambda t}.
\end{aligned}\tag{5.34}$$

Consider

$$\frac{\partial\Big(n_{SI0}(\tau)e^{\lambda t}\Big)}{\partial\tau}+\frac{\partial\Big(n_{SI0}(\tau)e^{\lambda t}\Big)}{\partial t}=-(m_0+r_{2,prim})n_{SI0}(\tau)e^{\lambda t}.$$

Then by taking derivatives, we have

$$\begin{aligned}e^{\lambda t}\left(\frac{dn_{SI0}(\tau)}{d\tau}\right)+\lambda n_{SI0}(\tau)e^{\lambda t}&=-(m_0+r_{2,prim})n_{SI0}(\tau)e^{\lambda t}\\ e^{\lambda t}\left(\frac{dn_{SI0}(\tau)}{d\tau}\right)&=-(m_0+r_{2,prim}+\lambda)n_{SI0}(\tau)e^{\lambda t}.\end{aligned}$$

We can do this similarly for the other partial differential equations. In summary, we have that the partial differential equations in system (5.33) can be written as

$$\begin{aligned}e^{\lambda t}\left(\frac{dn_{SI0}(\tau)}{d\tau}\right)&=-(m_0+r_{2,prim}+\lambda)n_{SI0}(\tau)e^{\lambda t},\\ e^{\lambda t}\left(\frac{dn_{IS0}(\tau)}{d\tau}\right)&=-(m_0+r_{1,prim}+\lambda)n_{IS0}(\tau)e^{\lambda t},\\ e^{\lambda t}\left(\frac{dn_{RI0}(\tau)}{d\tau}\right)&=-(m_0+r_{2,sec}+\lambda)n_{RI0}(\tau)e^{\lambda t},\\ e^{\lambda t}\left(\frac{dn_{IR0}(\tau)}{d\tau}\right)&=-(m_0+r_{1,sec}+\lambda)n_{IR0}(\tau)e^{\lambda t}.\end{aligned}\tag{5.35}$$

After taking the derivatives as described in (5.34) and (5.35), a term of $e^{\lambda t}$ can be factored out of every equation of system (5.33). This term of $e^{\lambda t}$ can then be eliminated from every

equation of system (5.33). Therefore, we have that system (5.33) can be written as

$$
\begin{aligned}
\lambda N_{SS0} &= -m_0 N_{SS0} \\
&\quad - \frac{m_0 N^*_{SS}}{\Lambda} \int_0^\infty \Big[bV_{1,prim}(\tau) n_{IS0}(\tau) + bV_{2,prim}(\tau) n_{SI0}(\tau) \\
&\qquad\qquad + bV_{1,sec}(\tau) n_{IR0}(\tau) + bV_{2,sec}(\tau) n_{RI0}(\tau) \Big] d\tau \\
&\quad - \frac{m_0 N_{SS0}}{\Lambda} \int_0^\infty \Big[bV_{1,prim}(\tau) n^*_{IS}(\tau) + bV_{2,prim}(\tau) n^*_{SI}(\tau) \\
&\qquad\qquad + bV_{1,sec}(\tau) n^*_{IR}(\tau) + bV_{2,sec}(\tau) n^*_{RI}(\tau) \Big] d\tau, \\
\lambda N_{SR0} &= -m_0 N_{SR0} - \frac{m_0 N^*_{SR}}{\Lambda} \int_0^\infty \Big[bV_{1,prim}(\tau) n_{IS0}(\tau) + bV_{1,sec}(\tau) n_{IR0}(\tau) \Big] d\tau \\
&\quad - \frac{m_0 N_{SR0}}{\Lambda} \int_0^\infty \Big[bV_{1,prim}(\tau) n^*_{IS}(\tau) + bV_{1,sec}(\tau) n^*_{IR}(\tau) \Big] d\tau + \int_0^\infty r_{2,prim} n_{SI0}(\tau)\, d\tau, \\
\lambda N_{RS0} &= -m_0 N_{RS0} - \frac{m_0 N^*_{RS}}{\Lambda} \int_0^\infty \Big[bV_{2,prim}(\tau) n_{SI0}(\tau) + bV_{2,sec}(\tau) n_{RI0}(\tau) \Big] d\tau \\
&\quad - \frac{m_0 N_{RS0}}{\Lambda} \int_0^\infty \Big[bV_{2,prim}(\tau) n^*_{SI}(\tau) + bV_{2,sec}(\tau) n^*_{RI}(\tau) \Big] d\tau + \int_0^\infty r_{1,prim} n_{IS0}(\tau)\, d\tau, \\
\lambda N_{RR0} &= -m_0 N_{RR0} + \int_0^\infty \Big[r_{2,prim} n_{IR0}(\tau) + r_{2,sec} n_{RI0}(\tau) \Big] d\tau,
\end{aligned}
$$

$$
\begin{aligned}
\frac{dn_{SI0}(\tau)}{d\tau} &= -(m_0 + r_{2,prim} + \lambda) n_{SI0}(\tau), \\
\frac{dn_{IS0}(\tau)}{d\tau} &= -(m_0 + r_{1,prim} + \lambda) n_{IS0}(\tau), \\
\frac{dn_{RI0}(\tau)}{d\tau} &= -(m_0 + r_{2,sec} + \lambda) n_{RI0}(\tau), \\
\frac{dn_{IR0}(\tau)}{d\tau} &= -(m_0 + r_{1,sec} + \lambda) n_{IR0}(\tau),
\end{aligned}
$$

$$
\begin{aligned}
n_{SI0}(0) &= \frac{m_0 N^*_{SS}}{\Lambda}\int_0^\infty \Big[bV_{2,prim}(\tau)n_{SI0}(\tau) + bV_{2,sec}(\tau)n_{RI0}(\tau)\Big]d\tau \\
&+ \frac{m_0 N_{SS0}}{\Lambda}\int_0^\infty \Big[bV_{2,prim}(\tau)n^*_{SI}(\tau) + bV_{2,sec}(\tau)n^*_{RI}(\tau)\Big]d\tau, \\
n_{IS0}(0) &= \frac{m_0 N^*_{SS}}{\Lambda}\int_0^\infty \Big[bV_{1,prim}(\tau)n_{IS0}(\tau) + bV_{1,sec}(\tau)n_{IR0}(\tau)\Big]d\tau \\
&+ \frac{m_0 N_{SS0}}{\Lambda}\int_0^\infty \Big[bV_{1,prim}(\tau)n^*_{IS}(\tau) + bV_{1,sec}(\tau)n^*_{IR}(\tau)\Big]d\tau, \\
n_{RI0}(0) &= \frac{m_0 N^*_{RS}}{\Lambda}\int_0^\infty \Big[bV_{2,prim}(\tau)n_{SI0}(\tau) + bV_{2,sec}(\tau)n_{RI0}(\tau)\Big]d\tau \\
&+ \frac{m_0 N_{RS0}}{\Lambda}\int_0^\infty \Big[bV_{2,prim}(\tau)n^*_{SI}(\tau) + bV_{2,sec}(\tau)n^*_{RI}(\tau)\Big]d\tau, \\
n_{IR0}(0) &= \frac{m_0 N^*_{SR}}{\Lambda}\int_0^\infty \Big[bV_{1,prim}(\tau)n_{IS0}(\tau) + bV_{1,sec}(\tau)n_{IR0}(\tau)\Big]d\tau \\
&+ \frac{m_0 N_{SR0}}{\Lambda}\int_0^\infty \Big[bV_{1,prim}(\tau)n^*_{IS}(\tau) + bV_{1,sec}(\tau)n^*_{IR}(\tau)\Big]d\tau. \qquad (5.36)
\end{aligned}
$$

Solving the differential equations of system (5.36), we have the following.

$$
\begin{aligned}
n_{SI0}(\tau) &= n_{SI0}(0)e^{-(m_0+r_{2,prim}+\lambda)\tau}, \\
n_{IS0}(\tau) &= n_{IS0}(0)e^{-(m_0+r_{1,prim}+\lambda)\tau}, \\
n_{RI0}(\tau) &= n_{RI0}(0)e^{-(m_0+r_{2,sec}+\lambda)\tau}, \\
n_{IR0}(\tau) &= n_{IR0}(0)e^{-(m_0+r_{1,sec}+\lambda)\tau}. \qquad (5.37)
\end{aligned}
$$

Thus, substituting the solutions (5.37) into the other equations of system (5.36), we obtain

the system of equations

$$
\begin{aligned}
\lambda N_{SS0} &= -m_0 N_{SS0} \\
&\quad - \frac{m_0 N^*_{SS}}{\Lambda} \int_0^\infty \Big[bV_{1,prim}(\tau) n_{IS0}(0) e^{-(m_0+r_{1,prim}+\lambda)\tau} + bV_{2,prim}(\tau) n_{SI0}(0) e^{-(m_0+r_{2,prim}+\lambda)\tau} \\
&\qquad\qquad + bV_{1,sec}(\tau) n_{IR0}(0) e^{-(m_0+r_{1,sec}+\lambda)\tau} + bV_{2,sec}(\tau) n_{RI0}(0) e^{-(m_0+r_{2,sec}+\lambda)\tau} \Big] d\tau \\
&\quad - \frac{m_0 N_{SS0}}{\Lambda} \int_0^\infty \Big[bV_{1,prim}(\tau) n^*_{IS}(\tau) + bV_{2,prim}(\tau) n^*_{SI}(\tau) + bV_{1,sec}(\tau) n^*_{IR}(\tau) + bV_{2,sec}(\tau) n^*_{RI}(\tau) \Big] d\tau, \\
\lambda N_{SR0} &= -m_0 N_{SR0} \\
&\quad - \frac{m_0 N^*_{SR}}{\Lambda} \int_0^\infty \Big[bV_{1,prim}(\tau) n_{IS0}(0) e^{-(m_0+r_{1,prim}+\lambda)\tau} + bV_{1,sec}(\tau) n_{IR0}(0) e^{-(m_0+r_{1,sec}+\lambda)\tau} \Big] d\tau \\
&\quad - \frac{m_0 N_{SR0}}{\Lambda} \int_0^\infty \Big[bV_{1,prim}(\tau) n^*_{IS}(\tau) + bV_{1,sec}(\tau) n^*_{IR}(\tau) \Big] d\tau + \int_0^\infty r_{2,prim} n_{SI0}(0) e^{-(m_0+r_{2,prim}+\lambda)\tau}\, d\tau, \\
\lambda N_{RS0} &= -m_0 N_{RS0} \\
&\quad - \frac{m_0 N^*_{RS}}{\Lambda} \int_0^\infty \Big[bV_{2,prim}(\tau) n_{SI0}(0) e^{-(m_0+r_{2,prim}+\lambda)\tau} + bV_{2,sec}(\tau) n_{RI0}(0) e^{-(m_0+r_{2,sec}+\lambda)\tau} \Big] d\tau \\
&\quad - \frac{m_0 N_{RS0}}{\Lambda} \int_0^\infty \Big[bV_{2,prim}(\tau) n^*_{SI}(\tau) + bV_{2,sec}(\tau) n^*_{RI}(\tau) \Big] d\tau + \int_0^\infty r_{1,prim} n_{IS0}(0) e^{-(m_0+r_{1,prim}+\lambda)\tau}\, d\tau, \\
\lambda N_{RR0} &= -m_0 N_{RR0} + \int_0^\infty \Big[r_{1,sec} n_{IR0}(0) e^{-(m_0+r_{1,sec}+\lambda)\tau} + r_{2,sec} n_{RI0}(0) e^{-(m_0+r_{2,sec}+\lambda)\tau} \Big] d\tau,
\end{aligned}
$$

$$
\begin{aligned}
n_{SI0}(0) &= \frac{m_0 N^*_{SS}}{\Lambda} \int_0^\infty \Big[bV_{2,prim}(\tau) n_{SI0}(0) e^{-(m_0+r_{2,prim}+\lambda)\tau} + bV_{2,sec}(\tau) n_{RI0}(0) e^{-(m_0+r_{2,sec}+\lambda)\tau} \Big] d\tau \\
&\quad + \frac{m_0 N_{SS0}}{\Lambda} \int_0^\infty \Big[bV_{2,prim}(\tau) n^*_{SI}(\tau) + bV_{2,sec}(\tau) n^*_{RI}(\tau) \Big] d\tau, \\
n_{IS0}(0) &= \frac{m_0 N^*_{SS}}{\Lambda} \int_0^\infty \Big[bV_{1,prim}(\tau) n_{IS0}(0) e^{-(m_0+r_{1,prim}+\lambda)\tau} + bV_{1,sec}(\tau) n_{IR0}(0) e^{-(m_0+r_{1,sec}+\lambda)\tau} \Big] d\tau \\
&\quad + \frac{m_0 N_{SS0}}{\Lambda} \int_0^\infty \Big[bV_{1,prim}(\tau) n^*_{IS}(\tau) + bV_{1,sec}(\tau) n^*_{IR}(\tau) \Big] d\tau, \\
n_{RI0}(0) &= \frac{m_0 N^*_{RS}}{\Lambda} \int_0^\infty \Big[bV_{2,prim}(\tau) n_{SI0}(0) e^{-(m_0+r_{2,prim}+\lambda)\tau} + bV_{2,sec}(\tau) n_{RI0}(0) e^{-(m_0+r_{2,sec}+\lambda)\tau} \Big] d\tau \\
&\quad + \frac{m_0 N_{RS0}}{\Lambda} \int_0^\infty \Big[bV_{2,prim}(\tau) n^*_{SI}(\tau) + bV_{2,sec}(\tau) n^*_{RI}(\tau) \Big] d\tau, \\
n_{IR0}(0) &= \frac{m_0 N^*_{SR}}{\Lambda} \int_0^\infty \Big[bV_{1,prim}(\tau) n_{IS0}(0) e^{-(m_0+r_{1,prim}+\lambda)\tau} + bV_{1,sec}(\tau) n_{IR0}(0) e^{-(m_0+r_{1,sec}+\lambda)\tau} \Big] d\tau \\
&\quad + \frac{m_0 N_{SR0}}{\Lambda} \int_0^\infty \Big[bV_{1,prim}(\tau) n^*_{IS}(\tau) + bV_{1,sec}(\tau) n^*_{IR}(\tau) \Big] d\tau. \qquad (5.38)
\end{aligned}
$$

We can ignore the equation involving N_{RR0} in system (5.38) since N_{RR0} is uncoupled from all the other equations in system (5.38).

Note

$$\int_0^\infty e^{-a\tau}\, d\tau = \frac{1}{a},$$

and only exists if the real part of a is positive.

Recall that C_1, C_2, $\Gamma_{1,prim,\lambda}$, $\Gamma_{2,prim,\lambda}$, $\Gamma_{1,sec,\lambda}$, and $\Gamma_{2,sec,\lambda}$ are defined as

$$\begin{aligned}
C_1 &= \frac{m_0}{\Lambda}\int_0^\infty \left(bV_{1,prim}(\tau)n^*_{IS}(\tau) + bV_{1,sec}(\tau)n^*_{IR}(\tau)\right) d\tau,\\
C_2 &= \frac{m_0}{\Lambda}\int_0^\infty \left(bV_{2,prim}(\tau)n^*_{SI}(\tau) + bV_{2,sec}(\tau)n^*_{RI}(\tau)\right) d\tau,\\
\Gamma_{1,prim,\lambda} &= \frac{m_0}{\Lambda}\int_0^\infty bV_{1,prim}(\tau)e^{-(m_0+r_{1,prim}+\lambda)\tau}\, d\tau,\\
\Gamma_{2,prim,\lambda} &= \frac{m_0}{\Lambda}\int_0^\infty bV_{2,prim}(\tau)e^{-(m_0+r_{2,prim}+\lambda)\tau}\, d\tau,\\
\Gamma_{1,sec,\lambda} &= \frac{m_0}{\Lambda}\int_0^\infty bV_{1,sec}(\tau)e^{-(m_0+r_{1,sec}+\lambda)\tau}\, d\tau,\\
\Gamma_{2,sec,\lambda} &= \frac{m_0}{\Lambda}\int_0^\infty bV_{2,sec}(\tau)e^{-(m_0+r_{2,sec}+\lambda)\tau}\, d\tau.
\end{aligned}$$

Thus, using these definitions and the fact that the integrals must exist, we can write (5.38) as

$$\begin{aligned}
\lambda N_{SS0} &= -m_0 N_{SS0} - N^*_{SS}\Gamma_{1,prim,\lambda}n_{IS0}(0) - N^*_{SS}\Gamma_{2,prim,\lambda}n_{SI0}(0)\\
&\quad - N^*_{SS}\Gamma_{1,sec,\lambda}n_{IR0}(0) - N^*_{SS}\Gamma_{2,sec,\lambda}n_{RI0}(0) - C_1 N_{SS0} - C_2 N_{SS0},\\
\lambda N_{SR0} &= -m_0 N_{SR0} - N^*_{SR}\Gamma_{1,prim,\lambda}n_{IS0}(0) - N^*_{SR}\Gamma_{1,sec,\lambda}n_{IR0}(0)\\
&\quad - C_1 N_{SR0} + \frac{r_{2,prim}}{\lambda + m_0 + r_{2,prim}}n_{SI0}(0),\\
\lambda N_{RS0} &= -m_0 N_{RS0} - N^*_{RS}\Gamma_{2,prim,\lambda}n_{SI0}(0) - N^*_{RS}\Gamma_{2,sec,\lambda}n_{RI0}(0)\\
&\quad - C_2 N_{RS0} + \frac{r_{1,prim}}{\lambda + m_0 + r_{1,prim}}N_{IS0}(0),
\end{aligned}$$

$$
\begin{aligned}
n_{SI0}(0) &= N^*_{SS}\Gamma_{2,prim,\lambda}n_{SI0}(0) + N^*_{SS}\Gamma_{2,sec,\lambda}n_{RI0}(0) + C_2N_{SS0},\\
n_{IS0}(0) &= N^*_{SS}\Gamma_{1,prim,\lambda}n_{IS0}(0) + N^*_{SS}\Gamma_{1,sec,\lambda}n_{IR0}(0) + C_1N_{SS0},\\
n_{RI0}(0) &= N^*_{RS}\Gamma_{2,prim,\lambda}n_{SI0}(0) + N^*_{RS}\Gamma_{2,sec,\lambda}n_{RI0}(0) + C_2N_{RS0},\\
n_{IR0}(0) &= N^*_{SR}\Gamma_{1,prim,\lambda}n_{IS0}(0) + N^*_{SR}\Gamma_{1,sec,\lambda}n_{IR0}(0) + C_1N_{SR0}.
\end{aligned} \tag{5.39}
$$

Rewriting the equations of system (5.39), we obtain

$$
\begin{aligned}
(\lambda + m_0 + C_1 + C_2)N_{SS0} + N^*_{SS}\Gamma_{2,prim,\lambda}n_{SI0}(0) + N^*_{SS}\Gamma_{1,prim,\lambda}n_{IS0}(0)&\\
+N^*_{SS}\Gamma_{2,sec,\lambda}n_{RI0}(0) + N^*_{SS}\Gamma_{1,sec,\lambda}n_{IR0}(0) &= 0,\\
(\lambda + m_0 + C_1)N_{SR0} - \frac{r_{2,prim}}{\lambda + m_0 + r_{2,prim}}n_{SI0}(0) + N^*_{SR}\Gamma_{1,prim,\lambda}n_{IS0}(0) + N^*_{SR}\Gamma_{1,sec,\lambda}n_{IR0}(0) &= 0,\\
(\lambda + m_0 + C_2)N_{RS0} + N^*_{RS}\Gamma_{2,prim,\lambda}n_{SI0}(0) - \frac{r_{1,prim}}{\lambda + m_0 + r_{1,prim}}n_{IS0}(0) + N^*_{RS}\Gamma_{2,sec,\lambda}n_{RI0}(0) &= 0,\\
-C_2N_{SS0} + (1 - N^*_{SS}\Gamma_{2,prim,\lambda})n_{SI0}(0) - N^*_{SS}\Gamma_{2,sec,\lambda}n_{RI0}(0) &= 0,\\
-C_1N_{SS0} + (1 - N^*_{SS}\Gamma_{1,prim,\lambda})n_{IS0}(0) - N^*_{SS}\Gamma_{1,sec,\lambda}n_{IR0}(0) &= 0,\\
-C_2N_{RS0} - N^*_{RS}\Gamma_{2,prim,\lambda}n_{SI0}(0) + (1 - N^*_{RS}\Gamma_{2,sec,\lambda})n_{RI0}(0) &= 0,\\
-C_1N_{SR0} - N^*_{SR}\Gamma_{1,prim,\lambda}n_{IS0}(0) + (1 - N^*_{SR}\Gamma_{1,sec,\lambda})n_{IR0}(0) &= 0.
\end{aligned} \tag{5.40}
$$

We can now write system (5.40) as

$$M_\lambda \mathbf{y} = \mathbf{0}, \tag{5.41}$$

where

$$\mathbf{y}^T = \Big(N_{SS0}, N_{SR0}, N_{RS0}, n_{SI0}(0), n_{IS0}(0), n_{RI0}(0), n_{IR0}(0)\Big),$$

$$\mathbf{0} = (0,0,0,0,0,0,0),$$

and

$$M_\lambda = \begin{pmatrix} M_1 & M_2 \end{pmatrix},$$

where

$$M_1 = \begin{pmatrix} \lambda + m_0 + C_1 + C_2 & 0 & 0 \\ 0 & \lambda + m_0 + C_1 & 0 \\ 0 & 0 & \lambda + m_0 + C_2 \\ -C_2 & 0 & 0 \\ -C_1 & 0 & 0 \\ 0 & 0 & -C_2 \\ 0 & -C_1 & 0 \end{pmatrix}$$

and

$$M_2 = \begin{pmatrix} N^*_{SS}\Gamma_{2,prim,\lambda} & N^*_{SS}\Gamma_{1,prim,\lambda} & N^*_{SS}\Gamma_{2,sec,\lambda} & N^*_{SS}\Gamma_{1,sec,\lambda} \\ \frac{-r_{2,prim}}{\lambda+m_0+r_{2,prim}} & N^*_{SR}\Gamma_{1,prim,\lambda} & 0 & N^*_{SR}\Gamma_{1,sec,\lambda} \\ N^*_{RS}\Gamma_{2,prim,\lambda} & \frac{-r_{1,prim}}{\lambda+m_0+r_{1,prim}} & N^*_{RS}\Gamma_{2,sec,\lambda} & 0 \\ 1 - N^*_{SS}\Gamma_{2,prim,\lambda} & 0 & -N^*_{SS}\Gamma_{2,sec,\lambda} & 0 \\ 0 & 1 - N^*_{SS}\Gamma_{1,prim,\lambda} & 0 & -N^*_{SS}\Gamma_{1,sec,\lambda} \\ -N^*_{RS}\Gamma_{2,prim,\lambda} & 0 & 1 - N^*_{RS}\Gamma_{2,sec,\lambda} & 0 \\ 0 & -N^*_{SR}\Gamma_{1,prim,\lambda} & 0 & 1 - N^*_{SR}\Gamma_{1,sec,\lambda} \end{pmatrix}.$$

M_λ is a 7×7 matrix.

Since $\mathbf{y}^T$ is nonzero, equation (5.41) implies

$$\det(M_\lambda) = 0. \tag{5.42}$$

Equation (5.42) is an equation of λ. However, this is not a normal characteristic equation of λ due to the definitions of $\Gamma_{1,prim,\lambda}$, $\Gamma_{2,prim,\lambda}$, $\Gamma_{1,sec,\lambda}$, and $\Gamma_{2,sec,\lambda}$.

Adding rows to other rows does not change the determinant of M_λ. Thus, we can simplify M_λ slightly.

We add rows 4 and 5 to row 1, we add row 7 to row 2, and we add row 6 to row 3. Thus,

we have $M_\lambda =$

$$\begin{pmatrix}
\lambda+m_0 & 0 & 0 & 1 & 1 & 0 & 0 \\
0 & \lambda+m_0 & 0 & \frac{-r_{2,prim}}{\lambda+m_0+r_{2,prim}} & 0 & 0 & 1 \\
0 & 0 & \lambda+m_0 & 0 & \frac{-r_{1,prim}}{\lambda+m_0+r_{1,prim}} & 1 & 0 \\
-C_2 & 0 & 0 & 1-N^*_{SS}\Gamma_{2,prim,\lambda} & 0 & -N^*_{SS}\Gamma_{2,sec,\lambda} & 0 \\
-C_1 & 0 & 0 & 0 & 1-N^*_{SS}\Gamma_{1,prim,\lambda} & 0 & -N^*_{SS}\Gamma_{1,sec,\lambda} \\
0 & 0 & -C_2 & -N^*_{RS}\Gamma_{2,prim,\lambda} & 0 & 1-N^*_{RS}\Gamma_{2,sec,\lambda} & 0 \\
0 & -C_1 & 0 & 0 & -N^*_{SR}\Gamma_{1,prim,\lambda} & 0 & 1-N^*_{SR}\Gamma_{1,sec,\lambda}
\end{pmatrix}. \quad (5.43)$$

In summary, as described when we defined solutions (5.32), we have shown that the stability of the generic equilibrium can be determined by analyzing the solutions λ to equation (5.42). If the solutions all have negative real parts, the equilibrium will be locally asymptotically stable. If at least one solution has positive real parts, then the solution will be unstable.

Note that (5.43) is the same matrix described in definition (5.26).

Thus, the proposition is proved. □

5.4.8 Extinction stability

Proposition 5.4.7. *The extinction equilibrium*

$$\left(N^*_{SS}, N^*_{SR}, N^*_{RS}, N^*_{RR}, n^*_{SI}(\tau), n^*_{IS}(\tau), n^*_{RI}(\tau), n^*_{IR}(\tau)\right) = \left(\frac{\Lambda}{m_0}, 0, 0, 0, 0, 0, 0, 0\right) \quad (5.44)$$

1) is locally asymptotically stable if $\Gamma_{1,prim} < 1$ *and* $\Gamma_{2,prim} < 1$*;*

2) is unstable if $\Gamma_{1,prim} > 1$ *or* $\Gamma_{2,prim} > 1$*.*

Proof. To determine stability of the equilibrium, we can use the matrix M_λ defined in (5.26).

Recall

$$\Gamma_{1,prim,\lambda} = \frac{m_0}{\Lambda}\int_0^\infty bV_{1,prim}(\tau)e^{-(m_0+r_{1,prim}+\lambda)\tau}\,d\tau,$$
$$\Gamma_{2,prim,\lambda} = \frac{m_0}{\Lambda}\int_0^\infty bV_{2,prim}(\tau)e^{-(m_0+r_{2,prim}+\lambda)\tau}\,d\tau.$$

We plug in the extinction equilibrium as defined in (5.44) into the matrix M_λ.

Using Mathematica, we find that

$$\det(M_\lambda) = (\lambda+m_0)^3\left(\frac{\Lambda}{m_0}\Gamma_{1,prim,\lambda}-1\right)\left(\frac{\Lambda}{m_0}\Gamma_{2,prim,\lambda}-1\right).$$

Solutions λ must satisfy $\det(M_\lambda)=0$.

Thus, we have solutions λ_1, λ_2, and λ_3 that satisfy the equations

$$\begin{aligned}\lambda_1+m_0&=0,\\ \frac{\Lambda}{m_0}\Gamma_{1prim\lambda_2}-1&=0,\\ \frac{\Lambda}{m_0}\Gamma_{2prim\lambda_3}-1&=0.\end{aligned} \tag{5.45}$$

Let

$$H_{1,prim}(\lambda) = \int_0^\infty bV_{1,prim}(\tau)e^{-(m_0+r_{1,prim}+\lambda)\tau}\,d\tau, \tag{5.46}$$
$$H_{2,prim}(\lambda) = \int_0^\infty bV_{2,prim}(\tau)e^{-(m_0+r_{2,prim}+\lambda)\tau}\,d\tau. \tag{5.47}$$

From equations (5.45), we consider

$$\frac{\Lambda}{m_0}\Gamma_{1,prim,\lambda_2}-1=0.$$

This is equivalent to

$$H_{1,prim}(\lambda_2) = 1, \tag{5.48}$$

where $H_{1,prim}$ is defined in equation (5.46).

Similarly, equation

$$\frac{\Lambda}{m_0}\Gamma_{2,prim,\lambda_3} - 1 = 0$$

from equations (5.45) is equivalent to

$$H_{2,prim}(\lambda_3) = 1, \tag{5.49}$$

where $H_{2,prim}$ is defined in equation (5.47).

Lemma 5.4.1. *If $\Gamma_{1,prim} < 1$, then solution λ_2 from equations (5.45) has negative real parts.*

Proof. Assume $\lambda_2 = \alpha + \beta i$ where $\alpha \geq 0$.

Note $|e^{\beta i}| = 1$ for all β.

Using $H_{1,prim}$ as defined in equation (5.46), we have

$$\begin{aligned}
|H_{1,prim}(\lambda_2)| &= \left| \int_0^\infty bV_{1,prim}(\tau)e^{-(m_0+r_{1,prim}+\lambda_2)\tau}\, d\tau \right| \\
&\leq \int_0^\infty bV_{1,prim}(\tau)e^{-(m_0+r_{1,prim})\tau}|e^{-(\alpha+\beta i)\tau}|\, d\tau \\
&= \int_0^\infty bV_{1,prim}(\tau)e^{-(m_0+r_{1,prim})\tau}|e^{-\alpha\tau}||e^{-\beta i\tau}|\, d\tau \\
&= \int_0^\infty bV_{1,prim}(\tau)e^{-(m_0+r_{1,prim})\tau}e^{-\alpha\tau}\, d\tau \\
&\leq \int_0^\infty bV_{1,prim}(\tau)e^{-(m_0+r_{1,prim})\tau}\, d\tau \\
&= \Gamma_{1,prim} < 1
\end{aligned}$$

In summary, if $\Gamma_{1,prim} < 1$ and λ_2 has positive real parts, then $|H_{1,prim}(\lambda_2)| < 1$.

However, solution λ_2 must satisfy $H_{1,prim}(\lambda_2) = 1$, as shown in equation (5.48).

Therefore, in order to satisfy $H_{1,prim}(\lambda_2) = 1$, solution λ_2 must have negative real parts. □

Lemma 5.4.2. *If $\Gamma_{2,prim} < 1$, then solution λ_3 from equations (5.45) has negative real parts.*

Proof. The lemma is proved similar to Lemma 5.4.1 by replacing λ_2 with λ_3, $\Gamma_{1,prim}$ with $\Gamma_{2,prim}$, and $H_{1,prim}(\lambda)$ with $H_{2,prim}(\lambda)$, where $H_{2,prim}$ is defined in equation (5.47). □

Lemma 5.4.3. *If $\Gamma_{1,prim} < 1$ and $\Gamma_{2,prim} < 1$, then the extinction equilibrium is locally asymptotically stable.*

Proof. We show that the solutions λ_1, λ_2, and λ_3 from equations (5.45) have negative real parts.

Note that $\lambda_1 + m_0 = 0$ implies $\lambda_1 = -m_0$. Since $m_0 > 0$, solution λ_1 always has negative real parts.

If $\Gamma_{1,prim} < 1$, then from Lemma 5.4.1, solution λ_2 has negative real parts.

If $\Gamma_{2,prim} < 1$, then from Lemma 5.4.2, solution λ_3 has negative real parts.

Thus, if $\Gamma_{1,prim} < 1$ and $\Gamma_{2,prim} < 1$, all solutions λ_1, λ_2, and λ_3 from equations (5.45) have negative real parts.

Thus, the extinction equilibrium is locally asymptotically stable. □

Lemma 5.4.4. *If $\Gamma_{1,prim} > 1$, then solution λ_2 from equations (5.45) has positive real parts.*

Proof. Consider $H_{1,prim}(\lambda)$ as defined in equation (5.46).

The solution λ_2 must satisfy the equation $H_{1,prim}(\lambda_2) = 1$, as shown in equation (5.48).

Note that

$$H_{1,prim}(0) = \int_0^\infty bV_{1,prim}(\tau)e^{-(m_0+r_{1,prim})\tau}\, d\tau = \Gamma_{1,prim}.$$

If $\Gamma_{1,prim} > 1$, then $H_{1,prim}(0) > 1$.

Treating $H_{1,prim}(\lambda_2)$ as a function of the real variable λ_2, we note that

$$\lim_{\lambda_2 \to \infty} H_{1,prim}(\lambda_2) = 0$$

Since $H_{1,prim}(0) > 1$, we have that the equation $H_{1,prim}(\lambda_2^*) = 1$ is only satisfied for some $\lambda_2^* > 0$.

In summary, if $\Gamma_{1,prim} > 1$, then solution λ_2 must have positive real parts. □

Lemma 5.4.5. *If $\Gamma_{2,prim} > 1$, then solution λ_3 from equations (5.45) has positive real parts.*

Proof. The lemma is proved similar to Lemma 5.4.4 by replacing λ_2 with λ_3, $\Gamma_{1,prim}$ with $\Gamma_{2,prim}$, and $H_{1,prim}(\lambda)$ with $H_{2,prim}(\lambda)$, where $H_{2,prim}$ is defined in equation (5.47). □

Lemma 5.4.6. *If $\Gamma_{1,prim} > 1$ or $\Gamma_{2,prim} > 1$, the extinction equilibrium is unstable.*

Proof. If $\Gamma_{1,prim} > 1$, then from Lemma 5.4.4, solution λ_2 from equations (5.45) has positive real parts.

If $\Gamma_{2,prim} > 1$, then from Lemma 5.4.5, solution λ_3 from equations (5.45) has positive real parts.

Thus, if $\Gamma_{1,prim} > 1$ or $\Gamma_{2,prim} > 1$, the extinction equilibrium is unstable. □

In summary, we proved statement 1) in Proposition 5.4.7 using Lemma 5.4.3.

We proved statement 2) in Proposition 5.4.7 using Lemma 5.4.6.

Thus, the proposition is proved. □

5.4.9 Strain 1 stability

Proposition 5.4.8. *The equilibrium where only strain 1 persists*

$$\begin{aligned}&\left(N^*_{SS}, N^*_{SR}, N^*_{RS}, N^*_{RR}, n^*_{SI}(\tau), n^*_{IS}(\tau), n^*_{RI}(\tau), n^*_{IR}(\tau)\right)\\ =&\left(\frac{\Lambda}{\Gamma_{1,prim}}, 0, \frac{\Lambda r_{1,prim}(\Gamma_{1,prim}-1)}{m_0(m_0+r_{1,prim}\Gamma_{1,prim})}, 0, 0, \frac{\Lambda(\Gamma_{1,prim}-1)}{\Gamma_{1,prim}}e^{-(m_0+r_{1,prim})\tau}, 0, 0\right)\end{aligned} \tag{5.50}$$

1) exists if $\Gamma_{1,prim} > 1$*;*

2) is locally asymptotically stable if $\mathcal{R}_{0_1} < 1$*;*

3) is unstable if $\mathcal{R}_{0_1} > 1$*,*

where

$$\mathcal{R}_{0_1} = \frac{\Gamma_{2,prim}}{\Gamma_{1,prim}} + \frac{r_{1,prim}(\Gamma_{1,prim}-1)\Gamma_{2,sec}}{(m_0+r_{1,prim})\Gamma_{1,prim}}. \tag{5.51}$$

Proof. We first use the following lemma.

Lemma 5.4.7. *The equilibrium where only strain 1 persists exists only if* $\Gamma_{1,prim} > 1$*.*

Proof. Assuming nonnegative initial conditions on System (5.1), it can be shown that all solutions are unique and nonnegative. Thus, in order for this equilibrium to exist, we need $\Gamma_{1,prim} - 1 > 0$. Thus, if the equilibrium exists, we must have $\Gamma_{1,prim} > 1$. □

From the definition of the equilibrium in (5.50), we have $n^*_{SI}(\tau) = 0$ and $n^*_{RI}(\tau) = 0$.

Thus, we have

$$C_2 = \frac{m_0}{\Lambda} \int_0^\infty bV_{2,prim}(\tau)n^*_{SI}(\tau) + bV_{2,sec}(\tau)n^*_{RI}(\tau)\, d\tau = 0.$$

Also, since

$$n^*_{IS}(\tau) = \frac{\Lambda(\Gamma_{1,prim} - 1)}{\Gamma_{1,prim}} e^{-(m_0 + r_{1,prim})\tau}$$

and

$$n^*_{IR}(\tau) = 0,$$

we have

$$\begin{aligned} C_1 =& \frac{m_0}{\Lambda} \int_0^\infty bV_{1,prim}(\tau)n^*_{IS}(\tau) + bV_{1,sec}(\tau)n^*_{IR}(\tau)\, d\tau \\ =& \left(\frac{m_0}{\Lambda}\right) \left(\frac{\Lambda(\Gamma_{1,prim} - 1)}{\Gamma_{1,prim}}\right) \int_0^\infty bV_{1,prim}(\tau) e^{-(m_0 + r_{1,prim})\tau} \\ =& \left(\frac{m_0}{\Lambda}\right) \left(\frac{\Lambda(\Gamma_{1,prim} - 1)}{\Gamma_{1,prim}}\right) \Gamma_{1,prim} \\ =& (m_0)(\Gamma_{1,prim} - 1). \end{aligned} \tag{5.52}$$

Using the equilibrium where only the first strain persists as defined in (5.50),

$$\begin{aligned} &\left(N^*_{SS}, N^*_{SR}, N^*_{RS}, N^*_{RR}, n^*_{SI}(\tau), n^*_{IS}(\tau), n^*_{RI}(\tau), n^*_{IR}(\tau)\right) \\ =&\left(\frac{\Lambda}{\Gamma_{1,prim}}, 0, \frac{\Lambda r_{1,prim}(\Gamma_{1,prim} - 1)}{m_0(m_0 + r_{1,prim}\Gamma_{1,prim})}, 0, 0, \frac{\Lambda(\Gamma_{1,prim} - 1)}{\Gamma_{1,prim}} e^{-(m_0 + r_{1,prim})\tau}, 0, 0\right), \end{aligned}$$

we plug these values along with C_1 and C_2 into the matrix M_λ as defined in (5.26).

Using Mathematica, we find that

$$\begin{aligned}\det(M_\lambda) = &\left(\frac{1}{\Gamma_{1,prim}^2 m_0^2(m_0 + r_{1,prim})}\right)(\lambda + m_0)(\lambda + m_0\Gamma_{1,prim}) \\ &\Big(m_0\Gamma_{1,prim}(\lambda + m_0\Gamma_{1,prim}) - \Lambda\Gamma_{1,prim,\lambda}(\lambda + m_0)\Big) \\ &\Big((m_0 + r_{1,prim})(m_0\Gamma_{1,prim} - \Lambda\Gamma_{2,prim,\lambda}) + \Lambda r_{1,prim}\Gamma_{2,sec,\lambda}(1 - \Gamma_{1,prim})\Big)\end{aligned}$$

Note that solutions λ must satisfy $\det(M_\lambda) = 0$.

Thus, we have solutions λ_1, λ_2, λ_3, and λ_4 that satisfy the following equations.

$$\begin{aligned}\lambda_1 + m_0 &= 0, \\ \lambda_2 + m_0\Gamma_{1,prim} &= 0, \\ m_0\Gamma_{1,prim}(\lambda_3 + m_0\Gamma_{1,prim}) - \Lambda\Gamma_{1,prim,\lambda_3}(\lambda_3 + m_0) &= 0, \\ (m_0 + r_{1,prim})(m_0\Gamma_{1,prim} - \Lambda\Gamma_{2,prim,\lambda_4}) + \Lambda r_{1,prim}(1 - \Gamma_{1,prim})\Gamma_{2,sec,\lambda_4} &= 0.\end{aligned} \tag{5.53}$$

Lemma 5.4.8. *Solutions λ_1, λ_2, and λ_3 from equations (5.53) always have negative real parts.*

Proof. From equations (5.53), $\lambda_1 + m_0 = 0$, which implies $\lambda_1 = -m_0$. Since $m_0 > 0$, solution λ_1 always has negative real parts.

From equations (5.53), $\lambda_2 + m_0\Gamma_{1,prim} = 0$, which implies $\lambda_2 = -m_0\Gamma_{1,prim}$. Since $m_0 > 0$ and $\Gamma_{1,prim} > 1$, solution λ_2 always has negative real parts. From equations (5.53), we consider

$$m_0\Gamma_{1,prim}(\lambda_3 + m_0\Gamma_{1,prim}) - \Lambda\Gamma_{1,prim,\lambda_3}(\lambda_3 + m_0) = 0.$$

Then,

$$m_0\Gamma_{1,prim}(\lambda_3 + m_0\Gamma_{1,prim}) = \Lambda\Gamma_{1,prim,\lambda_3}(\lambda_3 + m_0).$$

Thus,

$$\frac{\Gamma_{1,prim}(\lambda_3 + m_0\Gamma_{1,prim})}{\lambda_3 + m_0} = \left(\frac{\Lambda}{m_0}\right)\Gamma_{1,prim,\lambda_3}. \tag{5.54}$$

Assume $\lambda_3 = \alpha + \beta i$ where $\alpha \geq 0$. Now consider the left side of equation (5.54).

Since $\Gamma_{1,prim} > 1$, we have

$$\left|\frac{\Gamma_{1,prim}(\lambda_3 + m_0\Gamma_{1,prim})}{\lambda_3 + m_0}\right| = \Gamma_{1,prim}\left(\frac{\sqrt{(\alpha + m_0\Gamma_{1,prim})^2 + \beta^2}}{\sqrt{(\alpha + m_0)^2 + \beta^2}}\right) > \Gamma_{1,prim}.$$

Now consider the right side of equation (5.54).

Note that $|e^{\beta i}| = 1$ for all β.

Also, note that

$$\Gamma_{1,prim,\lambda_3} = \frac{m_0}{\Lambda}\int_0^\infty bV_{1,prim}(\tau)e^{-(m_0+r_{1,prim})\tau}e^{-\lambda_3\tau}\,d\tau.$$

Thus,

$$\begin{aligned}
\left|\left(\frac{\Lambda}{m_0}\right)\Gamma_{1,prim,\lambda_3}\right| &= \left|\int_0^\infty bV_{1,prim}(\tau)e^{-(m_0+r_{1,prim})\tau}e^{-\lambda_3\tau}\,d\tau\right| \\
&\leq \int_0^\infty bV_{1,prim}(\tau)e^{-(m_0+r_{1,prim})\tau}|e^{-(\alpha+\beta i)\tau}|\,d\tau \\
&\leq \int_0^\infty bV_{1,prim}(\tau)e^{-(m_0+r_{1,prim})\tau}|e^{-\alpha\tau}||e^{-\beta i\tau}|\,d\tau \\
&\leq \int_0^\infty bV_{1,prim}(\tau)e^{-(m_0+r_{1,prim})\tau}e^{-\alpha\tau}\,d\tau \\
&\leq \int_0^\infty bV_{1,prim}(\tau)e^{-(m_0+r_{1,prim})\tau}\,d\tau \\
&= \Gamma_{1,prim}
\end{aligned}$$

Thus, if $\lambda_3 = \alpha + \beta i$ where $\alpha \geq 0$, then the right side of equation (5.54) is less than or equal to $\Gamma_{1,prim}$, but the left side of equation (5.54) is greater than $\Gamma_{1,prim}$.

Therefore, to satisfy equation (5.54), λ_3 cannot have positive real parts, and thus λ_3 must have negative real parts.

In summary, solutions λ_1, λ_2, and λ_3 always have negative real parts. □

From equations (5.53), we consider

$$(m_0 + r_{1,prim})(m_0\Gamma_{1,prim} - \Lambda\Gamma_{2,prim,\lambda_4}) + \Lambda r_{1,prim}(1 - \Gamma_{1,prim})\Gamma_{2,sec,\lambda_4} = 0.$$

Thus,

$$(m_0 + r_{1,prim})(m_0\Gamma_{1,prim} - \Lambda\Gamma_{2,prim,\lambda_4}) = \Lambda r_{1,prim}(1 - \Gamma_{1,prim})\Gamma_{2,sec,\lambda_4},$$

which implies

$$m_0(m_0 + r_{1,prim})\Gamma_{1,prim} = \Lambda\left((m_0 + r_{1,prim})\Gamma_{2,prim,\lambda_4} + r_{1,prim}(1 - \Gamma_{1,prim})\Gamma_{2,sec,\lambda 4}\right),$$

which implies

$$\left(\frac{\Lambda}{m_0(m_0 + r_{1,prim})\Gamma_{1,prim}}\right)\left((m_0+r_{1,prim})\Gamma_{2,prim,\lambda_4}+r_{1,prim}(1-\Gamma_{1,prim})\Gamma_{2,sec,\lambda_4}\right) = 1. \quad (5.55)$$

Thus, solution λ_4 must satisfy equation (5.55).

Note

$$\Gamma_{2,prim,\lambda_4} = \frac{m_0}{\Lambda}\int_0^\infty bV_{2,prim}(\tau)e^{-(m_0+r_{2,prim}+\lambda_4)\tau}\,d\tau,$$
$$\Gamma_{2,sec,\lambda_4} = \frac{m_0}{\Lambda}\int_0^\infty bV_{2,sec}(\tau)e^{-(m_0+r_{2,sec}+\lambda_4)\tau}\,d\tau.$$

Let

$$c = (m_0 + r_{1,prim})\Gamma_{1,prim},$$

$$d = r_{1,prim}(\Gamma_{1,prim} - 1),$$

$$H_1(\lambda) = \frac{1}{c}\int_0^\infty b\left[\frac{c}{\Gamma_{1,prim}}V_{2,prim}(\tau)e^{-(m_0+r_{2,prim})\tau} + dV_{2,sec}(\tau)e^{-(m_0+r_{2,sec})\tau}\right]e^{-\lambda\tau}d\tau. \quad (5.56)$$

Then we have that equation (5.55) is equivalent to

$$H_1(\lambda_4) = 1. \quad (5.57)$$

Thus, solution λ_4 must satisfy equation (5.57).

Lemma 5.4.9. *If $R_{0_1} < 1$, the equilibrium where only strain 1 persists is locally asymptotically stable.*

Proof. To prove this statement, we just need to to show that the solution λ_4 from equations (5.53) has negative real parts due to Lemma 5.4.8.

The solution λ_4 must satisfy $H_1(\lambda_4) = 1$ as shown in equation (5.57), where H_1 is defined in (5.56).

Suppose $\lambda_4 = \alpha + \beta i$ where $\alpha \geq 0$.

Note $|e^{\beta i}| = 1$ for all β.

Thus, using c, d, and H_1 as defined in (5.56),

$$\begin{aligned}
|H_1(\lambda_4)| &= \left| \frac{1}{c} \int_0^\infty \left[\frac{c}{\Gamma_{1,prim}} b V_{2,prim}(\tau) e^{-(m_0+r_{2,prim})\tau} + dbV_{2,sec}(\tau) e^{-(m_0+r_{2,sec})\tau} \right] e^{-\lambda_4 \tau} d\tau \right| \\
&\leq \frac{1}{c} \int_0^\infty \left[\frac{c}{\Gamma_{1,prim}} b V_{2,prim}(\tau) e^{-(m_0+r_{2,prim})\tau} + dbV_{2,sec}(\tau) e^{-(m_0+r_{2,sec})\tau} \right] |e^{-(\alpha+\beta i)\tau}| d\tau \\
&\leq \frac{1}{c} \int_0^\infty \left[\frac{c}{\Gamma_{1,prim}} b V_{2,prim}(\tau) e^{-(m_0+r_{2,prim})\tau} + dbV_{2,sec}(\tau) e^{-(m_0+r_{2,sec})\tau} \right] |e^{-\alpha\tau}||e^{-\beta i\tau}| d\tau \\
&= \frac{1}{c} \int_0^\infty \left[\frac{c}{\Gamma_{1,prim}} b V_{2,prim}(\tau) e^{-(m_0+r_{2,prim})\tau} + dbV_{2,sec}(\tau) e^{-(m_0+r_{2,sec})\tau} \right] e^{-\alpha\tau} d\tau \\
&\leq \frac{1}{c} \int_0^\infty \left[\frac{c}{\Gamma_{1,prim}} b V_{2,prim}(\tau) e^{-(m_0+r_{2,prim})\tau} + dbV_{2,sec}(\tau) e^{-(m_0+r_{2,sec})\tau} \right] d\tau \\
&= \frac{1}{c} \left(\frac{c}{\Gamma_{1,prim}} \Gamma_{2,prim} + d\Gamma_{2,sec} \right) \\
&= \frac{\Gamma_{2,prim}}{\Gamma_{1,prim}} + \frac{d}{c} \Gamma_{2,sec} \\
&= \frac{\Gamma_{2,prim}}{\Gamma_{1,prim}} + \frac{r_{1,prim}(\Gamma_{1,prim}-1)\Gamma_{2,sec}}{(m_0+r_{1,prim})\Gamma_{1,prim}} \\
&= \mathcal{R}_{0_1} < 1.
\end{aligned}$$

In summary, $|H_1(\lambda_4)| < 1$ if λ_4 has positive real parts.

Therefore, in order to satisfy $H_1(\lambda_4) = 1$, solution λ_4 must have negative real parts.

In conclusion, from Lemma 5.4.8, the solutions λ_1, λ_2, λ_3 to the equations (5.53) always have negative real parts.

We then showed that since $\mathcal{R}_{0_1} < 1$, the solution λ_4 to the equations (5.53) must have negative real parts.

Therefore, if $\mathcal{R}_{0_1} < 1$, the equilibrium is locally asymptotically stable. □

Lemma 5.4.10. *If $\mathcal{R}_{0_1} > 1$, the equilibrium where only strain 1 persists is unstable.*

Proof. We show that the solution λ_4 from equations (5.53) has positive real parts if $\mathcal{R}_{0_1} > 1$.

We use c, d, and H_1 as defined in (5.56).

Since $\mathcal{R}_{0_1} > 1$,

$$\begin{aligned} H_1(0) &= \frac{1}{c}\int_0^\infty b\left[\frac{c}{\Gamma_{1,prim}}V_{2,prim}(\tau)e^{-(m_0+r_{2,prim})\tau} + dV_{2,sec}(\tau)e^{-(m_0+r_{2,sec})\tau}\right]d\tau \\ &= \frac{1}{c}\left(\frac{c}{\Gamma_{1,prim}}\Gamma_{2,prim} + d\Gamma_{2,sec}\right) \\ &= \frac{\Gamma_{2,prim}}{\Gamma_{1,prim}} + \frac{d}{c}\Gamma_{2,sec} \\ &= \frac{\Gamma_{2,prim}}{\Gamma_{1,prim}} + \frac{r_{1,prim}(\Gamma_{1,prim}-1)\Gamma_{2,sec}}{(m_0+r_{1,prim})\Gamma_{1,prim}} \\ &= \mathcal{R}_{0_1} > 1. \end{aligned}$$

The solution λ_4 must satisfy $H_1(\lambda_4) = 1$, as shown in equation (5.57).

Treating $H_1(\lambda_4)$ as a function of the real variable λ_4, we note

$$\lim_{\lambda_4\to\infty} H_1(\lambda_4) = 0.$$

Thus, since $H_1(0) > 1$, we have that $H_1(\lambda_4^*) = 1$ for some $\lambda_4^* > 0$.

Thus, $H_1(\lambda_4) = 1$ has a solution with a positive real part.

Therefore, if $\mathcal{R}_{0_1} > 1$, the equilibrium is unstable. □

In summary, we proved statement 1) in Proposition 5.4.8 using Lemma 5.4.7.

We proved statement 2) in Proposition 5.4.8 using Lemma 5.4.9.

We proved statement 3) in Proposition 5.4.8 using Lemma 5.4.10.

Thus, the proposition is proved. □

5.4.10 Strain 2 stability

Proposition 5.4.9. *The equilibrium where only strain 2 persists*

$$\begin{aligned}&\left(N^*_{SS}, N^*_{SR}, N^*_{RS}, N^*_{RR}, n^*_{SI}(\tau), n^*_{IS}(\tau), n^*_{RI}(\tau), n^*_{IR}(\tau)\right)\\ =&\left(\frac{\Lambda}{\Gamma_{2,prim}}, \frac{\Lambda r_{2,prim}(\Gamma_{2,prim}-1)}{m_0(m_0+r_{2,prim}\Gamma_{2,prim})}, 0, 0, \frac{\Lambda(\Gamma_{2,prim}-1)}{\Gamma_{2,prim}}e^{-(m_0+r_{2,prim})\tau}, 0, 0, 0\right).\end{aligned}$$

1) exists if $\Gamma_{1,prim} > 1$*;*

2) is locally asymptotically stable if $\mathcal{R}_{0_1} < 1$*;*

3) is unstable if $\mathcal{R}_{0_1} > 1$*,*

where

$$\mathcal{R}_{0_2} = \frac{\Gamma_{1,prim}}{\Gamma_{2,prim}} + \frac{r_{2,prim}(\Gamma_{2,prim}-1)\Gamma_{1,sec}}{\Gamma_{2,prim}(m_0+r_{2,prim})}. \tag{5.58}$$

Proof. The proof is similar to Proposition 5.4.8. □

5.4.11 Coexistence stability

Conjecture 5.4.1. *The coexistence equilibrium*

$$\left(N^*_{SS}, N^*_{SR}, N^*_{RS}, N^*_{RR}, n^*_{SI}(\tau), n^*_{IS}(\tau), n^*_{RI}(\tau), n^*_{IR}(\tau)\right)$$

exists and is locally asymptotically stable if

$$\Gamma_{1,prim} > 1 \text{ (and/or) } \Gamma_{2,prim} > 1$$

and the following dependent conditions are met.

If $\Gamma_{1,prim} > 1$*, then also require* $\mathcal{R}_{0_1} > 1$*; if* $\Gamma_{2,prim} > 1$*, then also require* $\mathcal{R}_{0_2} > 1$*.*

While we cannot prove this remark analytically, numerical results allow us to conjecture this statement.

If $\Gamma_{1,prim} > 1$ (and/or) $\Gamma_{2,prim} > 1$, then the extinction equilibrium is unstable from Proposition 5.4.7.

If $\Gamma_{1,prim} > 1$ and $\mathcal{R}_{0_1} > 1$, then the equilibrium where only strain 1 persists is unstable from Proposition 5.4.8.

If $\Gamma_{2,prim} > 1$ and $\mathcal{R}_{0_2} > 1$, then the equilibrium where only strain 2 persists is unstable from Proposition 5.4.9.

Also note the solutions to System (5.1) must be bounded, as shown in Proposition 5.4.1.

Therefore, if the statements listed in Remark 5.4.1 are true, the solution must approach an equilibrium that is locally asymptotically stable.

Since no other equilibria are locally asymptotically stable, the coexistence equilibrium must be locally asymptotically stable.

In our numerical simulations, we do not find a situation where the coexistence equilibrium exists when one of the other equilibria is stable.

Thus, we postulate that the coexistence equilibrium only exists and is locally asymptotically stable when all other equilibria are unstable.

5.5 Numerical results

5.5.1 Numerical algorithm

We provide a complete set of equations for the numerical algorithm required to simulate our time-since-infection immunoepidemiological model, system (5.1). Here, denote time by t and time-since-infection by τ. Δt $(= \Delta\tau)$ is the step size used; K is the maximum number of

steps in τ-time; k is the reference index to denote the k-th step in time-since-infection; and q is the reference index to denote the q-th step in system time. Note that this derivation requires $\Delta t = \Delta\tau$, and the numerical scheme is in a format so that it can be readily adapted to code (i.e. the indices for τ have been shifted such that the lower bound starts at 1). We also assume that $N_T = \dfrac{\Lambda}{m_0}$.

The algorithm for the PDEs in System (5.1) is

$$\begin{aligned}
n_{SI}^{k+1,q+1} &= \frac{n_{SI}^{k,q}}{1+(m_0+r_{2,prim})\Delta t},\\
n_{IS}^{k+1,q+1} &= \frac{n_{IS}^{k,q}}{1+(m_0+r_{1,prim})\Delta t},\\
n_{RI}^{k+1,q+1} &= \frac{n_{RI}^{k,q}}{1+(m_0+r_{2,sec})\Delta t},\\
n_{IR}^{k+1,q+1} &= \frac{n_{IR}^{k,q}}{1+(m_0+r_{1,sec})\Delta t},
\end{aligned} \tag{5.59}$$

with boundary conditions

$$\begin{aligned}
n_{SI}^{1,q+1} &= \frac{N_{SS}^{q+1}}{N_T}\left[b\sum_{k=2}^{K+1}\left(V_{2,prim}^{k}n_{SI}^{k,q+1}+V_{2,sec}^{k}n_{RI}^{k,q+1}\right)\Delta t\right],\\
n_{IS}^{1,q+1} &= \frac{N_{SS}^{q+1}}{N_T}\left[b\sum_{k=2}^{K+1}\left(V_{1,prim}^{k}n_{IS}^{k,q+1}+V_{1,sec}^{k}n_{IR}^{k,q+1}\right)\Delta t\right],\\
n_{RI}^{1,q+1} &= \frac{N_{RS}^{q+1}}{N_T}\left[b\sum_{k=2}^{K+1}\left(V_{2,prim}^{k}n_{SI}^{k,q+1}+V_{2,sec}^{k}n_{RI}^{k,q+1}\right)\Delta t\right],\\
n_{IR}^{1,q+1} &= \frac{N_{SR}^{q+1}}{N_T}\left[b\sum_{k=2}^{K+1}\left(V_{1,prim}^{k}n_{IS}^{k,q+1}+V_{1,sec}^{k}n_{IR}^{k,q+1}\right)\Delta t\right].
\end{aligned} \tag{5.60}$$

The algorithm for the ODEs in System (5.1) is given by

$$
\begin{aligned}
N_{SS}^{q+1} &= \frac{\Lambda\Delta t + N_{SS}^{q}}{1 + m_0\Delta t + \frac{\Delta t}{N_T}\left[b\sum_{k=2}^{K+1}\left(V_{2,prim}^{k}n_{SI}^{k,q+1} + V_{1,prim}^{k}n_{IS}^{k,q+1} + V_{2,sec}^{k}n_{RI}^{k,q+1} + V_{1,sec}^{k}n_{IR}^{k,q+1}\right)\Delta t\right]},\\
N_{SR}^{q+1} &= \frac{N_{SR}^{q} + r_{2,prim}\Delta t\left[\sum_{k=2}^{K+1} n_{SI}^{k,q+1}\Delta t\right]}{1 + m_0\Delta t + \frac{\Delta t}{N_T}\left[b\sum_{k=2}^{K+1}\left(V_{1,prim}^{k}n_{IS}^{k,q+1} + V_{1,sec}^{k}n_{IR}^{k,q+1}\right)\Delta t\right]},\\
N_{RS}^{q+1} &= \frac{N_{RS}^{q} + r_{1,prim}\Delta t\left[\sum_{k=2}^{K+1} n_{IS}^{k,q+1}\Delta t\right]}{1 + m_0\Delta t + \frac{\Delta t}{N_T}\left[b\sum_{k=2}^{K+1}\left(V_{2,prim}^{k}n_{SI}^{k,q+1} + V_{2,sec}^{k}n_{RI}^{k,q+1}\right)\Delta t\right]},\\
N_{RR}^{q+1} &= \frac{N_{RR}^{q} + \Delta t\left[\sum_{k=2}^{K+1}\left(r_{1,sec}n_{IR}^{k,q+1} + r_{2,sec}n_{RI}^{k,q+1}\right)\Delta t\right]}{1 + m_0\Delta t}.
\end{aligned}
\tag{5.61}
$$

The initial conditions are

$$
\begin{aligned}
N_{SS}(0) &= N_{SS0}, \qquad & N_{SI}(0) &= \sum_{k=2}^{K+1} n_{SI0}^{k}\Delta t,\\
N_{SR}(0) &= N_{SR0}, \qquad & N_{IS}(0) &= \sum_{k=2}^{K+1} n_{IS0}^{k}\Delta t,\\
N_{RS}(0) &= N_{RS0}, \qquad & N_{RI}(0) &= \sum_{k=2}^{K+1} n_{RI0}^{k}\Delta t,\\
N_{RR}(0) &= N_{RR0}, \qquad & N_{IR}(0) &= \sum_{k=2}^{K+1} n_{IR0}^{k}\Delta t.
\end{aligned}
$$

We follow [71] (pp. 351-356) to develop the numerical algorithm. We include a discussion of several important assumptions made throughout the derivation, which is intended to provide some intuition in the choices that led to our final numerical scheme.

Notation and Truncation of the Domain

We denote time by t and time-since-infection by τ. To discretize the domain, we divide the age of infection direction by equally spaced steps using a step size of $\Delta\tau$ such that after the k-th step, $\tau_k = k\Delta\tau$. Similarly, the time direction is divided into equally spaced steps of size Δt such that after the q-th step, $t_q = q\Delta t$. We assume variables in the ODEs in System (5.1) evaluated at time t_q have the form $N_{SS}(t_q)$, and are approximated numerically by N_{SS}^q. The variables in the PDEs in System (5.1) have the form $n_{SI}(\tau_k, t_q)$, and are approximated numerically by $n_{SI}^{k,q}$.

As the domain of the system is infinite,

$$D = \{(\tau, t) : \tau \geq 0, t \geq 0\},$$

we must create a reasonable approximation and truncate the domain in both age of infection (τ) and time (t)

$$D = \{(\tau, t) : 0 \leq \tau \leq G, 0 \leq t \leq T\}.$$

Because individuals eventually succumb to natural mortality if infected for a sufficiently long period of time, $\lim_{\tau \to \infty} n_{SI}(\tau, t) = 0$. To evaluate the infinite integral

$$\int_0^\infty r_{2,prim} n_{SI}(\tau, t)\, d\tau,$$

we choose G large enough so that $n_{SI}(\tau, t) < \epsilon$ for all $\tau \geq G$. Thus, we guarantee the difference between the finite sum and the infinite integral is sufficiently small. Similar reasoning can be applied for the infinite integrals involving $n_{IS}(\tau, t)$, $n_{RI}(\tau, t)$, and $n_{IR}(\tau, t)$.

For the numerical simulations, we assume a constant recovery rate, implying an underlying exponential distribution in τ. Even with a moderate average length of infection, there remain individuals with long infections, so we must take care to choose G large enough to minimize the proportion of the class discarded. We have found $G = 100$ to be sufficient.

Partial Differential Equations

We first consider the partial differential equation for n_{SI} from System (5.1) and evaluate it at t_{q+1} and τ_k, which results in

$$\frac{\partial}{\partial \tau} n_{SI}(\tau_k, t_{q+1}) + \frac{\partial}{\partial t} n_{SI}(\tau_k, t_{q+1}) = -(m_0 + r_{2,prim}) n_{SI}(\tau_k, t_{q+1}). \tag{5.62}$$

Using forward differentiation for the derivative in τ, such that the term on the right hand side occurs at time τ_k (step k), and backward differentiation for the derivative in t, such that the term on the right hand side occurs at time $t_q + \Delta t$ (step q+1), we have

$$\frac{n_{SI}^{k+1,q+1} - n_{SI}^{k,q+1}}{\Delta \tau} + \frac{n_{SI}^{k,q+1} - n_{SI}^{k,q}}{\Delta t} = -(m_0 + r_{2,prim}) n_{SI}^{k,q+1}. \tag{5.63}$$

The choice of forward differentiation for the derivative in τ and backward differentiation for the derivative in t is needed for the cancellation of mixed terms (evaluated at the k-th step with respect to τ and the q+1-th step with respect to t) on the left hand side.

To simplify, we assume both age of infection and time proceed at the same rate such that $\Delta \tau = \Delta t$. This assumption is necessary for cancellation of the mixed terms in equation (5.63), and forms a square mesh for the discretized domain.

Following cancellation on the left hand side of equation (5.63), the mixed term $n_{SI}^{k,q+1}$ only appears on the right hand side. However, it is necessary that we approximate this variable with a similar term to one appearing on the left hand side. Thus, we use the assumption $n_{SI}^{k,q+1} \approx n_{SI}^{k+1,q+1}$. Without such an assumption, the solution for $n_{SI}^{k+1,q+1}$ in equation (5.63) depends on $n_{SI}^{k,q+1}$ and the solution for $n_{SI}^{1,q+1}$ in the boundary conditions (5.60) depends on $n_{SI}^{k+1,q+1}$, which cannot be numerically computed.

With $\Delta \tau = \Delta t$, and with the assumption that $n_{SI}^{k,q+1} \approx n_{SI}^{k+1,q+1}$, equation (5.63) simplifies

to

$$\frac{n_{SI}^{k+1,q+1} - n_{SI}^{k,q}}{\Delta t} = -(m_0 + r_{2,prim}) n_{SI}^{k+1,q+1}. \tag{5.64}$$

Solving equation (5.64) for $n_{SI}^{k+1,q+1}$, we obtain

$$n_{SI}^{k+1,q+1} = \frac{n_{SI}^{k,q}}{1 + (m_0 + r_{2,prim})\Delta t}. \tag{5.65}$$

Similar equations are obtained for the other PDEs, $n_{IS}^{k+1,q+1}$, $n_{IR}^{k+1,q+1}$, and $n_{RI}^{k+1,q+1}$, which are summarized in equations (5.59).

We return to the boundary conditions for the PDEs later in Section 5.5.1 as they depend on N_{SS}, N_{SR}, and N_{RS} at time t_{q+1}, which we have not yet computed.

Ordinary Differential Equations

We consider the ordinary differential equation for N_{SS} from System (5.1) and evaluate it at t_{q+1}, which results in

$$\begin{aligned}\frac{dN_{SS}(t_{q+1})}{dt} = \Lambda &- m_0 N_{SS}(t_{q+1}) \\ &- \frac{N_{SS}(t_{q+1})}{N_T(t_{q+1})} \int_0^\infty \Big[bV_{1,prim}(\tau) n_{IS}(\tau, t_{q+1}) + bV_{2,prim}(\tau) n_{SI}(\tau, t_{q+1}) \\ &\qquad + bV_{1,sec}(\tau) n_{IR}(\tau, t_{q+1}) + bV_{2,sec}(\tau) n_{RI}(\tau, t_{q+1}) \Big] d\tau. \end{aligned} \tag{5.66}$$

We then use backward differentiation from time t_{q+1}, such that all terms on the right hand side of equation (5.66) occur at step $q+1$. The choice of backward differentiation comes from the need to match the boundary condition which will be evaluated at step $q+1$ (see Boundary Conditions subsection).

The integral terms evaluate the τ-dependent variables across the entire history of infection.

We approximate the integral with a sum by employing the right Riemann sum with step size $\Delta\tau$ up to our maximum infection length considered, G. This results in $K = \frac{G}{\Delta\tau}$ intervals of length $\Delta\tau$. On each interval, we evaluate the integrand at the right endpoint. A component of these integrands is the output of our within-host model after the k^{th} interval, i.e. $V_{i,j}^k$ with $i \in \{1, 2\}$ and $j \in \{prim, sec\}$.

Thus, using backward differentiation from time t_{q+1} and approximating the integral using a right Riemann sum, we can write equation (5.66) as

$$\begin{aligned}\frac{N_{SS}^{q+1} - N_{SS}^{q}}{\Delta t} &= \Lambda - m_0 N_{SS}^{q+1} \\ &\quad - \frac{N_{SS}^{q+1}}{N_T^{q+1}} \left[b \sum_{k=1}^{K} \left(V_{2,prim}^k n_{SI}^{k,q+1} + V_{1,prim}^k n_{IS}^{k,q+1} + V_{2,sec}^k n_{RI}^{k,q+1} + V_{1,sec}^k n_{IR}^{k,q+1} \right) \Delta\tau \right].\end{aligned} \tag{5.67}$$

We use that fact that there is constant population size such that $N_T^{q+1} = N_T^q = N_T = \frac{\Lambda}{m_0}$, i.e. System (5.1) sums to 0. Without a constant total population, it would not be possible in our numerical scheme to explicitly solve for the variables from our ODEs, since N_T^{q+1} depends on N_{SS}^{q+1}, which depends on N_T^{q+1}, as can be seen in equations (5.67) and (5.68). Additionally, we note that many available pre-packaged software programs assume a step-size of $\Delta t = \Delta\tau = 1$. We caution that this step-size may be too large to observe all the dynamics, and may possibly lead to inconsistency in total population size.

Using the knowledge of constant population size and the assumption $\Delta t = \Delta\tau$, we solve equation (5.67) for N_{SS}^{q+1} and obtain

$$N_{SS}^{q+1} = \frac{\Lambda \Delta t + N_{SS}^{q}}{1 + m_0 \Delta t + \frac{\Delta t}{N_T} \left[b \sum_{k=1}^{K} \left(V_{2,prim}^k n_{SI}^{k,q+1} + V_{1,prim}^k n_{IS}^{k,q+1} + V_{2,sec}^k n_{RI}^{k,q+1} + V_{1,sec}^k n_{IR}^{k,q+1} \right) \Delta\tau \right]}. \tag{5.68}$$

Next, we consider the ordinary differential equation for N_{SR} in System (5.1). We use back-

ward differentiation from time t_{q+1} and approximate the integrals using right Riemann sums to obtain

$$\frac{N_{SR}^{q+1}-N_{SR}^{q}}{\Delta t}=-m_0N_{SR}^{q+1}-\frac{N_{SR}^{q+1}}{N_T^{q+1}}\left[b\sum_{k=1}^{K}\left(V_{1,prim}^{k}n_{IS}^{k,q+1}+V_{1,sec}^{k}n_{IR}^{k,q+1}\right)\Delta\tau\right]$$
$$+r_{2,prim}\left[\sum_{k=1}^{K}n_{SI}^{k,q+1}\Delta\tau\right].$$

Again we consider constant population size N_T, $\Delta t=\Delta\tau$ and solve for N_{SR}^{q+1} to obtain

$$N_{SR}^{q+1}=\frac{N_{SR}^{q}+r_{2,prim}\Delta t\left[\sum_{k=1}^{K}n_{SI}^{k,q+1}\Delta t\right]}{1+m_0\Delta t+\frac{\Delta t}{N_T}\left[b\sum_{k=1}^{K}\left(V_{1,prim}^{k}n_{IS}^{k,q+1}+V_{1,sec}^{k}n_{IR}^{k,q+1}\right)\Delta t\right]}.$$

Similar arguments are used to obtain N_{RS}^{q+1} and N_{RR}^{q+1}.

It is important to note, that as currently written, we start our reference indices k at $k=0$. We see that since we use right Riemann sums and we begin the sums at $k=1$, this implies the first interval used in τ-time is $[\tau_0,\tau_1]$. To avoid confusion when coding this algorithm in coding languages that start with a default initial index of 1 (e.g. MATLAB), we shift the indices for the τ variable up by one, thus starting our reference indices k at $k=1$. This results in a change to the bounds of the sums. For example, equation (5.68) becomes

$$N_{SS}^{q+1}=\frac{\Lambda\Delta t+N_{SS}^{q}}{1+m_0\Delta t+\frac{\Delta t}{N_T}\left[b\sum_{k=2}^{K+1}\left(V_{2,prim}^{k}n_{SI}^{k,q+1}+V_{1,prim}^{k}n_{IS}^{k,q+1}+V_{2,sec}^{k}n_{RI}^{k,q+1}+V_{1,sec}^{k}n_{IR}^{k,q+1}\right)\Delta t\right]}.$$

We summarize the algorithm for the ODEs in equations (5.61).

Boundary Conditions

We now return to consider the boundary conditions for our PDEs in System (5.1). We note that since they depend on both the PDEs and ODEs, we must compute those before we can

compute our boundary conditions.

As described in the Ordinary Differential Equations subsection, we start our reference indices k at $k = 1$. Thus, we evaluate the boundary conditions at $\tau_1 = 0$ and t_{q+1}. For example, the boundary condition associated with n_{SI} is

$$n_{SI}(\tau_1, t_{q+1}) = \frac{N_{SS}(t_{q+1})}{N_T(t_{q+1})} \int_0^\infty \left[bV_{2,prim}(\tau) n_{SI}(\tau, t_{q+1}) + bV_{2,sec}(\tau) n_{RI}(\tau, t_{q+1}) \right] d\tau. \quad (5.69)$$

As done previously, we assume constant total population N_T and $\Delta t = \Delta\tau$, and we use right Riemann sums to evaluate the integrals. We note we also computed $N_{SS}(t_{q+1})$ previously. Thus, we write equation (5.69) as

$$n_{SI}^{1,q+1} = \frac{N_{SS}^{q+1}}{N_T} \left[b \sum_{k=2}^{K+1} \left(V_{2,prim}^k n_{SI}^{k,q+1} + V_{2,sec}^k n_{RI}^{k,q+1} \right) \Delta t \right]. \quad (5.70)$$

We can write the other boundary conditions similarly using our previously computed PDEs and ODEs. The boundary conditions are summarized in equations (5.60).

5.5.2 Generating numerical results

We simulate two virus profiles that are defined for $\tau \geq 0$, where $V_{\mathrm{F}}(\tau)$ is the profile associated with dengue fever, and $V_{\mathrm{H}}(\tau)$ is the profile associated with dengue hemorrhagic fever (see Figure 5.2). The recovery rates r_{F} and r_{H}, associated with dengue fever and dengue hemorrhagic fever respectively, are also determined from the virus profiles as one over the average length of infection (see Table 5.2). We determine the total infectiousness under each condition based on the shape of virus profiles in Figure 5.2 as

$$\text{Dengue fever: } \int_0^\infty V_{\mathrm{F}}(\tau) e^{-(m_0 + r_{\mathrm{F}})\tau} \, d\tau \approx 40.8003,$$
$$\text{Dengue hemorrhagic fever: } \int_0^\infty V_{\mathrm{H}}(\tau) e^{-(m_0 + r_{\mathrm{H}})\tau} \, d\tau \approx 52.4801.$$

The choice of parameterization will impact the quantitative values for the existence and stability of the different equilibria, which we refer to as equilibrium structure. The derivation of the equilibrium structure under our chosen parameterization is described in Section 5.6.

Table 5.2: Parameter values for simulations.

Parameter	Standard value	Units
Λ	$\frac{10000}{365}$	people $\cdot$ day^{-1}
m_0	$\frac{1}{365 \cdot 70}$	day^{-1}
b	varied in [0,0.03]	ml$\cdot$(RNA $\cdot$ day)$^{-1}$
r_{F}	$\frac{1}{12}$	day^{-1}
r_{H}	$\frac{1}{14}$	day^{-1}
V_{F}	see Figure 2 solid line	RNA $\cdot$ ml^{-1}
V_{H}	see Figure 2 dashed line	RNA $\cdot$ ml^{-1}

5.5.3 Numerical simulations

We determine the equilibrium structure based on the course of infection, i.e. which strain infects first and whether each infection results in dengue fever or dengue hemorrhagic fever. Therefore, we consider all possible combinations of strain order and disease type. Since we assume infection with one strain induces immunity against secondary infections with the same strain, we only consider primary-secondary infection events caused by two different virus strains. For example, in Figure 5.3, the course of infection is either (i) primary infection with strain 1 resulting in dengue fever followed by secondary infection with strain 2 resulting in dengue fever ($V_{1,prim} = \mathrm{F}$, $V_{2,sec} = \mathrm{F}$) or (ii) primary infection with strain 2 resulting in dengue hemorrhagic fever followed by secondary infection with strain 1 resulting in dengue hemorrhagic fever ($V_{2,prim} = \mathrm{H}$, $V_{1,sec} = \mathrm{H}$). For each combination we determine whether both strains can coexist within the population, both strains go extinct, or only one strain persists. The equilibrium reached is based on parameter b, the constant that relates viral load to between-host transmission rate, and the disease type each strain induced (F versus H). Under fixed model parameterization and changing b, we can obtain all the described between-

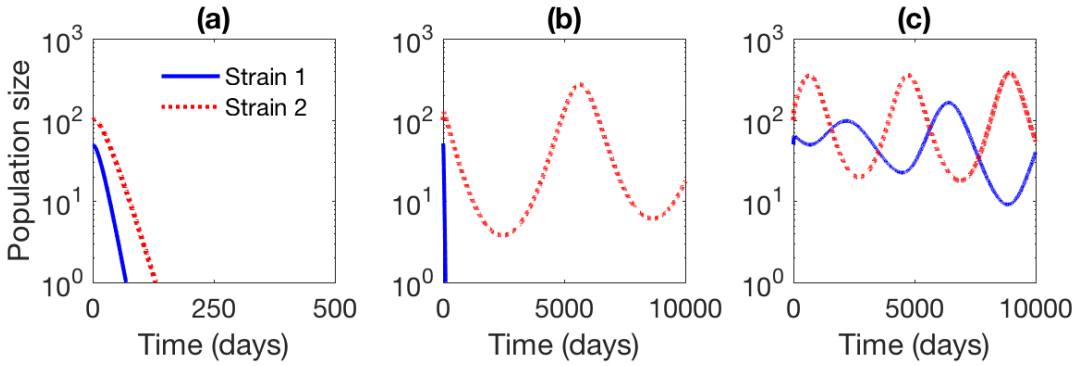

Figure 5.3: **Between-host infected population dynamics.** The total infected population (combining both primary and secondary infections) of strain 1 (blue solid) and strain 2 (red dashed) over 10,000 days results in (a) the extinction equilibrium, (b) persistence of only strain 2 and (c) the coexistence equilibrium. In (a), $b = 0.018$, $N_{SR0} = 5 \times 10^4$, and $N_{SS0} = 5.2485 \times 10^5$. In (b), $b = 0.023$, $N_{SR0} = 5 \times 10^4$, and $N_{SS0} = 5.2485 \times 10^5$. In (c), $b = 0.028$, $N_{SR0} = 1.4 \times 10^5$, and $N_{RS0} = 4.3485 \times 10^5$. Parameters: Λ, m_0, r_{F}, r_{H} found in Table 5.2, $V_{1,prim} = V_{\mathrm{F}}$, $V_{2,prim} = V_{\mathrm{H}}$, $V_{1,sec} = V_{\mathrm{H}}$, $V_{2,sec} = V_{\mathrm{F}}$. Initial conditions: $N_{RS0} = 6.5 \times 10^4$, $N_{RR0} = 6 \times 10^4$, $N_{SI0} = 90$, $N_{IS0} = 40$, $N_{RI0} = N_{IR0} = 10$. See Section 5.6.4 for the τ distribution of initial values. Numerical algorithm parameters: $\Delta t = \Delta\tau = 0.5$, $\max(\tau) = 100$, $\max(t) = 10,000$.

host dynamics: extinction, persistence of one virus strain and coexistence (see Figure 5.3).

Our model predicts that both the strain order and disease type can lead to different between-host stable equilibria (see Figures 5.4 and 5.5). When both virus strains produce a primary infection resulting in dengue fever, there is between-host extinction of both infections, assuming that b is sufficiently low ($b < 0.024096$). In contrast, primary infection by either strain resulting in dengue hemorrhagic fever is more likely to lead to between-host coexistence, or at least the persistence of a single strain in the population for a minimum b ($0.0190548 < b$). Over a range of b ($0.0190548 < b < 0.024096$), all equilibria are possible, and the between-host equilibrium structure depends on the strain order and disease severity (see Figure 5.5). It is important to recognize that these results demonstrate the equilibrium structure under our chosen parameterization as b is varied. While this shows the overall importance of strain order and disease type for shaping the between-host equilibrium structure, similar analyses should be conducted to determine the structure for strains with different characteristics.

Because dengue fever usually occurs during primary infection and dengue hemorrhagic fever is more likely to occur during secondary infection, the most biologically relevant scenario to analyze when considering a *de novo* infection is the case F-H/F-H, where both courses of infection lead to dengue fever in primary infection and dengue hemorrhagic fever in secondary infection. In this scenario, the only possible outcomes are either extinction or coexistence. This is often the case with dengue viral infection, as areas either have no strains circulating or multiple strains circulating. However, our model can also account for two later infections (e.g. third and forth exposure in the population) in which case an H-F/H-F scenario is possible.

5.6 Equilibrium structure

5.6.1 Introduction

The parameter b is the proportionality constant relating the viral load to the transmission rate. For a particular strain order and disease type, we can calculate how changing the value of b will affect the equilibrium structure.

Let

$$\begin{aligned} V_{1P} &= \int_0^\infty V_{1,prim}(\tau)e^{-(m_0+r_{1,prim})\tau}\,d\tau, \\ V_{2P} &= \int_0^\infty V_{2,prim}(\tau)e^{-(m_0+r_{2,prim})\tau}\,d\tau, \\ V_{1S} &= \int_0^\infty V_{1,sec}(\tau)e^{-(m_0+r_{1,sec})\tau}\,d\tau, \\ V_{2S} &= \int_0^\infty V_{2,sec}(\tau)e^{-(m_0+r_{2,sec})\tau}\,d\tau. \end{aligned} \tag{5.71}$$

The following four equations come up in our stability conditions that determine the difference

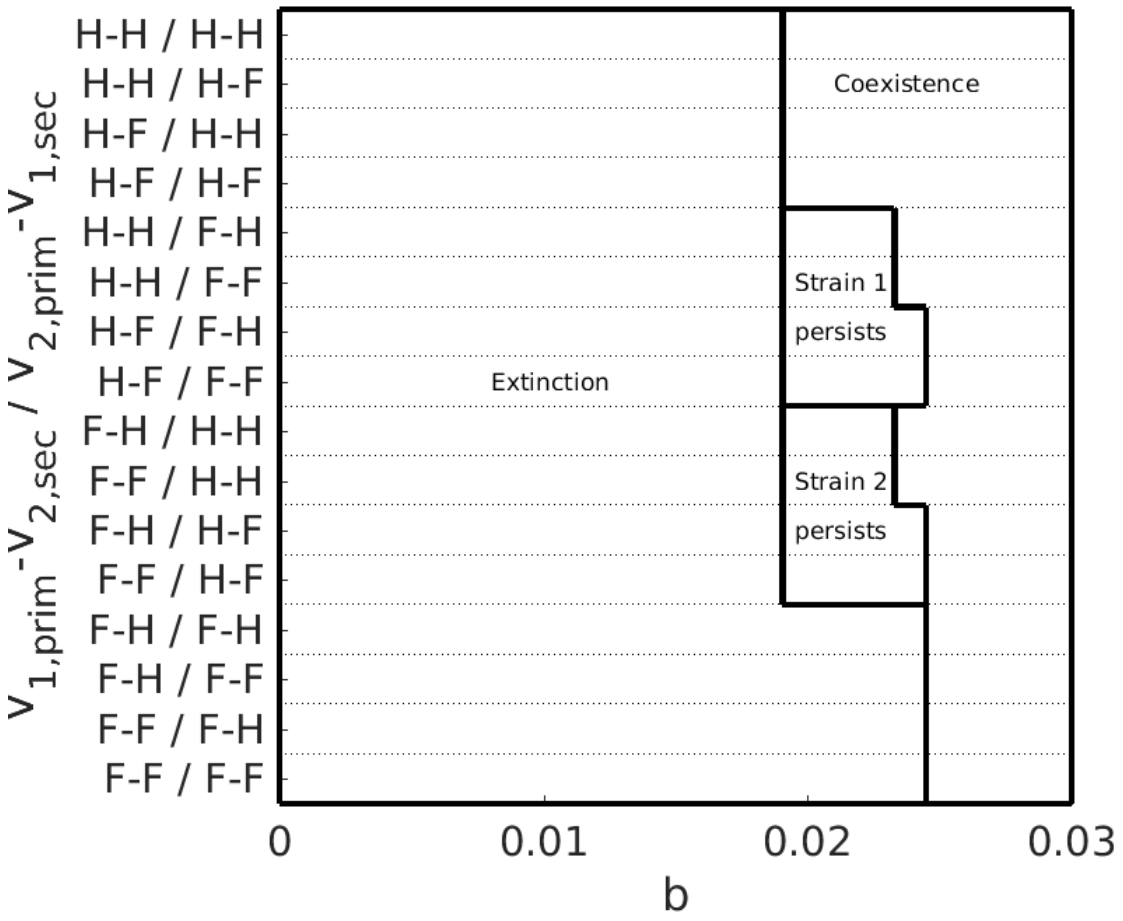

Figure 5.4: **Qualitative between-host equilibrium structure varying the proportionality constant relating viral load to between-host transmission rate, b.** In addition to the impact of b, the strain order and disease type (F = dengue fever, H = dengue hemorrhagic fever) affect the between-host equilibrium structure. The two possible courses of infection are $V_{1,prim} - V_{2,sec}$ and $V_{2,prim} - V_{1,sec}$.

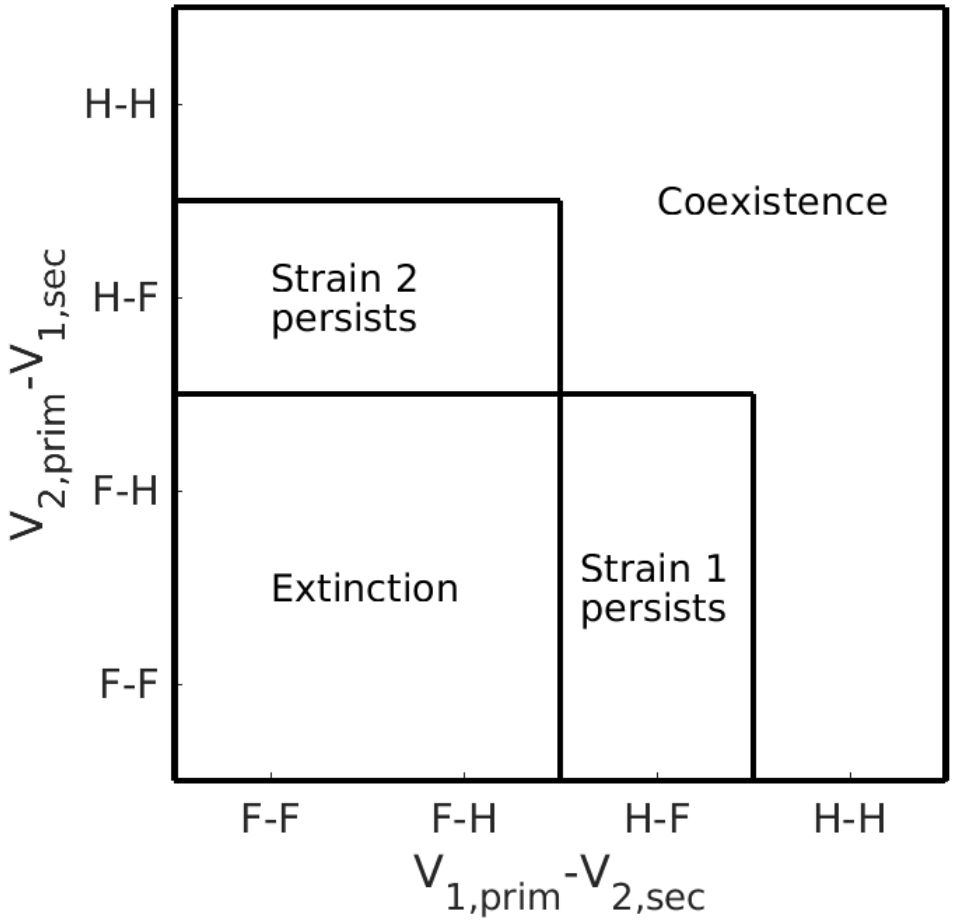

Figure 5.5: **Qualitative between-host equilibrium structure when** $b = 0.024$**.** The strain order and disease type (F = dengue fever, H = dengue hemorrhagic fever) affect the between-host equilibrium structure. The two possible courses of infection are $V_{1,prim} - V_{2,sec}$ and $V_{2,prim} - V_{1,sec}$. This plot summarizes the qualitative between-host equilibria when $b = 0.024$ as displayed in Fig. 5.4.

between an equilibrium being locally asymptotically stable or unstable.

$$\Gamma_{1,prim} = 1, \tag{5.72}$$

$$\Gamma_{2,prim} = 1, \tag{5.73}$$

$$\mathcal{R}_{0_1} = 1, \tag{5.74}$$

$$\mathcal{R}_{0_2} = 1, \tag{5.75}$$

where

$$\begin{aligned} \Gamma_{1,prim} &= \int_0^\infty bV_{1,prim}(\tau)e^{-(m_0+r_{1,prim})\tau}\,d\tau, \\ \Gamma_{2,prim} &= \int_0^\infty bV_{2,prim}(\tau)e^{-(m_0+r_{2,prim})\tau}\,d\tau, \end{aligned} \tag{5.76}$$

and $\mathcal{R}_{0_1}$ and $\mathcal{R}_{0_2}$ are defined in (5.51) and (5.58) respectively. Note that all of these equations involve b and at least one of the definitions in (5.71).

Thus, we can solve for the values of b that satisfy these conditions.

5.6.2 Solving for values of b

We now solve the equations (5.72), (5.73), (5.74), and (5.75) for b. We associate each of these equations with a different value of b, i.e $b_{G_{1P}}$, $b_{G_{2P}}$, $b_{R_{01}}$, and $b_{R_{02}}$.

Solving equation (5.72) for b, we have

$$\begin{aligned} \Gamma_{1,prim} &= 1 \\ \int_0^\infty bV_{1,prim}(\tau)e^{-(m_0+r_{1,prim})\tau}\,d\tau &= 1 \\ b \cdot V_{1P} &= 1 \\ b &= \frac{1}{V_{1P}}. \end{aligned} \tag{5.77}$$

Thus, we label

$$b_{G_{1P}} = \frac{1}{V_{1P}}. \tag{5.78}$$

Similarly, by solving equation (5.73) for b, we find

$$b_{G_{2P}} = \frac{1}{V_{2P}}. \tag{5.79}$$

Solving equation (5.74) for b, we have

$$\begin{aligned}
\mathcal{R}_{0_1} &= 1 \\
\frac{\Gamma_{2,prim}}{\Gamma_{1,prim}} + \frac{r_{1,prim}(\Gamma_{1,prim}-1)\Gamma_{2,sec}}{\Gamma_{1,prim}(m_0+r_{1,prim})} &= 1 \\
\frac{bV_{2P}}{bV_{1P}} + \frac{r_{1,prim}(bV_{1P}-1)bV_{2S}}{bV_{1P}(m_0+r_{1,prim})} &= 1 \\
\frac{V_{2P}}{V_{1P}} + \frac{r_{1,prim}(bV_{1P}-1)bV_{2S}}{bV_{1P}(m_0+r_{1,prim})} &= 1 \\
\frac{V_{2P}}{V_{1P}} + \frac{br_{1,prim}V_{2S}(bV_{1P}-1)}{bV_{1P}(m_0+r_{1,prim})} &= 1 \\
\frac{V_{2P}}{V_{1P}} + \frac{r_{1,prim}V_{2S}V_{1P}b - r_{1,prim}V_{2S}}{V_{1P}(m_0+r_{1,prim})} &= 1 \\
V_{2P}(m_0+r_{1,prim}) + r_{1,prim}V_{2S}V_{1P}b - r_{1,prim}V_{2S} &= V_{1P}(m_0+r_{1,prim}) \\
\frac{m_0(V_{1P}-V_{2P}) + r_{1,prim}(V_{1P}+V_{2S}-V_{2P})}{r_{1,prim}V_{1P}V_{2S}} &= b.
\end{aligned}$$

Thus, we label

$$b_{R_{01}} = \frac{m_0(V_{1P}-V_{2P}) + r_{1,prim}(V_{1P}+V_{2S}-V_{2P})}{r_{1,prim}V_{1P}V_{2S}}. \tag{5.80}$$

Similarly, by solving equation (5.75) for b, we find

$$b_{R_{02}} = \frac{m_0(V_{2P}-V_{1P}) + r_{2,prim}(V_{2P}+V_{1S}-V_{1P})}{r_{2,prim}V_{2P}V_{1S}}. \tag{5.81}$$

Note the equations (5.77) show $\Gamma_{1,prim} = 1$ is equivalent to $b = b_{G_{1P}}$. Thus, $\Gamma_{1,prim} < 1$ is equivalent to $b < b_{G_{1P}}$ and $\Gamma_{1,prim} > 1$ is equivalent to $b > b_{G_{1P}}$. We have similar equivalences for $b_{G_{2P}}$, b_{R01}, and b_{R02}.

In summary, from the above derivations, we have the following equivalences.

$$\begin{aligned}
\Gamma_{1,prim} < 1 &\iff b < b_{G_{1P}} \\
\Gamma_{1,prim} \geq 1 &\iff b \geq b_{G_{1P}} \\
\Gamma_{2,prim} < 1 &\iff b < b_{G_{2P}} \\
\Gamma_{2,prim} \geq 1 &\iff b \geq b_{G_{2P}} \\
\mathcal{R}_{0_1} < 1 &\iff b < b_{R_{01}} \\
\mathcal{R}_{0_1} \geq 1 &\iff b \geq b_{R_{01}} \\
\mathcal{R}_{0_2} < 1 &\iff b < b_{R_{02}} \\
\mathcal{R}_{0_2} \geq 1 &\iff b \geq b_{R_{02}}
\end{aligned} \tag{5.82}$$

5.6.3 Determining equilibrium structure

We use the definitions (5.78)-(5.81) and the equivalences (5.82) to determine for which values of b each equilibrium is locally asymptotically stable.

Extinction equilibrium

From Proposition 5.4.3, the extinction equilibrium is locally asymptotically stable when $\Gamma_{1,prim} < 1$ and $\Gamma_{2,prim} < 1$.

From the equivalences (5.82), the extinction equilibrium is locally asymptotically stable if $b < b_{G_{1P}}$ and $b < b_{G_{2P}}$.

Thus, the extinction equilibrium is locally asymptotically stable if

$$0 < b < \min(b_{G_{1P}}, b_{G_{2P}}). \tag{5.83}$$

Equilibrium where only strain 1 persists

From Proposition 5.4.4, the equilibrium where only strain 1 persists is locally asymptotically stable if $\Gamma_{1,prim} > 1$ and $\mathcal{R}_{0_1} < 1$.

From the equivalences (5.82), the equilibrium where only strain 1 persists is locally asymptotically stable if $b > b_{G_{1P}}$ and $b < b_{R_{01}}$.

Thus, the equilibrium where only strain 1 persists is locally asymptotically stable if

$$b_{G_{1P}} < b < b_{R_{01}}. \tag{5.84}$$

Note if $V_{1P} = V_{2P}$ (meaning the virus types of both strains during primary infection are the same), then $b_{G_{1P}} = b_{R_{01}}$. Therefore, the equilibrium can never be stable in this case.

Equilibrium where only strain 2 persists

From Proposition 5.4.5, the equilibrium where only strain 2 persists is locally asymptotically stable if $\Gamma_{2,prim} > 1$ and $\mathcal{R}_{0_2} < 1$.

From the equivalences (5.82), the equilibrium where only strain 2 persists is locally asymptotically stable if $b > b_{G_{2P}}$ and $b < b_{R02}$.

Thus, the equilibrium where only strain 2 persists is locally asymptotically stable if

$$b_{G_{2P}} < b < b_{R_{02}}. \tag{5.85}$$

Note if $V_{1P} = V_{2P}$ (meaning the virus types of both strains during primary infection are the same), then $b_{G_{2P}} = b_{R_{02}}$. Therefore, the equilibrium can never be stable in this case.

Coexistence equilibrium

From Conjecture 5.4.1, the coexistence equilibrium is locally asymptotically stable if all of the other states are unstable.

If the extinction equilibrium is unstable, then $b > \min(b_{G_{1P}}, b_{G_{2P}})$.

If the equilibrium where only strain 1 persists is unstable (and the extinction equilibrium is also unstable), then $b > b_{R_{01}}$.

If the equilibrium where only strain 2 persists is unstable (and the extinction equilibrium is also unstable), then $b > b_{R_{02}}$.

Thus, based on these results, the coexistence equilibrium is locally asymptotically stable if

$$b > \max\big(\min(b_{G_{1P}}, b_{G_{2P}}), b_{R_{01}}, b_{R_{02}}\big). \tag{5.86}$$

5.6.4 Generating figures 5.3 and 5.4

Introduction

Note Section 5.6.3 gives the general conditions for stability of the equilibria in terms of b. In order to calculate the definitions (5.78)-(5.81), we use the definitions (5.71), which depend on the virus profiles of strain order and disease type.

In our simulations, we use two virus profiles $V_{\mathrm{F}}(\tau)$ and $V_{\mathrm{H}}(\tau)$, where $V_{\mathrm{F}}(\tau)$ is the virus profile associated with dengue fever and $V_{\mathrm{H}}(\tau)$ is the virus profile associated with dengue hemorrhagic fever. These virus profiles are shown in Figure 5.2.

The recovery rates for dengue fever and dengue hemorrhagic fever are $r_{\mathrm{F}} = \frac{1}{12}$ and $r_{\mathrm{H}} = \frac{1}{14}$ respectively, since the virus profile for dengue fever in Figure 5.2 clears in 12 days and the virus profile for dengue hemorrhagic fever in Figure 5.2 clears in 14 days.

We also use $m_0 = \frac{1}{70(365)} \approx 3.9139 \times 10^{-5}$ to represent an average lifespan of 70 years.

We define

$$v_{\mathrm{F}} = \int_0^\infty V_{\mathrm{F}}(\tau) e^{-(m_0+r_{\mathrm{F}})\tau}\, d\tau,$$
$$v_{\mathrm{H}} = \int_0^\infty V_{\mathrm{H}}(\tau) e^{-(m_0+r_{\mathrm{H}})\tau}\, d\tau,$$

which we can calculate using the above parameters. These parameters are summarized in Table 5.2.

We note that based on the particular combination of strain order and disease type, each of V_{1P}, V_{2P}, V_{1S}, and V_{2S} as defined in (5.71) will be equal to either v_{F} or v_{H}. Also, each of $r_{1,prim}$, $r_{2,prim}$, $r_{1,sec}$, and $r_{2,sec}$ will be equal to either r_{F} or r_{H}.

Figure 5.4

Based on the parameters in Table 5.2, we calculate the values of $b_{G_{1P}}$, $b_{G_{2P}}$, $b_{R_{01}}$, and $b_{R_{02}}$ as defined in (5.78)-(5.81) for a particular combination of strain order and disease type.

Thus, we can determine the equilibrium structure for the particular combination of strain order and disease type.

For example, if we have $V_{1,prim} = \mathrm{F}$, $V_{2,prim} = \mathrm{H}$, $V_{1,sec} = \mathrm{H}$, $V_{2,sec} = \mathrm{F}$, we have that $V_{1P} = v_{\mathrm{F}}$, $V_{2P} = v_{\mathrm{H}}$, $V_{1S} = v_{\mathrm{H}}$, and $V_{2S} = v_{\mathrm{F}}$.

Therefore, $b_{G_{1P}} = 0.0245096$, $b_{G_{2P}} = 0.0190548$, $b_{R_{01}} = 0.01749$, and $b_{R_{02}} = 0.0232979$.

From equation (5.83), the extinction equilibrium is locally asymptotically stable if $0 < b < 0.0190548$.

From equation (5.84), the equilibrium where only strain 1 persists must always be unstable since $b_{R_{01}} < b_{G_{1P}}$.

From equation (5.85), the equilibrium where only strain 2 persists is locally asymptotically stable if $0.0190548 < b < 0.0232979$.

From equation (5.86), the coexistence equilibrium is locally asymptotically stable if $b > 0.0232979$.

We can use this same process to determine the equilibrium structure for all possible combinations of strain order and disease type. These results are summarized in Figure 5.4.

Figure 5.3

We use the F-F/H-H row of Figure 5.4 to produce the three different outcomes of extinction, single-strain persistence, and coexistence as shown in Figure 5.3. Here, extinction occurs if $0 < b < 0.0190548$, strain 2 persists if $0.0190548 < b < 0.0232979$, and coexistence occurs if $b > 0.0232979$.

Thus, we choose $b = 0.018$ to produce the extinction equilibrium, $b = 0.023$ to produce the equilibrium where strain 2 persists, and $b = 0.028$ to produce the coexistence equilibrium.

We use the parameters as described in the Figure 5.3 caption. The τ-distribution of our initial conditions is

$$n_{SI0}(\tau) = \left\{ r_{2,prim} N_{SI0} \text{ if } 0 \leq \tau \leq \frac{1}{r_{2,prim}};\ 0 \text{ if } \tau > \frac{1}{r_{2,prim}} \right\},$$

$$n_{IS0}(\tau) = \left\{ r_{1,prim} N_{IS0} \text{ if } 0 \leq \tau \leq \frac{1}{r_{1,prim}};\ 0 \text{ if } \tau > \frac{1}{r_{1,prim}} \right\},$$

$$n_{RI0}(\tau) = \left\{ r_{2,sec} N_{RI0} \text{ if } 0 \leq \tau \leq \frac{1}{r_{2,sec}};\ 0 \text{ if } \tau > \frac{1}{r_{2,sec}} \right\},$$

$$n_{IR0}(\tau) = \left\{ r_{1,sec} N_{IR0} \text{ if } 0 \leq \tau \leq \frac{1}{r_{1,sec}};\ 0 \text{ if } \tau > \frac{1}{r_{1,sec}} \right\}.$$

5.7 Discussion

The precise mechanisms generating the population-level dynamics of dengue serotypes remain difficult to uncover as a result of the complexity of the pathogen itself. For example, four distinct dengue serotypes exist and there is a marked increase in disease severity following a secondary infection with a heterologous serotype. Multiple competing hypotheses exist to explain this phenomenon, and further uncertainty exists surrounding the role of both primary and secondary infection and the disease type induced (F vs H) in driving the transmission and persistence of multiple serotypes in the population. We developed a time-since-infection immunoepidemiological model as a means of integrating the within-host and population-level dynamics of two co-circulating strains of dengue. Through both model analysis and numerical simulations, we demonstrate that the between-host equilibrium structure critically depends on both the strain order and disease type. To be precise, it may be more appropriate to consider this model as an infection-age structured model with transmission rate related to within-host viral load. Even though our virus profiles are generated from within-host models [88, 89], we simplify these profiles to triangular distributions during our simulations. This is different than other self-described immunoepidemiological models [111, 41], which generate the within-host model using differential equations. Our simplifications may have an affect on our results and is something worth exploring in the future.

Although dengue has four serotypes, we simplified our analysis to consider two co-circulating strains. At the population level, we assumed that the transmission dynamics for each strain followed the classic SIR paradigm and we simultaneously tracked the infection status for both strains in the population. Importantly, we assumed that the transmission rate associated with each dengue infection is directly proportional to the viral load of an infectious individual. Because viral load is directly related to an individual's time-since-infection, we coupled our population-level model with the within-host virus dynamics, where we considered that primary and secondary infections may result in either dengue fever or dengue

hemorrhagic fever. We find that, for large enough transmission rates, we can observe either between-hosts extinction of both virus infections, persistence of one virus infection, or coexistence of both virus infections depending on the profiles of infection. In particular, if the within-host primary infections for both strains result in dengue hemorrhagic fever then one or both strains will remain endemic in the population. That is true even if the within-host secondary infection by either or both strains results in dengue fever. This implies that the severity of infection in the population is not dependent on the increased severity of a secondary heterologous infection in an individual, and only depends of the profile of the individual's primary infection.

Our model assumes that the individual's virus profile influences transmission to another individual. These results may change if we change our assumption to account for an individual's immunological responses [89], their role in transmission [4, 5, 14, 16, 25, 104], or if we consider cross-immunity between virus strains [15, 84]. Moreover, we assume a linear relationship between the transmission rate and viral load. Further investigation is needed to determine whether these results will change if we use density dependent transmission rates [105], Hill-type transmission rates [35], or strain variability in per contact transmission probability [106].

Dengue persistence and extinction in a population are influenced by factors other than order of infection and viral type. Previous studies focusing on the role of spatial spread [115], stochastic extinction events [109, 123], and seasonal forcing [4] have all shown that these characteristics can drive the spread of dengue infection in a population. Understanding the impacts of such added complexities is important to obtain a more global picture of this system; however, it will likely impact the analytic tractability of our system and is beyond the scope of our current work.

5.8 Conclusion

Using a modeling framework that integrated the within-host transmission dynamics and between-host virus dynamics of dengue virus infection, we investigated the roles of order and type of infection in driving the long term persistence of co-circulating dengue serotypes in a population. Our findings indicate that these processes can determine whether both strains co-exist, both become extinct, or only one persists. The integration of multiple scales – in our case both within-host and between-hosts dynamics – provides a means to investigate complex processes that have significant dependence on input from different levels.

Chapter 6

Conclusion

In summary, we have outlined different mathematical models describing dengue viral infection, both at the within-host level and at the epidemiological level.

We first developed within-host models of dengue viral infections that considered the contributions of T cells to disease severity. We fitted these models to published patient data and showed that the overall infected cell killing is similar in dengue secondary infections resulting in DF and DHF cases. The contribution to overall killing, however, is dominated by non-specific, less efficacious, T cell responses during secondary DHF cases compared with strain-specific, high avidity T cell responses in at least half of secondary DF cases. Therefore, the cross-reactive cellular immune responses, as described in the hypothesis of original antigenic sin, may be present and responsible for the disease enhancement during heterologous infections.

Using the results from our within-host models and certain simplifying assumptions, we studied the effects of incorporating the within-host viral dynamics into the transmission dynamics at the betwen-host level. We investigated the roles of order and type of infection in driving the long term persistence of co-circulating dengue serotypes in a population. Our findings indicate that these processes can determine whether both strains co-exist, both become

extinct, or only one persists.

In the future, we are interested in expanding the dengue infection immuno-epidemiolgical study to address the effects of vaccination. Due to the higher risk of more severe disease during secondary infections due to cross-reactive immune responses, a vaccine that is not protective across all strains may induce prevalence of more severe diseases [45]. Mathematical models are a cost-efficient way to study this possible outcome, and to predict prevention methods that limit negative effects that may arise from the introduction of vaccines. We are also interested in including vector transmission explicitly and analyzing how different control methods may affect the spread of the virus in different populations. Even though we have mainly studied dengue viral infection, we are interested in applying models of a similar nature to other diseases.

In our review of immunoepidemiological models, we only focused on models of HIV. In the future, we would like to review how immunoepidemiological models are applied to infectious diseases on a broader scale, categorize how these models are validated against data, and classify how their results differ from epidemiological models.

Since we would like the work we do to have an impact on the spread of the diseases we are studying, we would like to collaborate with biologists to determine whether we can design experiments that can further inform the models. For example, we would like to verify our explanation for the role of original antigenic sin during dengue viral infection, which may give more insight into developing better vaccines. We are also interested in how the results of the immunoepidemiological model can be validated experimentally, and further studying optimization algorithms to obtain better model predictions.

Bibliography

[1] J. Aaskov, K. Buzacott, H. M. Thu, K. Lowry, and E. C. Holmes. Long-term transmission of defective RNA viruses in humans and *Aedes* mosquitoes. *Science*, 311(5758):236–238, 2006.

[2] L. J. Abu-Raddad, A. S. Magaret, C. Celum, A. Wald, I. M. Longini, Jr., S. G. Self, and L. Corey. Genital herpes has played a more important role than any other sexually transmitted infection in driving HIV prevalence in Africa. *PLoS One*, 3(5):e2230, 2008.

[3] B. Adams and M. Boots. Modelling the relationship between antibody-dependent enhancement and immunological distance with application to dengue. *J. Theor. Biol.*, 242:337–346, 2006.

[4] M. Aguiar, S. Ballesteros, B. W. Kooi, and N. Stollenwerk. The role of seasonality and import in a minimalistic multi-strain dengue model capturing differences between primary and secondary infections: Complex dynamics and its implications for data analysis. *J. Theor. Biol.*, 289:181–196, 2011.

[5] M. Aguiar, B. Kooi, and N. Stollenwerk. Epidemiology of dengue fever: A model with temporary cross-immunity and possible secondary infection shows bifurcations and chaotic behaviour in wide parameter regions. *Math. Model. Nat. Phenom.*, 3:48–70, 2008.

[6] B. Alberts, D. Bray, J. Lewis, M. Raff, K. Roberts, and J. Watson. *Molecular biology of the cell*. Garland Publishing, New York, 4 edition, 1994.

[7] M. Andraud, N. Hens, C. Marais, and P. Beutels. Dynamic epidemiological models for dengue transmission: A systematic review of structural approaches. *PloS One*, 7(11):e49085, 2012.

[8] H. Ansari and M. Hesaaraki. A with-in host dengue infection model with immune response and Beddington-Deangelis incidence rate. *Appl. Math.*, 3:177–184, 2012.

[9] S. Attia, M. Egger, M. Müller, M. Zwahlen, and N. Low. Sexual transmission of HIV according to viral load and antiretroviral therapy: Systematic review and meta-analysis. *AIDS*, 23(11):1397–1404, 2009.

[10] N. T. Bailey. *The mathematical theory of infectious diseases and its applications.* Charles Griffin & Company Ltd, 5a Crendon Street, High Wycombe, Bucks HP13 6LE., 1975.

[11] R. Ben-Shachar and K. Koelle. Minimal within-host dengue models highlight the specific roles of the immune response in primary and secondary dengue infections. *J. R. Soc. Interface*, 12(103):20140886, 2015.

[12] R. Ben-Shachar, S. Schmidler, and K. Koelle. Drivers of inter-individual variation in dengue viral load dynamics. *PLoS Comput. Biol.*, 12:1–26, 2016.

[13] S. Bhatt, P. W. Gething, O. J. Brady, J. P. Messina, A. W. Farlow, C. L. Moyes, J. M. Drake, J. S. Brownstein, A. G. Hoen, O. Sankoh, et al. The global distribution and burden of dengue. *Nature*, 496:504–507, 2013.

[14] S. Bianco and L. B. Shaw. Asymmetry in the presence of migration stabilizes multi-strain disease outbreaks. *Bull. Math. Biol.*, 73:248–260, 2011.

[15] S. Bianco, L. B. Shaw, and I. B. Schwartz. Epidemics with multistrain interactions: The interplay between cross immunity and antibody-dependent enhancement. *Chaos*, 19:043123, 2009.

[16] L. Billings, A. Fiorillo, and I. B. Schwartz. Vaccinations in disease models with antibody-dependent enhancement. *Math. Biosci.*, 211:265–281, 2008.

[17] J. D. Capra, C. A. Janeway, P. Travers, and M. Walport. *Immunobiology: The immune system in health and disease*. Garland Publishing, New York, 8 edition, 1999.

[18] S. Ciupe, P. De Leenheer, and T. Kepler. Paradoxical suppression of broadly neutralizing antibodies in the presence of strain specific antibodies during HIV infection. *J. Theor. Biol.*, 277:55–66, 2011.

[19] S. Ciupe, R. Ribeiro, P. Nelson, G. Dusheiko, and A. Perelson. The role of cells refractory to productive infection in acute hepatitis B viral dynamics. *Proc. Natl. Acad. Sci. USA*, 104:5050–5055, 2007.

[20] H. E. Clapham, V. Tricou, N. V. V. Chau, C. P. Simmons, and N. M. Ferguson. Within-host viral dynamics of dengue serotype 1 infection. *J. R. Soc. Interface*, 11:20140094, 2014.

[21] J. Cohen. HIV treatment as prevention. *Science*, 334(6063):1628–1628, 2011.

[22] D. Coombs, M. A. Gilchrist, and C. L. Ball. Evaluating the importance of within- and between-host selection pressures on the evolution of chronic pathogens. *Theor. Popul. Biol.*, 72(4):576–591, 2007.

[23] L. Coudeville, N. Baurin, M. L'Azou, and B. Guy. Potential impact of dengue vaccination: Insights from two large-scale phase III trials with a tetravalent dengue vaccine. *Vaccine*, 34(50):6426–6435, 2016.

[24] D. F. Cuadros and G. García-Ramos. Variable effect of co-infection on the HIV infectivity: Within-host dynamics and epidemiological significance. *Theor. Biol. Med. Model.*, 9(1):9, 2012.

[25] D. A. Cummings, I. B. Schwartz, L. Billings, L. B. Shaw, and D. S. Burke. Dynamic effects of antibody-dependent enhancement on the fitness of viruses. *Proc. Natl. Acad. Sci. USA*, 102:15259–15264, 2005.

[26] S. DebRoy and M. Martcheva. Immuno-epidemiology and HIV-AIDS: A modeling perspective. In *Mathematical biology research trends*, pages 175–192. Nova Science Publishers, 2008.

[27] P. DeLeenheer and S. Pilyugin. Multi-strain virus dynamics with mutations: A global analysis. *Math. Med. Biol.*, 26:285–322, 2008.

[28] O. Diekmann, J. A. P. Heesterbeek, and J. A. Metz. On the definition and the computation of the basic reproduction ratio R0 in models for infectious diseases in heterogeneous populations. *J. Math. Biol.*, 28(4):365–382, 1990.

[29] H. M. Doekes, C. Fraser, and K. A. Lythgoe. Effect of the latent reservoir on the evolution of HIV at the within- and between-host levels. *PLoS Comput. Biol.*, 13(1):1–27, 2017.

[30] N. Dorratoltaj, R. Nikin-Beers, S. M. Ciupe, S. G. Eubank, and K. M. Abbas. Multi-scale immunoepidemiological modeling of within-host and between-host HIV dynamics: Systematic review of mathematical models. *PeerJ*, 5:e3877, 2017.

[31] N. Dung, H. Duyen, N. Thuy, T. Ngoc, N. Chau, T. Hien, and et al. Timing of CD8+ T cell responses in relation to commencement of capillary leakage in children with dengue. *J. Immunol.*, 184:7281–7287, 2010.

[32] P. V. Effler, L. Pang, P. Kitsutani, V. Vorndam, M. Nakata, T. Ayers, J. Elm, T. Tom, P. Reiter, J. G. Rigau-Perez, et al. Dengue fever, Hawaii, 2001–2002. *Emerg. Infect. Diseases*, 11(5):742, 2005.

[33] R. A. Erickson, S. M. Presley, L. J. Allen, K. R. Long, and S. B. Cox. A stage-structured, *Aedes albopictus* population model. *Ecol. Model.*, 221(9):1273–1282, 2010.

[34] N. Ferguson, R. Anderson, and S. Gupta. The effect of antibody-dependent enhancement on the transmission dynamics and persistence of multiple-strain pathogens. *Proc. Natl. Acad. Sci. USA*, 96(2):790–794, 1999.

[35] C. Fraser, T. D. Hollingsworth, R. Chapman, F. de Wolf, and W. P. Hanage. Variation in HIV-1 set-point viral load: Epidemiological analysis and an evolutionary hypothesis. *Proc. Natl. Acad. Sci. USA*, 104(44):17441–17446, 2007.

[36] H. Friberg, L. Burns, M. Woda, S. Kalayanarooj, T. Endy, H. Stephens, S. Green, A. Rothman, and A. Mathew. Memory CD8+ T cells from naturally acquired primary dengue virus infection are highly cross-reactive. *Immunol. Cell Biol.*, 89:122–129, 2011.

[37] V. V. Ganusov and R. Antia. Imperfect vaccines and the evolution of pathogens causing acute infections in vertebrates. *Evolution*, 60(5):957–969, 2006.

[38] D. Gubler. Dengue and dengue hemmoragic fever. *Clin. Microbiol. Rev.*, 11:480–493, 1998.

[39] D. Guha-Sapir and B. Schimmer. Dengue fever: New paradigms for a changing epidemiology. *Emerg. Themes Epidemiol.*, 2(1):1, 2005.

[40] T. P. Gujarati and G. Ambika. Virus antibody dynamics in primary and secondary dengue infections. *J. Math. Biol.*, 69:1773–1800, 2014.

[41] H. Gulbudak, V. L. Cannataro, N. Tuncer, and M. Martcheva. Vector-borne pathogen and host evolution in a structured immuno-epidemiological system. *Bull. Math. Biol.*, 79(2):325–355, 2017.

[42] M. G. Guzmán, G. Kourí, L. Valdés, J. Bravo, S. Vázquez, and S. B. Halstead. Enhanced severity of secondary dengue-2 infections: Death rates in 1981 and 1997 Cuban outbreaks. *Rev. Panam. Salud Publica*, 11:223–227, 2002.

[43] M. G. Guzmán, G. P. Kouri, J. Bravo, M. Soler, S. Vazquez, and L. Morier. Dengue hemorrhagic fever in Cuba, 1981: A retrospective seroepidemiologic study. *Am. J. Trop. Med. Hyg.*, 42(2):179–184, 1990.

[44] S. B. Halstead. Dengue. *Lancet*, 370(9599):1644–1652, 2007.

[45] S. B. Halstead. Which dengue vaccine approach is the most promising, and should we be concerned about enhanced disease after vaccination? There is only one true winner. *Cold Spring Harb. Perspect. Biol.*, page a030700, 2017.

[46] S. B. Halstead, S. Mahalingam, M. A. Marovich, S. Ubol, and D. M. Mosser. Intrinsic antibody-dependent enhancement of microbial infection in macrophages: Disease regulation by immune complexes. *Lancet Infect. Dis.*, 10:712–722, 2010.

[47] S. B. Halstead, S. Rojanasuphot, and N. Sangkawibha. Original antigenic sin in dengue. *Am. J. Trop. Med. Hyg.*, 32:154–156, 1983.

[48] R. L. Hamers, C. L. Wallis, C. Kityo, M. Siwale, K. Mandaliya, F. Conradie, M. E. Botes, M. Wellington, A. Osibogun, K. C. Sigaloff, I. Nankya, R. Schuurman, F. W. Wit, W. S. Stevens, M. Vugt, and T. F. R. de Wit. HIV-1 drug resistance in antiretroviral-naive individuals in sub-Saharan Africa after rollout of antiretroviral therapy: A multicentre observational study. *Lancet Infect. Dis.*, 11(10):750–759, 2011.

[49] A. Handel and P. Rohani. Crossing the scale from within-host infection dynamics to between-host transmission fitness: A discussion of current assumptions and knowledge. *Phil. Trans. R. Soc. B*, 370(1675):20140302, 2015.

[50] L. Hartley, C. Donnelly, and G. Garnett. The seasonal pattern of dengue in endemic areas: Mathematical models of mechanisms. *Trans. R. Soc. Trop. Med. Hyg.*, 96(4):387–397, 2002.

[51] F. G. Hayden, J. J. Treanor, R. F. Betts, M. Lobo, J. D. Esinhart, E. K. Hussey,

et al. Safety and efficacy of the neuraminidase inhibitor gg167 in experimental human influenza. *JAMA*, 275(4):295–299, 1996.

[52] M. Hellerstein, M. Hanley, D. Cesar, S. Siler, C. Papageorgopoulos, E. Wieder, D. Schmidt, R. Hoh, R. Neese, D. Macallan, et al. Directly measured kinetics of circulating T lymphocytes in normal and HIV-1-infected humans. *Nature Med.*, 5(1):83, 1999.

[53] H. W. Hethcote. Three basic epidemiological models. In *Applied mathematical ecology*, pages 119–144. Springer, 1989.

[54] H. W. Hethcote. The mathematics of infectious diseases. *SIAM Rev.*, 42(4):599–653, 2000.

[55] T. J. Hladish, C. A. Pearson, D. L. Chao, D. P. Rojas, G. L. Recchia, H. Gómez-Dantés, M. E. Halloran, J. R. Pulliam, and I. M. Longini. Projected impact of dengue vaccination in Yucatán, Mexico. *PLoS Negl. Trop. Dis.*, 10:e0004661, 2016.

[56] D. D. Ho, A. U. Neumann, A. S. Perelson, W. Chen, J. M. Leonard, and M. Markowitz. Rapid turnover of plasma virions and CD4 lymphocytes in HIV-1 infection. *Nature*, 373(6510):123–126, 1995.

[57] T. D. Hollingsworth, R. M. Anderson, and C. Fraser. HIV-1 transmission, by stage of infection. *J. Infect. Dis.*, 198(5):687–693, 2008.

[58] S. Hué, R. J. Gifford, D. Dunn, E. Fernhill, D. Pillay, and UK Collaborative Group on HIV Drug Resistance. Demonstration of sustained drug-resistant human immunodeficiency virus type 1 lineages circulating among treatment-naive individuals. *J. Virol.*, 83(6):2645–2654, 2009.

[59] B. L. Innis. Antibody responses to dengue virus infection. In *Dengue and dengue hemorrhagic fever*, pages 221–243. CAB International, 1997.

[60] R. D. Kouyos, V. von Wyl, T. Hinkley, C. J. Petropoulos, M. Haddad, J. M. Whitcomb, J. Böni, S. Yerly, C. Cellerai, T. Klimkait, H. F. Günthard, S. Bonhoeffer, and the Swiss HIV Cohort Study. Assessing predicted HIV-1 replicative capacity in a clinical setting. *PLoS Pathog.*, 7(11):1–5, 11 2011.

[61] J. G. Kublin, P. Patnaik, C. S. Jere, W. C. Miller, I. F. Hoffman, N. Chimbiya, R. Pendame, T. E. Taylor, and M. E. Molyneux. Effect of plasmodium falciparum malaria on concentration of HIV-1-RNA in the blood of adults in rural Malawi: A prospective cohort study. *Lancet*, 365(9455):233–240, 2005.

[62] J. Lagarias, J. Reeds, M. Wright, and W. P. Convergence properties of the Nelder-Mead simplex method in low dimensions. *SIAM J. Optim.*, 9:112–147, 1998.

[63] P. Lemey, A. Rambaut, and O. G. Pybus. HIV evolutionary dynamics within and among hosts. *AIDS Rev.*, 8(3):125–140, 2006.

[64] B. L. Levine, L. M. Humeau, J. Boyer, R.-R. MacGregor, T. Rebello, X. Lu, G. K. Binder, V. Slepushkin, F. Lemiale, J. R. Mascola, et al. Gene transfer in humans using a conditionally replicating lentiviral vector. *Proc. Natl. Acad. Sci. USA*, 103(46):17372–17377, 2006.

[65] D. H. Libraty, T. P. Endy, H.-S. H. Houng, S. Green, S. Kalayanarooj, S. Suntayakorn, W. Chansiriwongs, D. W. Vaughn, A. Nisalak, F. A. Ennis, et al. Differing influences of virus burden and immune activation on disease severity in secondary dengue-3 virus infections. *J. Infect. Dis.*, 185:1213–1221, 2002.

[66] I. M. Longini, A. Nizam, S. Xu, K. Ungchusak, W. Hanshaoworakul, D. A. Cummings, and M. E. Halloran. Containing pandemic influenza at the source. *Science*, 309(5737):1083–1087, 2005.

[67] J. Lourenço, W. Tennant, N. R. Faria, A. Walker, S. Gupta, and M. Recker. Challenges in dengue research: A computational perspective. *Evol. Appl.*, 2017.

[68] P. M. Luz, T. Vanni, J. Medlock, A. D. Paltiel, and A. P. Galvani. Dengue vector control strategies in an urban setting: An economic modelling assessment. *Lancet*, 377(9778):1673–1680, 2011.

[69] K. A. Lythgoe, L. Pellis, and C. Fraser. Is HIV short-sighted? Insights from a multi-strain nested model. *Evolution*, 67(10):2769–2782, 2013.

[70] G. N. Malavige and G. S. Ogg. T cell responses in dengue viral infections. *J. Clin. Virol.*, 58:605–611, 2013.

[71] M. Martcheva. *An introduction to mathematical epidemiology*, volume 61 of *Texts in applied mathematics*. Springer US, 2015.

[72] M. Martcheva and X.-Z. Li. Linking immunological and epidemiological dynamics of HIV: The case of super-infection. *J. Biol. Dyn.*, 7(1):161–182, 2013.

[73] P. Mas Lago et al. Dengue fever in Cuba in 1977: Some laboratory aspects. In *Dengue in the Caribbean, 1977: Proceedings of a workshop held in Montego Bay, Jamaica (8-11 May 1978)*, pages 40–43. Pan American Health Organization, 1979.

[74] A. Mathew, I. Kurane, A. Rothman, L. Zeng, M. Brinton, and F. Ennis. Dominant recognition by human CD8+ cytotoxic T lymphocytes of dengue virus nonstructural proteins NS3 and NS1.2a. *J. Clin. Invest.*, 98:1684 – 1692, 1996.

[75] V. T. Metzger, J. O. Lloyd-Smith, and L. S. Weinberger. Autonomous targeting of infectious superspreaders using engineered transmissible therapies. *PLoS Comput. Biol.*, 7(3):1–12, 03 2011.

[76] N. Mideo, S. Alizon, and T. Day. Linking within-and between-host dynamics in the evolutionary epidemiology of infectious diseases. *Trends Ecol. Evol.*, 23(9):511–517, 2008.

[77] C. M. Midgley, M. Bajwa-Joseph, S. Vasanawathana, W. Limpitikul, B. Wills, A. Flanagan, E. Waiyaiya, H. B. Tran, A. E. Cowper, P. Chotiyarnwon, et al. An

in-depth analysis of original antigenic sin in dengue virus infection. *J. Virol.*, 85(1):410–421, 2011.

[78] K. Modjarrad and S. H. Vermund. Effect of treating co-infections on HIV-1 viral load: A systematic review. *Lancet Infect. Dis.*, 10(7):455–463, 2010.

[79] H. Mohri, A. S. Perelson, K. Tung, R. M. Ribeiro, B. Ramratnam, M. Markowitz, R. Kost, L. Weinberger, D. Cesar, M. K. Hellerstein, et al. Increased turnover of T lymphocytes in HIV-1 infection and its reduction by antiretroviral therapy. *J. Exp. Med.*, 194(9):1277–1288, 2001.

[80] J. Mongkolsapaya, W. Dejnirattisai, X.-n. Xu, S. Vasanawathana, N. Tangthawornchaikul, A. Chairunsri, S. Sawasdivorn, T. Duangchinda, T. Dong, S. Rowland-Jones, et al. Original antigenic sin and apoptosis in the pathogenesis of dengue hemorrhagic fever. *Nature Med.*, 9:921–927, 2003.

[81] D. M. Morens. Antibody-dependent enhancement of infection and the pathogenesis of viral disease. *Clin. Infect. Dis.*, 19:500–512, 1994.

[82] B. R. Murphy and S. S. Whitehead. Immune response to dengue virus and prospects for a vaccine. *Annu. Rev. Immunol.*, 29:587–619, 2011.

[83] N. E. A. Murray, M. B. Quam, and A. Wilder-Smith. Epidemiology of dengue: past, present and future prospects. *Clin. Epidemiol.*, 5:299, 2013.

[84] Y. Nagao and K. Koelle. Decreases in dengue transmission may act to increase the incidence of dengue hemorrhagic fever. *Proc. Natl. Acad. Sci. USA*, 105:2238–2243, 2008.

[85] N. M. Nguyen, D. T. H. Kien, T. V. Tuan, N. T. H. Quyen, C. N. Tran, L. V. Thi, D. Le Thi, H. L. Nguyen, J. J. Farrar, E. C. Holmes, et al. Host and viral features of human dengue cases shape the population of infected and infectious *Aedes aegypti* mosquitoes. *Proc. Natl. Acad. Sci. USA*, 110:9072–9077, 2013.

[86] T. Nguyen, H. Lei, T. Nguyen, Y. Lin, K. Huang, B. Le, and et al. Dengue hemorrhagic fever in infants: A study of clinical and cytokine profiles. *J. Infect. Dis.*, 189:221–232, 2004.

[87] R. Nikin-Beers, J. C. Blackwood, L. M. Childs, and S. M. Ciupe. Unraveling within-host signatures of dengue infection at the population level. *J. Theor. Biol.*, 446:79–86, 2018.

[88] R. Nikin-Beers and S. M. Ciupe. The role of antibody in enhancing dengue virus infection. *Math. Biosci.*, 263:83–92, 2015.

[89] R. Nikin-Beers and S. M. Ciupe. Modelling original antigenic sin in dengue viral infection. *Math. Med. Biol.*, page dqx002, 2017.

[90] M. A. Nowak, S. Bonhoeffer, A. M. Hill, R. Boehme, H. C. Thomas, and H. McDade. Viral dynamics in hepatitis B virus infection. *Proc. Natl. Acad. Sci. USA*, 93(9):4398–4402, 1996.

[91] N. Nuraini, H. Tasman, E. Soewono, and K. A. Sidarto. A with-in host dengue infection model with immune response. *Math. Comput. Model.*, 49:1148–1155, 2009.

[92] F. W. Nutter. Understanding the interrelationships between botanical, human, and veterinary epidemiology: The Ys and Rs of it all. *Ecosys. Health*, 5(3):131–140, 1999.

[93] K. Pawelek, S. Liu, F. Pahlevani, and L. Rong. A model of HIV-1 infection with two time delays: Mathematical analysis and comparison with patient data. *Math. Biosci.*, 235:98–109, 2012.

[94] K. A. Pawelek, G. T. Huynh, M. Quinlivan, A. Cullinane, L. Rong, and A. S. Perelson. Modeling within-host dynamics of influenza virus infection including immune responses. *PLoS Comput. Biol.*, 8(6):e1002588, 2012.

[95] A. S. Perelson. Modelling viral and immune system dynamics. *Nature Rev. Immunol.*, 2(1):28, 2002.

[96] A. S. Perelson, A. U. Neumann, M. Markowitz, J. M. Leonard, and D. D. Ho. HIV-1 dynamics in vivo: Virion clearance rate, infected cell life-span, and viral generation time. *Science*, 271(5255):1582–1586, 1996.

[97] P. Pongsumpun, K. Patanarapelert, M. Sriprom, S. Varamit, and I. Tang. Infection risk to travelers going to dengue fever endemic regions. *Southeast Asian J. Trop. Med. Public Health*, 35(1):155, 2004.

[98] L. Priyamvada, A. Cho, N. Onlamoon, N.-Y. Zheng, M. Huang, Y. Kovalenkov, K. Chokephaibulkit, N. Angkasekwinai, K. Pattanapanyasat, R. Ahmed, P. Wilson, and J. Wrammert. B cell responses during secondary dengue virus infection are dominated by highly cross-reactive, memory-derived plasmablasts. *J. Virol.*, 90:5574–5585, 2016.

[99] M. Recker, K. B. Blyuss, C. P. Simmons, T. T. Hien, B. Wills, J. Farrar, and S. Gupta. Immunological serotype interactions and their effect on the epidemiological pattern of dengue. *Proc. R. Soc. Lond. B Biol. Sci.*, 276:2541–2548, 2009.

[100] N. G. Reich, S. Shrestha, A. A. King, P. Rohani, J. Lessler, S. Kalayanarooj, I.-K. Yoon, R. V. Gibbons, D. S. Burke, and D. A. Cummings. Interactions between serotypes of dengue highlight epidemiological impact of cross-immunity. *J. R. Soc. Interface*, 10(86):20130414, 2013.

[101] A. Rothman. Immunity to dengue virus: A tale of original antigenic sin and tropical cytokine storms. *Nature Rev. Immunol.*, 11:532–543, 2011.

[102] R. A. Saenz and S. Bonhoeffer. Nested model reveals potential amplification of an HIV epidemic due to drug resistance. *Epidemics*, 5(1):34–43, 2013.

[103] P. Schmid-Hempel and S. A. Frank. Pathogenesis, virulence, and infective dose. *PLoS Pathog.*, 3(10):e147, 2007.

[104] I. B. Schwartz, L. B. Shaw, D. A. Cummings, L. Billings, M. McCrary, and D. S. Burke. Chaotic desynchronization of multistrain diseases. *Phys. Rev. E*, 72:066201, 2005.

[105] M. Shen, Y. Xiao, and L. Rong. Global stability of an infection-age structured HIV-1 model linking within-host and between-host dynamics. *Math. Biosci.*, 263:37–50, 2015.

[106] R. J. Smith, J. T. Okano, J. S. Kahn, E. N. Bodine, and S. Blower. Evolutionary dynamics of complex networks of hiv drug-resistant strains: the case of San Francisco. *Science*, 327(5966):697–701, 2010.

[107] X. Sun, Y. Xiao, S. Tang, Z. Peng, J. Wu, and N. Wang. Early HAART initiation may not reduce actual reproduction number and prevalence of MSM infection: Perspectives from coupled within- and between-host modelling studies of Chinese MSM populations. *PLoS One*, 11(3):1–21, 03 2016.

[108] S. Susser, C. Welsch, Y. Wang, M. Zettler, F. S. Domingues, U. Karey, E. Hughes, R. Ralston, X. Tong, E. Herrmann, et al. Characterization of resistance to the protease inhibitor boceprevir in hepatitis C virus–infected patients. *Hepatology*, 50(6):1709–1718, 2009.

[109] H. M. Thu, K. Lowry, L. Jiang, T. Hlaing, E. C. Holmes, and J. Aaskov. Lineage extinction and replacement in dengue type 1 virus populations are due to stochastic events rather than to natural selection. *Virology*, 336(2):163–172, 2005.

[110] V. Tricou, N. N. Minh, J. Farrar, H. T. Tran, and C. P. Simmons. Kinetics of viremia and NS1 antigenemia are shaped by immune status and virus serotype in adults with dengue. *PLoS Negl. Trop. Dis.*, 5:e1309, 2011.

[111] N. Tuncer, H. Gulbudak, V. L. Cannataro, and M. Martcheva. Structural and practical identifiability issues of immuno-epidemiological vector–host models with application to rift valley fever. *Bull. Math. Biol.*, 78(9):1796–1827, 2016.

[112] A. Vatti, D. M. Monsalve, Y. Pacheco, C. Chang, J.-M. Anaya, and M. E. Gershwin. Original antigenic sin: A comprehensive review. *J. Autoimmun.*, 83:12–21, 2017.

[113] D. W. Vaughn, S. Green, S. Kalayanarooj, B. L. Innis, S. Nimmannitya, S. Suntayakorn, T. P. Endy, B. Raengsakulrach, A. L. Rothman, F. A. Ennis, et al. Dengue viremia titer, antibody response pattern, and virus serotype correlate with disease severity. *J. Infect. Dis.*, 181:2–9, 2000.

[114] D. W. Vaughn, S. Green, S. Kalayanarooj, B. L. Innis, S. Nimmannitya, S. Suntayakorn, A. L. Rothman, F. A. Ennis, and A. Nisalak. Dengue in the early febrile phase: Viremia and antibody responses. *J. Infect. Dis.*, 176:322–330, 1997.

[115] G. M. Vazquez-Prokopec, U. Kitron, B. Montgomery, P. Horne, and S. A. Ritchie. Quantifying the spatial dimension of dengue virus epidemic spread within a tropical urban environment. *PLoS Negl. Trop. Dis.*, 4(12):e920, 2010.

[116] L. Villar, G. H. Dayan, J. L. Arredondo-García, D. M. Rivera, R. Cunha, C. Deseda, H. Reynales, M. S. Costa, J. O. Morales-Ramírez, G. Carrasquilla, et al. Efficacy of a tetravalent dengue vaccine in children in Latin America. *N. Engl. J. Med.*, 372:113–123, 2015.

[117] W.-K. Wang, H.-L. Chen, C.-F. Yang, S.-C. Hsieh, C.-C. Juan, S.-M. Chang, C.-C. Yu, L.-H. Lin, J.-H. Huang, and C.-C. King. Slower rates of clearance of viral load and virus-containing immune complexes in patients with dengue hemorrhagic fever. *Clin. Infect. Dis.*, 43:1023–1030, 2006.

[118] D. Weiskopf, M. Angelo, E. de Azeredo, J. Sidney, J. Greenbaum, A. Fernando, A. Broadwater, R. Kolla, A. De Silva, A. de Silva, K. Mattia, B. Doranz, H. Grey, S. Shresta, B. Peters, and A. Sette. Comprehensive analysis of dengue virus-specific responses supports an HLA-linked protective role for CD8+ T cells. *Proc. Natl. Acad. Sci. USA*, 110:E2046–E2053, 2013.

[119] D. Weiskopf, M. Angelo, J. Sidney, B. Peters, S. Shresta, and A. Sette. Immunodominance changes as a function of the infecting dengue virus serotype and primary versus secondary infection. *J. Virol.*, 88:11383–94, 2014.

[120] D. Weiskopf and A. Sette. T-cell immunity to infection with dengue virus in humans. *Front. Immunol.*, 5:1–6, 2014.

[121] When To Start Consortium, J. A. C. Sterne, M. May, D. Costagliola, F. de Wolf, A. N. Phillips, R. Harris, M. J. Funk, R. B. Geskus, J. Gill, F. Dabis, J. M. Miró, A. C. Justice, B. Ledergerber, G. Fätkenheuer, R. S. Hogg, A. D. Monforte, M. Saag, C. Smith, S. Staszewski, M. Egger, and S. R. Cole. Timing of initiation of antiretroviral therapy in AIDS-free HIV-1-infected patients: A collaborative analysis of 18 HIV cohort studies. *Lancet*, 373(9672):1352–1363, 2009.

[122] S. Whitehead, J. Blaney, A. Durbin, and B. Murphy. Prospects for a dengue virus vaccine. *Nature Rev. Microbiol.*, 5:518–528, 2007.

[123] V. Wittke, T. Robb, H. Thu, A. Nisalak, S. Nimmannitya, S. Kalayanrooj, D. Vaughn, T. Endy, E. Holmes, and J. Aaskov. Extinction and rapid emergence of strains of dengue 3 virus during an interepidemic period. *Virology*, 301(1):148–156, 2002.

[124] World Health Organization. Global strategy for dengue prevention and control. *Geneva: World Health Organization*, 2012.

[125] L. Yeghiazarian, W. G. Cumberland, and O. O. Yang. A stochastic multi-scale model of HIV-1 transmission for decision-making: Application to a MSM population. *PLoS One*, 8(11), 2013.

[126] J. Zaidi, E. Grapsa, F. Tanser, M.-L. Newell, and T. Bärnighausen. Dramatic increases in HIV prevalence after scale-up of antiretroviral treatment: A longitudinal population-based HIV surveillance study in rural KwaZulu-Natal. *AIDS (London, England)*, 27(14):2301, 2013.